Swansea University
Prifysgol Abertawe

Masters Thesis

The Biophone: Developing and Testing a Bioacoustic Recorder for Science and Citizen Science

---

by:

David Todd-Jones

Student ID: [redacted]

Supervisors

Prof. M. R. Jennings, Dr. R. P. Lewis, Prof. O. J. Guy

Submitted to Swansea University in fulfilment of the requirements for the Degree of Masters of Science by Research

Department of Electronic and Electrical Engineering,
Faculty of Science and Engineering,
Swansea University

November 6, 2025

22396 words

Declarations

Statement 1

This work has not previously been accepted in substance for any degree and is not being concurrently submitted in candidature for any degree.

Signed: [redacted]

Date: November 6, 2025

Statement 2

This thesis is the result of my own investigations, except where otherwise stated. Other sources are acknowledged by footnotes giving explicit references. A bibliography is appended.

Signed: [redacted]

Date: November 6, 2025

Statement 3

I hereby give consent for my thesis, if accepted, to be available for electronic sharing.

Signed: [redacted]

Date: November 6, 2025

Statement 4

The University's ethical procedures have been followed and, where appropriate, that ethical approval has been granted.

Signed: [redacted]

Date: November 6, 2025

Abstract

Bioacoustic Recorders (BARs) are specialised audio sensors for monitoring wildlife that have gained significant traction in academia to track species and understand biodiversity. Advancements in the underlying hardware have been key drivers for this growing popularity. However, the cost, power constraints and expertise required have limited the scale of their use. This thesis documents the research, development and testing of a new BAR device, the "Biophone", designed for both academic researchers and non-expert citizen scientists. The context of use and underlying hardware for BAR devices are explored in a literature review. The investigated hardware includes: Microcontroller Units (MCUs), Single Board Computers (SBCs), power electronics, microphones, signal processing and flash storage. This project involved building and testing two versions of the device: v1.0, with a 10 A h Nickel-Metal Hydride (NiMH) battery, and v1.1, with a 30 A h Lithium-ion (Li-ion) battery, as well as several other improvements to the design. For laboratory-based tests, an intermediary current-sense circuit was built, and waveforms were taken from oscilloscope and voltage-logger readings, with key observed waveforms described. In the lab, the Biophones had an effective deployment time of 3.91 days and 24.73 days for v1.0 and v1.1 respectively, when recording at the maximum Root Mean Square (RMS) power consumption of 93.99 mA, or 310.17 mW. In the field, a deployment time of 23 days for v1.0 was observed, recording with a bespoke schedule for the internal boards. Analysis of this deployment data identified 26 species of birds using the BirdNET algorithm. Furthermore, the computed acoustic indices revealed a distinct dawn chorus across all sites, along with a discernible variation in acoustic diversity among them. The closing chapters of this thesis discuss the key takeaways, the contribution and limitations of the study and the necessary further tests and development of this device.

Acknowledgements

I would like to express my gratitude to my supervisor, Professor Mike R. Jennings for his advice, patience and generosity while I conducted this project. His help, knowledge and encouragement were key to ensuring that I pursued this thesis to its conclusion.

Similarly, I'd like to thank my second and third supervisors, Dr. Richard P. Lewis and Professor Owen J. Guy for their support, sage advice and for the initial inspiration when starting this project.

Several others at Swansea University supported me during my studies. I am grateful to Dr. Stephen Batcup for his guidance and access to the laboratory and the lab equipment. I'm also grateful to the technicians David Moody and Robert John for sharing their knowledge and assistance in troubleshooting the various issues that came up.

More generally, I'd like to express my thanks to Swansea University for letting me study this Masters of Science by Research, from which I've learned a great deal.

I would also like to thank the students and staff at Coleg y Cymoedd (CYC) for facilitating and participating in the "Build-a-Biophone" workshops that allowed me to build Biophones in greater numbers for field and lab testing. In addition, I'd like to thank the members of the company Wild Connections Ltd. for allowing me to work on this Masters project part-time, while facilitating the future use of these devices in further deployments across the United Kingdom (UK).

Finally, I am also grateful to my friends and family who supported my long studying and working hours to complete this project, as well as their advice through the many ups and downs.

Contents

Nomenclature

Values

ρ	Resistivity of Copper at 20°C	1.68×10^{-8} Ωcm

Symbols

V_o	Voltage out of an Op-Amp	V
I_{sense}	Current across a sense resistor	A
R_{sense}	Resistance of sense resistor	Ω
V_{cc}	Power supplied to Op-Amp rails or the internal power supply of a PCB. Also referred to as V_{DD}/VDD.	

Units of Measurement

Ω	Ohms
A	Amperes
Ah	Ampere-hours
B	Bytes
C	Coulombs
dB	Decibels
dB(A)	A-weighted Decibels: volume as perceived by the human ear

$\mathrm{Np\,m^{-1}}$	Nepers per metre
Pa	Pacals
S	Samples
$\mathrm{S\,s^{-1}}$	Samples per second
V	Volts
W	Watts
Wh	Watt-hours

Abbreviations

AAF Anti-Aliasing Filter.

ACI Acoustic Complexity Index.

ADC Analogue to Digital Conversion.

AI Artificial Intelligence.

ARM Advanced RISC Machine.

ASA Acrylonitrile Styrene Acrylate.

AUD Australian Dollar.

AWG American Wire Gauge.

BAR Bioacoustic Recorder.

BI Bioacoustic Index.

BMS Battery Management System.

BNC Bayonet Neill–Concelman.

BNG Biodiversity Net Gain.

BOCC5 Birds of Conservation Concern 5.

CAD Computer-Aided design.

CAGR Compound Annual Growth Rate.

CBD Convention on Biological Diversity.

CD Compact Disc.

CISC Complex Instruction Set Computing.

CMOS Complementary Metal-Oxide Semiconductor.

CNN Convolutional Neural Network.

COP Conference of Parties.

CPU Central Processing Unit.

CTD Conductivity, Temperature, and Depth.

CYC Coleg y Cymoedd.

DAC Digital to Analogue Conversion.

DC Direct Current.

DIP Dual In-line Package.

DMA Direct Memory Access.

DVFS Dynamic Voltage and Frequency Scaling.

ECM Electret Condenser Microphone.

EEPROM Electrically Erasable Programmable Read-Only Memory.

ELMS Environmental Land Management Schemes.

EMI Electromagnetic Interference.

FFT Fast Fourier Transform.

FGMOS Floating Gate Metal-Oxide Semiconductor.

FLAC Free Lossless Audio Codec.

FM Frequency-Modulated.

GBP Great British Pound.

GPIO General Purpose Input/Output.

GPS Global Positioning System.

H Acoustic Entropy Index.

HDD Hard Disk Drive.

HDMI High-Definition Multimedia Interface.

I/O Input/Output.

IC Integrated Circuit.

IPX7 Ingress Protection Rating 7.

JFET Junction-gate Field-Effect Transistor.

JST Japan Solderless Terminal.

LED Light-Emitting Diode.

Li-ion Lithium-ion.

LoRa Long Range.

MCU Microcontroller Unit.

MEMS Micro-Electromechanical Systems.

ML Machine Learning.

MOS Metal-Oxide-Semiconductor.

MOSFET Metal–Oxide–Semiconductor Field-Effect Transistor.

NDSI Normalised Difference Soundscape Index.

NGO Non-Governmental Organisation.

NI National Instruments.

NiMH Nickel-Metal Hydride.

NRW Natural Resources Wales.

NWMP North Wales Moorland Partnership.

OAD Open Acoustic Devices.

OLED Organic Light-Emitting Diode.

Op-Amp Operational Amplifier.

OS Operating System.

OTP ROM One-Time-Programmable Read-Only Memory.

PC Personal Computer.

PCB Printed Circuit Board.

PGA Programmable-Gain Amplifier.

PIP Plug In Power.

Preamp Pre Amplifier.

RAM Random-Access Memory.

RFID Radio-Frequency Identification.

RISC Reduced Instruction Set Computer.

RMS Root Mean Square.

ROM Read-Only Memory.

SBC Single Board Computer.

SD Secure Digital.

SMT Surface-Mount Technology.

SNR Signal-to-Noise Ratio.

SPI Serial Peripheral Interface.

SRAM Static Random Access Memory.

SSSI Site of Special Scientific Interest.

TTL Transistor-Transistor Logic.

UART Universal Asynchronous Receiver-Transmitter.

UK United Kingdom.

UN United Nations.

USART Universal Synchronous and Asynchronous Receiver-Transmitter.

USB Universal Serial Bus.

USD United States Dollar.

UV Ultraviolet.

VHF Very High Frequency.

VLSI Very Large Scale Integrated circuit.

WWF World Wide Fund for Nature.

Terminology

Bioacoustic The collection and study of sounds from biological sources, principally animal vocalisations.

Ecoacoustic The collection and study of sounds of ecological importance. This includes bioacoustic sounds, as well as planetary sounds (weather, water and earthquakes) and anthropogenic sounds (gunshots, chainsaws and heavy industry).

Soundscape All sounds present in an environment at a given time.

Spectrogram A visual representation of a sound file, plotting frequency over time, with amplitude represented by colour intensity.

Taxa A group of related species. This can be at the species level or higher, such as the taxa of frogs or the taxa of amphibians.

Interchangeable Terms

Bioacoustic Recorder Acoustic Sensor, Field Recorder, Wildlife Recorder, Autonomous Recording Unit (ARU), Passive/Autonomous Acoustic Recorder, PAM Device.

Bioacoustics Passive Acoustic Monitoring (PAM), Wildlife Acoustic Monitoring.

Ecoacoustics Acoustic Ecology, Soundscape Ecology.

List of Figures

List of Tables

List of Equations

1. Introduction

1.1 Context: Wildlife Conservation Technology

Traditional ecological surveying is a demanding, field-based process that requires trained experts making manual observations. This process can be slow, limited in time and scale, prone to human error, and expensive [1]. These factors have previously limited scientific study of the natural world. Hence, there has been shift in academia to a greater use of automated remote loggers, bespoke surveillance technologies, and advanced methods of data analysis to improve wildlife monitoring and wildlife conservation efforts. Some of the listed benefits of these "conservation technologies" in the literature include:

1. The quantity and quality of data that can be collected is dramatically increased, widening the previous data bottleneck.
   (a) Through increased automation, monitoring can be done in a continuous and/or scheduled manner and rapidly processed without a significant increase in price or man-hours [2].
   (b) This ability to collect and parse more biological information automatically allows for more comprehensive species and biodiversity assessments, providing greater insights [3].
2. Data collected can be of greater resolution, particularly with on-the ground sensors, and standardised to improve the scientific accuracy of surveys [4].
3. The technologies that allow passive recording of data, such as video image and audio capture, as opposed to trapping and tagging, reduce the impact of researchers on the site, allowing observation of more natural behaviours [2].
4. Arrays of sensors, Global Positioning System (GPS) tagging, and satellite imaging allow now for extensive geographical coverage, significantly increasing the

land area surveys can take [4].

Recent advancements in electronics have played a fundamental role in the capability of conservation technologies, both in the logging devices and connected sensors, as well as in the computing power required for analysis.

Figure 1.1 shows some examples of conservation technology tools available to today's researchers. The term "conservation technology" can refer to a wide array of sensors and collection/analysis methods for biological data, which can include:

1. Established wildlife monitoring technologies that have steadily improved with each technological advancement, like camera traps, Bioacoustic Recorders (BARs), biologgers and GPS collars [2].
2. The reapplication of existing surveillance technologies, like satellite imaging, for flora and fauna monitoring at scale [4].
3. New, bespoke data collection and analysis technologies, like collecting environmental DNA or Artificial Intelligence (AI) analysis of images, audio and other sensor data [4].

Figure 1.1: Examples of wildlife conservation technologies. Taken from [2].

(A) Camera trap images with night infrared.

(B) A BAR SBC deployed in a simple bag casing.

(C) A pulse radar used to study bird migration.

(D) A small drone with a colour camera and thermal sensor.

(E) A Raspberry Pi–based video logger for sea turtles.

(F) A Weddell seal with a satellite relay data logger on its head with Conductivity, Temperature, and Depth (CTD) sensors.

(G) Manual Very High Frequency (VHF) radio tracking of orange-bellied parrots.

(H) A drone fitted with components for bespoke VHF radio-tracking.

(I) Monitoring equipment attached to a harness for birds, with a geolocator and multisensor logger for ambient light, atmospheric pressure, temperature, and acceleration.

(J) Monitoring of visits to a feeder via Radio-Frequency Identification (RFID) microchipped individual birds

(K) A Raspberry Pi–based time-lapse cameras for penguin colonies in Antarctica. For this study, pictures were labelled by citizen scientists via the Zooniverse platform.

(L) A fixed-wing drone with a camera using a bespoke Machine Learning (ML) model to identify Marsh deer from photographs.

1.2 Context: Bioacoustic Recorders (BARs)

Bioacoustic Recorders (BARs) are specialised audio recorders that can be deployed remotely to capture animal vocalisations and environmental sound. The science underpinning the interpretation of this sound data is the field of "Bioacoustics". Animals, in particular, produce a wide variety of sounds to communicate. Animal vocalisations vary noticeably between species and can consist of varied rhythm, complicated frequency modulation, broadband pulses or rapid changes in amplitudes, while integrating pure tones and harmonic stacks [5]. These sounds carry useful information for a trained ecologist, such as what species are present, as well as their behaviour, health, movement, and migrations [6]. In addition to animal sounds, environmental sounds such as weather, running water, traffic, mining, gunshots and chainsaws have also been studied in this field [7]–[11], as these sounds can have profound implications for local wildlife. Collecting and interpreting this biological data is valuable for scientific research, animal welfare, wider wildlife conservation efforts, eco-friendly land management and environmental policymaking [6].

Bioacoustics represents one of the older wildlife conservation technologies, but one that has recently been revolutionised by the falling cost and increased functionality of underlying hardware, as well as the data-processing capacity of specialised software and new ML algorithms.

In particular, the ability to record and store sound data has been dramatically improved in recent years with advancements in sound recording electronics. BARs, have capitalised on developments in MCUs, SBCs, power-management electronics, microphones, signal processing and data storage technologies. This has resulted in more efficient, cheaper, more compact devices that can be deployed for longer periods, while capturing data at a high resolution. Furthermore, advances in software-based tools to automatically interpret sound data, such as spectrogram-based species identification ML algorithms and statistical metrics like acoustic indices, have played a growing role in the study of wildlife and environmental sound.

Figure 1.2 and fig. 1.3 show simplified block diagrams of a modern BAR device. They display the array of key components that consume power and handle the audio signal on a typical BAR device. These components and concepts are discussed in greater depth in the literature review (see chapter 2).

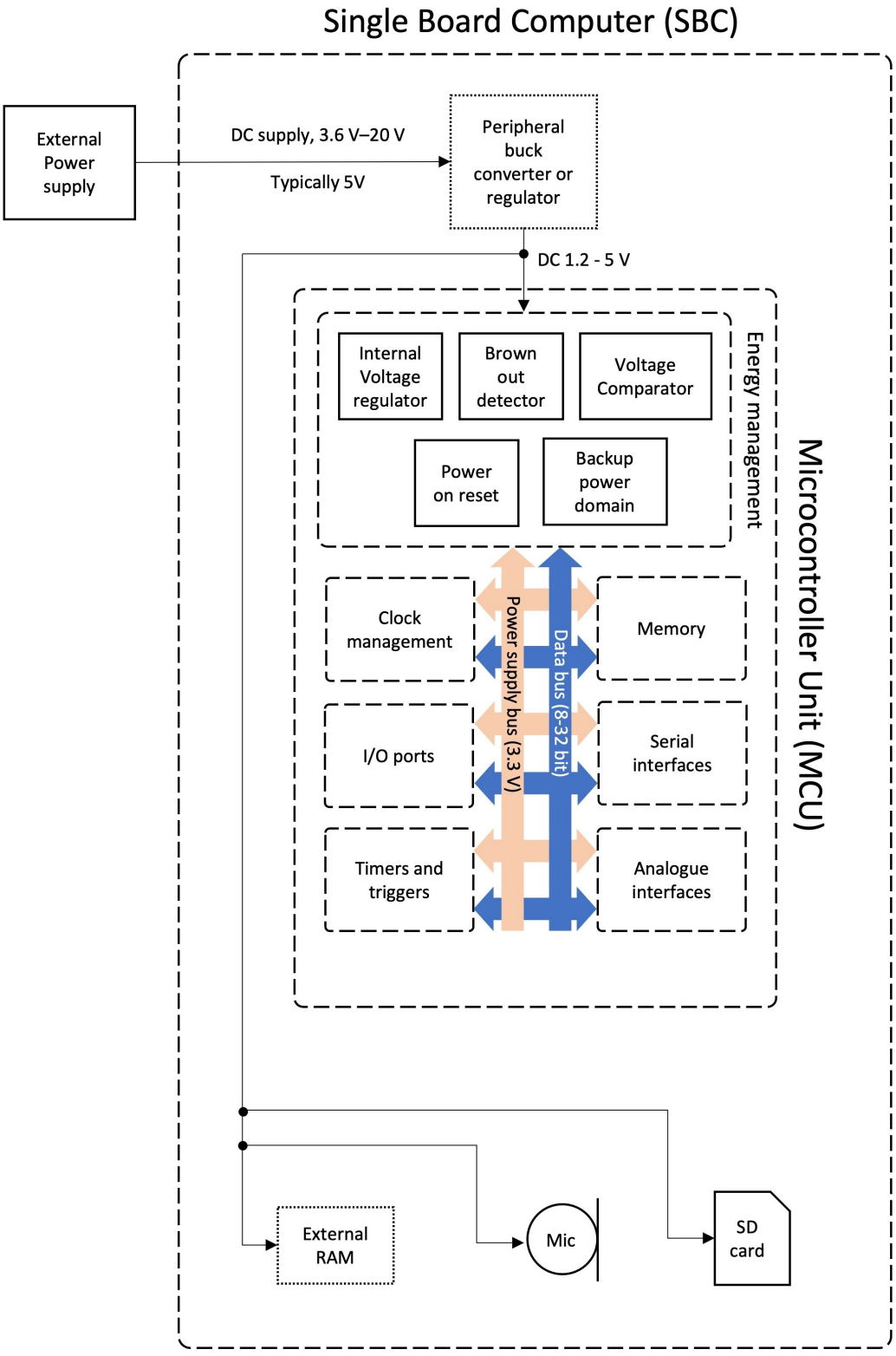

Figure 1.2: A simplified block diagram for power in a modern BAR device, showing typical key components. The dashed lines represent the borders of the SBC and MCU. Dotted lines represent optional extra components that can be involved. Other shorthands used include Random-Access Memory (RAM), Input/Output (I/O) and Secure Digital (SD) card.

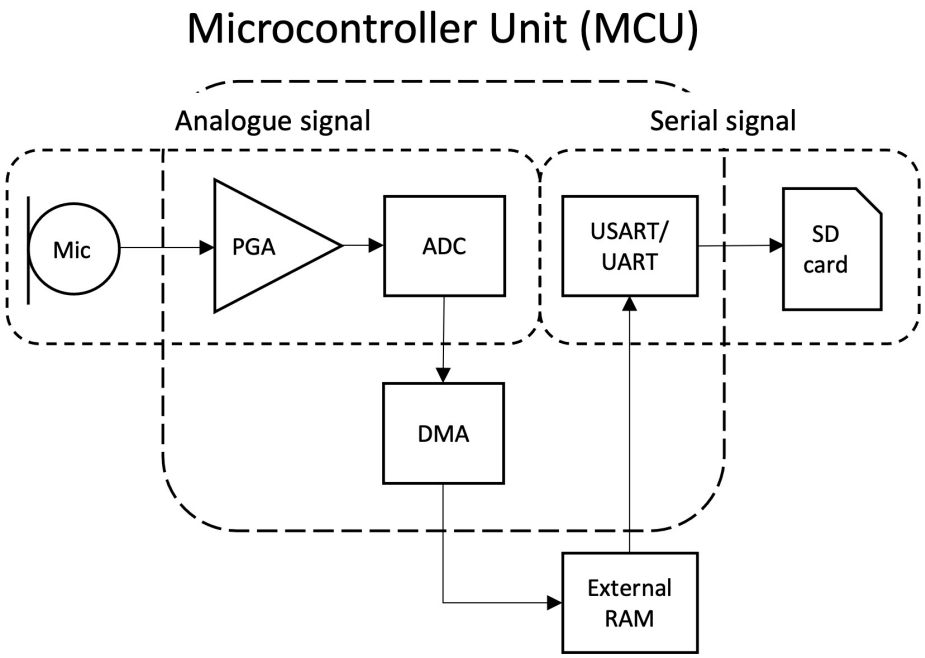

Figure 1.3: A simplified BAR block diagram for audio signal in a modern device, showing typical key components. The large dashed lines represent the borders of the MCU. Smaller dashes represent the different signal types. Shorthands include: Programmable-Gain Amplifier (PGA), Analogue to Digital Conversion (ADC), Direct Memory Access (DMA), Random-Access Memory (RAM), Universal Synchronous and Asynchronous Receiver-Transmitter (USART), Universal Asynchronous Receiver-Transmitter (UART) and SD card.

1.3 Context: The Wildlife Monitoring Market

According to one industry report, the global wildlife tracking systems market size was valued at £12.43 billion Great British Pound (GBP) in 2023 and is projected to reach £34.55 Billion GBP by 2031, with a Compound Annual Growth Rate (CAGR) of 14.3% [12].

The growth in these markets was attributed to a few key drivers:

1. Increased demand from existing researchers, due to falling costs of hardware and increased capability of the underlying technologies [12].

2. Growing scientific/public concern over biodiversity loss and local environmen-

tal concerns, driving up citizen science consumption of devices and putting pressure on policymakers [12].

3. New policies and public funding by governments and international groups on land use, protecting natural resources and nature-impact reporting [12].

The first of these points is addressed in the previous sections and in the literature review from section 2.2 onwards.

The second point, biodiversity loss (the global decline in wild flora and fauna) has been a topic of growing concern on the world stage. The majority of biodiversity loss has occurred in the last 70 years, with declines both in the number of species and the total abundance of living things. The World Wide Fund for Nature (WWF) Living Planet Report 2020 states that there has been an average 68% decline in vertebrate populations (mammals, birds, reptiles, amphibians and fish) worldwide since 1970 [13]. In addition to conservation concerns, multiple studies have shown biodiversity loss having measurable negative impacts on carbon sequestration, flooding, local climate, pollination, agriculture, and air and water quality [14]–[16].

As a response to growing concerns over biodiversity loss, policymakers attending the UN Convention on Biological Diversity (CBD) Conference of Parties (COP) have implemented new international policy agreements and national pro-biodiversity legislation. For instance, biodiversity monitoring is now also an integral part of the Aichi Biodiversity Targets as well as the United Nations' "Life on Land" and "Life Below Water" Sustainable Development Goals [4], [17].

1.4 Project Motivation

The recent proliferation of Bioacoustic Recorders (BARs) has been part of a larger scientific movement to monitor environments autonomously, continuously, and at scale. BARs represent a promising tool in the toolkit of researchers. And, continuing to optimise these devices for users of all kinds will have knock-on benefits for science and understanding the human impact on biodiversity.

According to a global study of biodiversity intactness by Newbold et al., the UK ranks in the bottom 10% of 240 nations. This has been primarily driven by urbanisation, pollution and intensive agriculture, leading to habitat degradation [18]. But, newly introduced policies offer an opportunity to reverse this trend of decline through remuneration and legal frameworks. These new policies include the Environmental Land Management Schemes (ELMS) [19] and Biodiversity Net Gain (BNG) [20] initiatives by the UK government (both officially launched in England in 2024), as well as the United Nations (UN) initiatives previously mentioned. That said, any progress made on biodiversity has to be tracked and stand up to scientific scrutiny. So, it is critical that robust and scalable wildlife monitoring tools are developed and tested to ensure that a measurable difference is made.

1.5 Aims and Objectives

This project's aim is to build, develop and test a custom Bioacoustic Recorder (BAR) for use by scientists and citizen scientists. The device should capitalise on recent technological advances, be capable of long-term, continuous monitoring, be affordable and be able to accommodate future hardware improvements.

The objectives are:

1. To research the current use of BARs and the requirements of potential end-users.
2. To research the underlying electronics of modern BARs and decide on components to use in the design.
3. To identify the research gap in previous studies and designs of commercially available device designs.
4. To design and build the required device based on the above considerations.
5. To test the BAR device:
   (a) Deployed in the field, testing the effective deployment time, durability in remote environments and usefulness of the data collected for ecologists.
   (b) In the lab, investigating power consumption in real-time and over the long term.
6. To evaluate the overall usefulness of the device for its intended user from the obtained results.
7. To recommend future improvements and research.

On completion of the project, readers will be able to make their own version of this BAR device, understand the technologies involved, and understand the trade-offs of building and deploying such devices. For highly-skilled academic use, further potential developments and tests of the devices are discussed, while methods for low-skilled deployment and data collection is demonstrated.

1.6 Organisation of Thesis

Chapter 2, the Literature Review, summarises the field of Bioacoustics, and constituent electronic components of BARs are discussed in the context of current academic literature and practitioner use. The reasoning behind the choice of SBC used and the SBC's underlying circuitry are also discussed. At this chapter's conclusion, the research gap is presented.

Chapter 3, Hardware Design, lays out the Biophone BAR device design.

Chapter 4, Methods, describes the tests used to build and interrogate the BAR device.

Chapter 5, Results, describes the results of tests.

Chapter 6, Discussion, covers the interpretation of results in the context of the literature.

Chapter 7, Conclusion, summarises the project and its contribution to science. It also discusses the limitations of the project and points for further study and hardware developments.

2. Literature Review

In this chapter, BARs are put in the context of current academic literature; the findings of previous authors are reviewed and the theory and trade-offs to consider for building and deploying a novel BAR device are discussed. Section 2.1 summarises bioacoustics, BARs and other considerations of their use by practitioners. Section 2.2 investigates the underpinning electronic components as well the reasoning and circuitry details for the chosen SBC used. Section 2.3 articulates the research gap.

2.1 Bioacoustics and Bioacoustic Recorders

2.1.1 Bioacoustics

Bioacoustics, particularly using automated sensors, has had a growing presence in academic literature. A systematic review by Sugai et al. found a fifteen-fold increase in publications in automated terrestrial bioacoustics since 1992 [21].

Sound has been used for some time to study terrestrial animals that are elusive, otherwise inconspicuous, and vocally active. For instance, bats, nocturnal animals, and animals in dense rainforests [22]. However, more recently, BARs have gained traction as a means of monitoring a wide variety of species and environment types [21], [23]. This is due to some inherent advantages of recording sound, discussed in section 2.1.2.1, and advancements made in the sound recording technologies, discussed in section 2.1.2. The limitations of bioacoustic analysis is discussed in section 2.1.1.6. It should also be noted that BARs have been extensively used to track marine life such as whales, dolphins and fish [24], but this literature review will mostly focus on terrestrial recording.

Broadly speaking, modern bioacoustics literature can be split into two camps:

1. Identifying specific biological sounds of interest: discussed in section 2.1.1.1.
2. Whole Soundscape Analysis (Ecoacoustics): discussed in section 2.1.1.3.

2.1.1.1 Tracking Specific Sounds

Biological sounds of significance can include:

1. Animal vocalisations (fig. 2.1A).
2. Indirect sounds from animal movement or metabolism (fig. 2.1B).

A wide array of biological sounds have been categorised as important for understanding animal presence, movement, behaviour and biodiversity. Figure 2.1 shows some examples of audio that can be captured and identified, displayed as Spectrograms: plotting audio frequency (in kHz) over time, in seconds, with the brightness of colour indicating amplitude. For each frame across the x axis (time) the frequency distribution is calculated using a Fast Fourier Transform (FFT) [5].

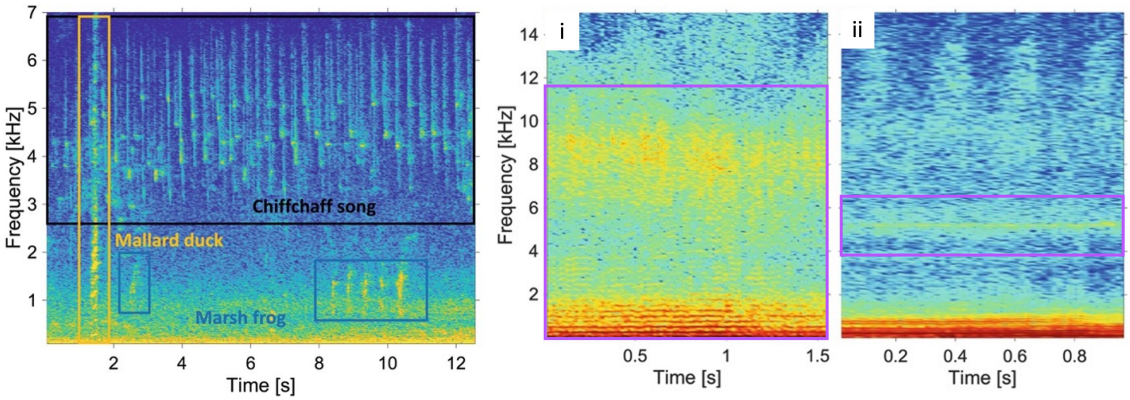

(A) A temperate forest at dusk, with calls from three species identified.

(B) Flight sounds of the European Honeybee (i) and the Japanese Yellow Hornet (ii).

Figure 2.1: Spectrogram examples of identified sounds. Taken from [25].

The unique acoustic signatures on a spectrogram can be used to identify and study species of interest in a variety of ways, either by manual inspection or with an

Machine Learning (ML) algorithm. For instance, Hughes et. al. were able to manually interrogate features from a spectrogram to determine different species of bat echolocation calls in Thailand, focusing on flying calls, referred to as Frequency-Modulated (FM) sweeps. The features their study focused on were start frequency, end frequency, maximum frequency, minimum frequency, middle frequency, maximum intensity, number of harmonics, inter-pulse interval, inter-harmonic distance, and call duration [26]. In addition to presence, Burnham argues that the large "vocal repertoire" of many animals can be used to track and differentiate between different behavioural calls such as those for foraging, feeding, weaning, mating, navigation, migration and territorial defence [27]. Furthermore, a cross-species study by Gilooly and Ophir also proposes that the differences between species in vocal repertoire can be explained by the energetic constraints of sound production. They observed an inverse relationship between the average species size and the peak frequency of the calls across taxa, with call features varying predictably with body size and metabolism/temperature. Larger species, with slower metabolisms were typically observed to invoke longer, deeper, or louder signals and vice versa [28]. This theory explains the typical separation of taxa observed by bioacousticians in a spectrogram, with small, high-metabolism animals in the higher frequencies, like bats, rodents, insects, small birds and amphibians, and larger animals in the lower frequencies, like larger mammals and reptiles. These studies together demonstrate the wealth of information that can be gathered from sound with the relevant expertise.

2.1.1.2 The Role of Machine Learning (ML) in Identifying Sounds

As with many fields of scientific research, Machine Learning (ML) algorithms have played a growing role in the academic literature to automate bioacoustic sound analysis [29]. Many of the ML algorithms developed build on recent advances in image recognition applied to spectrogram, identifying calls via their distinct visual fingerprint [30]. The model of ML algorithms used has also shifted in the past decade, moving towards greater efficiency, accuracy and coverage of novel species. Where

previously, Hidden Markov Models were used, now researchers typically rely on Convolutional Neural Networks (CNNs) models; which are more accurate and comprehensive, due to being trained on many terabytes (TB) of data [31]. With the advent of transformer-based models, like ChatGPT, there have also been transformer models developed for bioacoustics, which benefit form this architecture by having a more efficient pre-training process and less training data to recognise new animal vocalisations. These "few-shot" models propose a means for researchers to add novel species calls more efficiently and without requiring the immense, high-quality training datasets that CNNs rely on [32]. That said, there currently isn't one of these transformer-based models freely available for use in this study. One algorithm that has seen a lot of use in the literature is the CNN model BirdNET, developed by Cornell University. Pérez-Granados identifies this as a robust tool to use for bird species identification, but also notes some potential pitfalls that research can fall prey to when using this tool, including as a bias towards North American species, which make up the majority of the database [33]. The author recommends using the latitude and longitude features of the app as a way to counteract this. Sethi et al. also recommend setting a minimum confidence score of 0.7–0.8 as an appropriate range for most studies [34].

2.1.1.3 Whole Soundscape Analysis and Ecoacoustics

Whole Soundscape Analysis refers to analysis done on all sounds present in an recording at a given time [35]. This form of analysis comes under the wider scientific field of "Ecoacoustics", involving the capturing and interpreting all sounds of ecological relevance. This can include biological sound sources (bioacoustics), such as animal vocalisations, but also includes planetary sounds (such as weather and moving water) and anthropogenic sounds (such as gun shots, chainsaws, traffic and industry). There have been academic papers documenting the training ML algorithms to assess whole soundscapes without the need to identify individual calls, such as Omprakash et al. [36]. However, a more established method of measuring whole soundscapes is by us-

ing statistical metrics called "acoustic indices", which quantify objective "features" in recordings, such as frequency and amplitude, over time. Alcocer et al. describes the theory behind acoustic indices as follows: "Sounds can be described based on three interlinked acoustic dimensions: time, frequency, and energy. Acoustic indices are mathematical functions that rely on these three dimensions to summarise the global complexity or heterogeneity of a sound recording" [37]. These indices rely on the conceptual framework, referred to as the "acoustic niche hypothesis", that species will naturally partition themselves into different frequency ranges over evolutionary time to avoid acoustic clashes and maximise the chance for successful communication. Thus, environments with higher biodiversity will have more of these frequency niches filled and a measurably "fuller" soundscape [38]. Some cited benefits of using acoustic indices are that they demands far less computational power than ML algorithms and don't require the initial training with large annotated datasets. They are also reported to provide rapid and replicable values that can be used to infer an environment's biodiversity [39].

One commonly cited acoustic index, the Acoustic Complexity Index (ACI), represents a measure of the relative change in acoustic intensity (amplitude) in each frequency bin of an spectrogram - with "frequency bin" referring to an predefined partitioning of the frequency axis. Mathematically, ACI can be represented as:

The Acoustic Complexity Index

$$ACI(f) = \frac{\sum_i \mid A_{if} - A_{i-1,f} \mid}{\sum_i A_i} \tag{2.1.1}$$

Where A is the acoustic intensity, i is the index over all frames in the given time period and f is the index over all frequency bins.

The pre-analysis steps to calculating an acoustic index like ACI, include applying a digital filter to reduce the effects of microphone electrical noise, conducting a FFT to create a sonic matrix, and aggregating this data using a clumping procedure [40]. An average value is created for each input sound file, so long sound files have to be broken up into clips. Typically, 256 frequency bins are used for a 48 kHz sample rate

recording, and one minute is used as the time period [41].

Bradfer-Lawrence et. al. propose that acoustic indices offer a novel method for rapid and ongoing biodiversity assessment in UK bird species, both in richness and abundance. They found that patterns in these indices were coherent both between indices, and across habitat types. In addition, they propose that tracking shifting acoustic indices values could indicate changes in "species assemblages", and could be used to alert land managers to shifts in wildlife populations [42].

2.1.1.4 The Limitations of Acoustic Indices

While acoustic indices have shown promise in research, there are notable limitations to their use and interpretation. These include:

1. Understanding and accurately interpreting acoustic indices requires a degree of expertise. This can discourages new users and prevents the wider acceptance. To address this, Bradfer-Lawrence et al. provide a web app with step-by-step explanations of the most commonly used acoustic indices, with instructions on how to implement and interpret them (available here) [43].

2. There is still some dispute over the primary assumption behind acoustic indices: that there is a correlation between acoustic and biological diversity. In their meta-analysis of the literature, Alcocer et al.found a "moderate positive relationship with the diversity metrics ($r = 0.33$, CI [0.23, 0.43])", but found that use of acoustic indices showed "inconsistent performance, with highly variable effect sizes both within and among studies" [37].

3. Some non-biological acoustic events, like passing storms, can lead to high acoustic index values, which can skew results. For instance, dominant and interfering planetary noise, like extreme rain and wind, daily traffic, or droning insects like cicadas. Alcocer et al. recommend ground-truthing, long survey times (so that data can be analysed in aggregate), and using "weighted combinations" of different indices for comparison. They found that the indices Acoustic En-

tropy Index (H), Normalised Difference Soundscape Index (NDSI), and ACI performed the best in reflecting biological information. Ground-truthing such data sets would include a comparison with existing biodiversity datasets or an initial manual survey [37]. In their guidelines, Bradfer-Lawrence et al. recommend collecting a minimum of 120 hours of continuous recordings per site to achieve this [44].

4. There is some inherent biological acoustic variability that can occur over over multiple months/years, which could be misleading if not accounted for. These can include seasonal changes in species composition, due to migration and hibernation, and changes in vocal activity, due to specific vocalisations occurring only during seasons of breeding, rearing young and migration [6]. Furthermore, there are observed differences in acoustic complexity between temperate and equatorial habitats when both are at peak levels of biodiversity [37]. To combat this, researchers should seek to compare like-for-like in location and season, as well as control for other factors in sound data where possible. In addition, combining acoustic indices values with a species lists can allow researchers to track migration and hibernation periods.

For these reasons, Sethi et al. propose that a more appropriate use of acoustic indices might be to use them as a means of collecting low-resolution data for the initial phases of large scale monitoring programmes. In doing so, researchers could detect biological change across landscapes and pinpoint areas of interest. This could then be followed up by subsequent finer-scale surveying methods and allow for a more efficient use of limited resources [45].

2.1.1.5 The Importance of Sound Recording Technologies for Analysis

The amount of useful information that can be extracted from sound data has steadily increased with the development of more powerful analysis tools described in previous sections. But the quality and quantity of sound recorded still play a significant role

in its successful interpretation.

For instance, the quantity of data collected influences the accuracy of interpretation, either by allowing a greater data training set for ML algorithms or by allowing for a greater aggregation of data to remove short-term noise. Stowel et al. found that the performance of their CNN for whale vocalisations continued to improve towards the maximum accuracy with more data, even with poorly labelled datasets [31]. Collecting more data to improve accuracy requires more recorders, more continuous recording, and longer deployment times.

Similarly, the quality of sound data plays an important role. Particular reference in the literature is paid to lowering the artificial "noise floor" of recordings, with every 3 dB reduction in noise floor doubling the effective signal capture area [46]. This generally requires using microphones with a higher Signal-to-Noise Ratio (SNR) and sensitivity. Microphone dynamic range can also determine how close and loud an animal can be before the recording becomes distorted and unidentifiable [46].

2.1.1.6 The Limitations of Bioacoustic Analysis

One of the general limitations of bioacoustics highlighted in the literature includes an inherent bias towards animals that have frequent, loud and distinctive vocalisations. For terrestrial environments in the UK, the dominant sounds include those of birds, bats, livestock, frogs/toads and crickets. While other, less vocally active species, such as other insects, reptiles and mammals represent a smaller proportion of the soundscape. This can skew data when trying to predict species abundance and limits the amount of ML training data that can be collected for the less vocally active species [47]. Furthermore, groups that play pivotal roles in ecosystem function but don't make a detectable sound, like plants, fungi and microorganisms, are not surveyed with this method of data collection. Instead, bioacoustics relies on animals that interact with these groups (via the food chain, through disease, or otherwise) to indirectly serve as proxies for the ecosystem as a whole [47]. Another limitation is

that bioacoustics analysis currently cannot differentiate between the individuals of a population calling for most taxa, whereas this is more often possible with camera traps for larger animals [47].

Gibb et al. also ML identify technical barriers to researchers and a lack of clarity regarding the accuracy and transferability of analytical methods like bespoke ML algorithms or the implementation/interpretation of acoustic indices [47]. Furthermore, sound and different frequencies of sound do not travel uniformly through an environment, discussed further in section 2.1.3.3, meaning that certain species that are quieter or use higher frequencies may be under-represented in datasets. Finally, Potenza et. al. point out that some consideration is required when comparing soundscapes between different recordings. These authors call for equalisation of recordings made between different BAR devices during a study or when comparing between studies. This is due to the variability in microphone frequency response, sensitivity and noise floor. The paper also advocates for a standardised calibration of devices as a key initial step [48].

2.1.2 Bioacoustic Recorders (BARs)

Researchers' ability to capture, record and interpret bioacoustic sounds has been intrinsically tied to the sound recording technologies over the last decades. Reportedly, the first sound recording was made by Édouard-Léon Scott de Martinville in 1860 using a phonautograph, with a mechanical needle moving over soot-covered paper to draw a sound waveform [49]. The first documented recording of birdsong, of an Indian Shama bird, was later made with a needle on a wax cylinder in 1889 by Ludwig Koch, who would go on to create the largest private collection of birdsong of its time [50]. Since then, field recordists and enthusiasts, acting in a scientific or citizen science capacity, would go on to record with each successive technology, from vinyl records to magnetic tapes to cassette tapes, with increasing capacity to collect and store more data, as well as a dramatic decrease in the recording device's weight.

More compact and lighter recording equipment allowed transportation to more remote locations for longer deployment periods. The ability to record wildlife sound was dramatically improved again with the advent of digital data storage, with the Hard Disk Drive (HDD) in the 1950s, digital recording, with the CD in the 1980s, and the complementary computer-based sound analysis software in the 1990s with the first sound-acquisition board for Personal Computers (PCs) [49].

Modern BARs are specialised, programmable, self-contained units with bespoke circuitry and a high-capacity Direct Current (DC) power source. Some currently commercially available BARs are listed in fig. 2.2 below.

Model	Manufacturer	Channels	Price (US$)†	Power autonomy (hours)	Weight (g)‡	Dimensions (cm)	Warranty (yr)
Audiomoth	Open Acoustic Devices (open source)	1	50#	187	80	5.8 × 4.8 × 1.5	no
BAR	Frontier Labs	1 or 2	602	222	360	11 × 13 × 7	1
BAR-LT		1 or 2	811		890	11 × 16 × 7	1
SM4	Wildlife Acoustics	2	849	205	1,300	21.8 × 18.6 × 7.8	3
SM3Bat§		2	2,187	161	3,200	32.4 × 20 × 6.5	3
Whitlock and Christie (2016; Solo), Turner et al. (2015; ARUPI), Sethi et al. (2017, 2018), Beason et al. (2018; AURITA)	Raspberry-Pi-based open-source recorders	1 or 2	160–296	variable	~600	20 × 8 × 9.5	no
Swift	Cornell University (non-profit), Ithaca, New York, USA	1	250–300	550	1,088–2,494	20.3 × 12.7 × 10.-2 – 21.6 × 17.1 × -10.2	no¶

Note: A regularly updated version with more details is available from Darras (2019).
† With microphones, converted to US$ on 19 July 2018.
‡ With batteries.
§ recently discontinued.
¶ Technical support exists.
# does not include case.

Figure 2.2: A comparison of the most popular Bioacoustic Recorders, as of 2019. Taken from [51].

2.1.2.1 The Advantages of BARs for Environmental Monitoring

There are a few inherent advantages to recording sound for environmental monitoring. These include:

1. Sound can be collected without the need for a line-of-sight. Therefore, it is particularly effective at night, or in other low-visibility conditions, within a 360-degree radius. This therefore gives BARs a larger detection radius/area and means that they are not as restricted in the taxa they can record as camera traps, which require unobstructed animals of a certain size at close range [47]. BARs are also used for capturing sounds beyond physical barriers, such as dense foliage in forests. That said, these obstacles will absorb and reflect sound to some degree, as discussed in section 2.1.3.3, and so should be accounted for when considering detection radius.

2. Per unit time, sound takes up fewer bytes of space in digital storage terms than video from a camera traps, drones or satellite imagery. And, sound files can be further shrunk with compression algorithms such as Free Lossless Audio Codec (FLAC) and WavPack [52]. As a result of this, sound can be collected semi-continuously for long periods of time, increasing the likelihood of capturing rare and elusive species in remote environments [53] and allowing the tracking of long-term trends, such as the effects of climate change on biodiversity [54].

3. Sound recorders can be left to passively collect on the ground, with minimal disturbance to an environment or its wildlife [6], [54], as opposed to methods like attaching harnesses/collars or setting out traps, thus collecting the true behavioru of animals in the wild.

2.1.2.2 The Disadvantages of BARs for Environmental Monitoring

BAR devices and their electronic components have some notable limitations when using for environmental monitoring:

1. Each BAR device will have a limited radius that it can capture, and thus this method of recording is limited in geographical scale, typically to the hundreds of meters. This detection radius will be further limited by the target species' call amplitude and frequency, as well as obstacles that reflect/absorb sound, discussed in section 2.1.3.3. Thus, for surveying large landscapes, either many devices have to be purchased and deployed in large arrays/transects, or a small subsample of data must be used to extrapolate landscape-level trends [3]. And, since they are static, sites have to be chosen carefully to capture the desired sound. By contrast, GPS collars and drone imagery has successfully been used to track more mobile animals while satellite imagery for vegetation can be conducted at the km scale with meter-level resolution [4].

2. When continuously recording for long periods of time and with multiple devices, researchers can easily to create TBs of data within months or less. This then creates a knock-on storage and processing issue [3].

3. BAR devices still require manual deployment, troubleshooting and maintenance. They also require knowledgable users in throughout the collection to analysis steps [3].

4. There are a multitude of other trade-offs when considering components for a BAR device that can further limit the devices' ability to capture biological information. For instance, settling for a lower sampling rate, microphone Signal-to-Noise Ratio (SNR) or bit-depth to respectively save on power consumption, cost or memory [3]. These trade-offs are further discussed in section 2.2.

2.1.3 Other Considerations

This section considers:

1. Overall design considerations for use in the field.
2. The role of non-experts and citizen science in wildlife monitoring.
3. The physics of sound propagation, as relevant to terrestrial sensor deployment and design.

2.1.3.1 Overall Design

In their 2023 guidelines for researchers, Metcalf et al. describe several challenges that BARs are exposed in the field. These include:

1. The ingress of water from rain and humidity. They suggest all deployed BARs should be fully waterproof, but should also have vents to allow condensation to escape [3].
2. Variable outside temperatures. In the UK, these variations are mild, but they suggest that electronics should still be shielded from direct sunlight with a Ultraviolet (UV) resistant enclosure and/or contain components that are heat and cold resistant for the expected deployment climate. They also note that all battery types decline in performance in sub-zero temperatures, and this should be accounted for in deployment time [3].
3. Getting the audio recorder gain correct to collect the environmental noise without exceeding maximum amplitude in recordings (referred to as "clipping"), taking into account dominant sounds like running water, traffic, etc. They suggest using devices with adjustable gain and test deployments [3].
4. Weight, bulk and portability. As devices are often manually carried to deployment sites, they suggest using devices that can be transported in reasonable numbers by a small group on foot. [3].

5. Animals directly interacting with the device and any exposed components. They suggest using devices with internal or small external microphones and limited other protruding components to avoid damage [3].
6. Extreme sound events, like storms, that drown out other sounds. They suggest using devices that can record for longer periods to compensate for this data loss [3].
7. Theft, particularly in more urban areas. They suggest recorders with dull colours to avoid additional cost in camouflage and security cables where necessary [3].
8. Transporting internationally, due to border restrictions on certain components like Li-ion batteries. They suggest considering power sources based on study requirements and location. [3].
9. Current BAR user interfaces can vary in complexity. They suggest using recorders with simple actions, like an external on/off switch, for users in the field, without the need to open up ethe enclosure outside, where water can get in. They also suggest using devices that can be pre-programmed before deployment to avoid human errors [3].

Thus, any BAR device developed for the field should address these issues listed at the design stage to avoid problems during deployments.

In addition to the above, Darras et al. were able to remove a significant amount of noise from wind buffeting the microphone using simple and cheap furry or foam covers over the top, with a minimal observed change in frequency response of the microphones [55]. So a similar method of shielding should be used when deploying future BAR devices.

2.1.3.2 The Role of Non-experts and Citizen Science

The beginning of section 2.1.2 documents how wildlife sound recording has had a long history of amateur enthusiasts taking part. Even before the use of sound recording technology, one of the first documented citizen science projects in Finland, in 1749, collected data on bird migration from visual and audio observation [56]. Modern bioacoustics and wildlife conservation technology more generally have had many contributions from citizen science groups documented in the literature, both in the collection and analysis of data.

On the analysis side, researchers have been able to make use of platforms like Zooniverse to distribute data for manual analysis by participants, as well as cross-checking for accuracy [57]. This has allowed studies to be undertaken on a much larger scale. For instance, Simpson et al. document that citizen scientists using Zooniverse were able to successfully identify 18,000 wildebeest in images from camera traps in the Serengeti [57].

On the data collection side, in a study comparing citizen science recordings of nightingale birds to experts, Jäckel et al. found that citizen scientists were able to produce a significant number of recordings of valid quality for bioacoustic research. They found that the major differences in the recording quality between the citizen and expert groups were principally correlated to the technical quality of the devices used [58]. Thus, the technical aspects of a device built for non-experts should be well considered, tested and standardised to make full use of this community and allow for monitoring at a larger scale.

2.1.3.3 Sound Physics Considerations

Several considerations for how sound travels need to be made when deploying and analysing data from BAR devices.

2.1.3.3.1 Animal Vocalisation and Hearing Frequencies

Animals vocalise across a broad range of the frequency spectrum, from the low infrasound (0.1 Hz to 20 Hz) through the audible range (20 Hz to 20 kHz) and well into ultrasound (20 kHz to >200 kHz). The frequency ranges "infrasound", "audible" and "ultrasound" are based on the observed limits of human hearing [59]. On land, species of elephant, crocodiles and Cassowary birds have been observed to communicate using infrasound [60]–[62]. These vocalisations have their dominant, fundamental frequency below 20 Hz, but often contain harmonics that extend into the audible range [63]. A significantly larger proportion of species of amphibians, birds, reptiles, mammals and insects have been observed communicating within the human-audible range [64], several of which are shown in fig. 2.3A. For ultrasound, researchers have documented species of bats, stridulating insects and rodents communicating at these frequencies [65]–[70]. Ultrasound is also significantly used for echolocation by bats and several cave-dwelling birds species for navigation and foraging [67], [71].

An animals ability to produce sound within a particular frequency range is based on the physical properties of the animals' sound-producing-organ, such as the linear dimensions, density and elasticity of the organ material [63]. Methods of sound productions vary as well. Air-breathing animals using pulsating air pressure in the lungs to vibrate vocal chords in a larynx (mammals, reptiles and amphibians) or syrinx (birds). These air pressure waves then pass through the upper vocal tract and radiate from the mouth before travelling through the environment [72], [73]. Several authors have observed how vocal range in these animals typically correlates with animal body size/mass and hence the linear dimensions of its sound-producing-organ [28], [73]. For air-breathing animals, Fletcher calculates a general power rule to obtain the optimal frequency for maximising communication between individuals, equalling $mass^{-0.4}$ (see Figure 2.3A), with communication distance equal to $mass^{0.6}$ [73]. Insects have alternative methods of sound production for communication, which involve exciting/vibrating various specialised parts of their anatomy. For instance, crickets and grasshoppers will draw a wing or another thin panel across ridges on

the back of their legs to create sound, referred to as stridulation. Other insects, such a cicadas, use a different, specialised organs to produced sound, though operate on a similar principal of rubbing a ridged surface to cause vibration. According to Fletcher, The result is that the sounds of crickets, grasshoppers and cicadas typically occur between 2 kHz to 5 kHz, with the general rule of song frequency being inversely related to linear size, and a within-species communication distance equal to $mass^{0.5}$ [73].

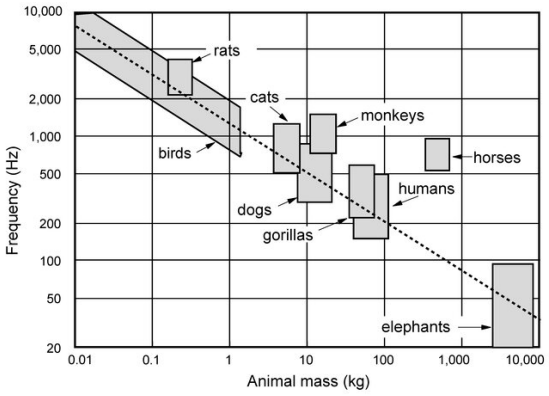

(A) The dominant vocalising frequency range of birds and mammals as a function of body mass. Taken from [73].

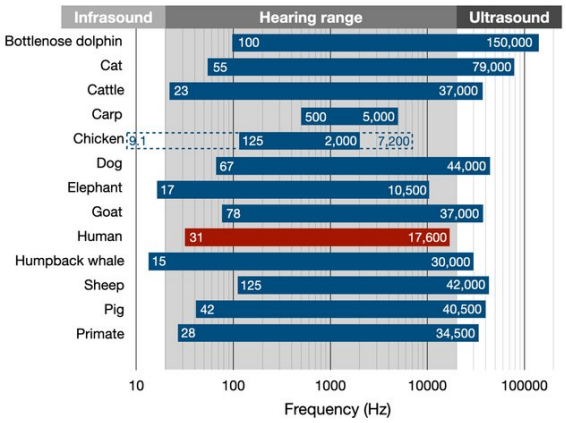

(B) The observed ranges of animal and human hearing, with boundaries for ultrasound and infrasound. Taken from [74].

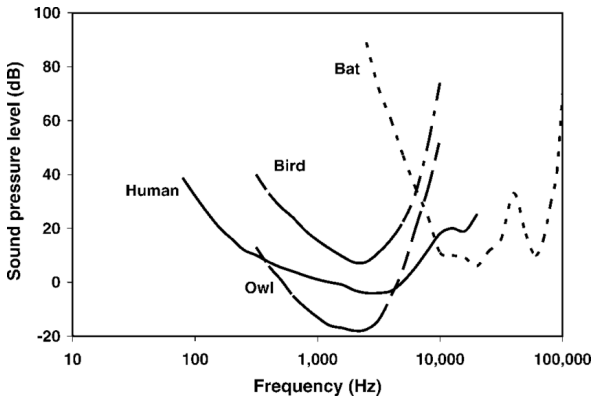

(C) An audiogram showing the average frequency response of the human ear against other animals. Taken from [75].

Figure 2.3: The varying frequency ranges of animal vocalisation and hearing. For **A** (vocalising ranges), Fletcher calculated a regression line of $mass^{-0.4}$ (shown as a dotted line on the chart) as a general power law that dictates the optimal vocalisation frequency for these animals to achieve maximum communication range. For **B** (hearing ranges), Human hearing is shown as the red bar, with hearing ranges established at a volume of 60 dB, coalescing findings from previous studies. The chicken's hearing range was also extended (shown as a blue dotted line) due to more recent findings suggesting greater hearing range. Details for the each specific animal measurement can be found in Figure 2 of [74]. For **C** (frequency response), audiograms for taxa groups are composite averages taken from previous publications. Details for how these were calculated can be found in Figure 2 of [75].

Similar to vocalisation, an animal's sensitivity to hearing certain frequencies is due to the physical properties of the co-evolved sound-sensing-organ and the frequency response of the attached nerve fibre [63]. For many species, hearing sensitivity is highest at the most commonly used frequencies for within-species communication. For instance, humans have the highest sensitivity between 2 kHz to 5 kHz, where most conversational sounds occur [59]. However, there are many examples of animals hearing sounds well outside their vocal range. Several species of birds, like the common pidgeon, have demonstrated behavioural responses to infrasound, which may indicate approaching storms or changing air currents in the wild [76]. Furthermore, moths and other flying insects have been shown to respond to ultrasound produced by predatory bats [77]. Figure fig. 2.3B and fig. 2.3C shows the hearing range and sensitivity to certain frequencies of humans and several animal groups.

Given this wide range of sounds produced and received in the animal kingdom, there is intrinsic scientific value in capturing sounds from the low infrasound to the high ultrasound on a BAR device, particularly in cases where it is advantageous to fully survey biodiversity. Capturing the "full soundscape" requires considering values for electronic components such as the microphone frequency response across low and high frequencies and the maximum ADC sampling rate (discussed further in section 2.2.5 and section 2.2.6).

2.1.3.3.2 Sound Pressure Waves and the Effect of the Environment

Sound consists of oscillating pressure waves travelling through physical matter. As these waves are passed by colliding molecules, the speed of sound is dependent on both the matter being travelled through, any water content or dissolved solids, the matter density, and temperature. Sound travels faster in materials with a higher bulk modulus (or stiffness), such as solid rock, relative to lower bulk modulus materials, like liquids or gases. In atmospheric air, the speed of sound is $\approx 331\,\mathrm{m\,s^{-1}}$ at 0°C and 1 atm [78], in pure water, it's $\approx 1404\,\mathrm{m\,s^{-1}}$ at 0°C [79], when travelling through loose soil, it ranges from $86\,\mathrm{m\,s^{-1}}$ to $260\,\mathrm{m\,s^{-1}}$ dependent on porosity, soil moisture, and compaction [80]. The principal focus of this section will be on sound travelling

through air. For a simplified bioacoustic sound event, sound waves can be said to radiate from a point source and propagate as a spherical wavefront that attenuates over distance [78]. This follows the Inverse-Squared (I^2) law, which can be expressed as:

The I^2 Law and Proportional Law for Sound Propagation

$$I = \frac{P}{4\pi r^2} \qquad (2.1.2a) \qquad\qquad I \propto \frac{1}{r^2} \qquad (2.1.2b)$$

Where I represents the sound intensity at a receiving sensor (in $\mathrm{W\,m^{-2}}$), P is the power of the sound source (in W) and r is the radial/Euclidean distance from the sound source (in m). The left-hand side shows the direct use of the I^2 law, while the right-hand side shows the proportional relationship.

In an ideal scenario, for a given value of power in eq. (2.1.2), it can be said that sound reduces in amplitude/power, or "attenuates", to one-quarter of the energy, as the distance r is doubled. This is equivalent to a reduction by $-6\,\mathrm{dB}$, referencing $20\,\mu\mathrm{Pa}$. It should be noted, however, that both animal ears and microphones are sensitive to a proportionally related physical property, "sound pressure" (the local pressure deviation caused by a sound wave, in $\mathrm{W\,m^{-2}}$), not the "sound intensity" (the total perpendicular sound power carried, per unit area, per unit time) [81].

There is also a greater level of sound pressure attenuation with increasing frequency due to the viscous forces of air molecules. Air absorption is most significant at high frequencies and at long distances, in effect, acting as a low-pass filter. The effect of distance can be rewritten as:

The Relationship Between the Sound Attenuation Coefficient and Distance

$$P = P_0 e^{\frac{\alpha x}{2}} \qquad (2.1.3)$$

Where P represents the sound pressure of a planar sound wave at a distance x, P_0 represents the starting sound pressure and α represents the attenuation coefficient

The relationship between air absorption and frequency, temperature, and pressure,

however, is more complicated. In this case, the "relaxation frequencies" of nitrogen and oxygen molecules present in the atmosphere have to be considered:

The Relationship Between the Atmospheric Sound Attenuation, Frequency, Temperature and Pressure

$$\alpha = f^2 \left[\left(\frac{1.84 \times 10^{-11}}{\left(\frac{T_0}{T}\right)^{\frac{1}{2}} \frac{p_s}{p_0}} \right) + \left(\frac{T_0}{T}\right)^{2.5} \times \left(\frac{0.10680 e^{\frac{-3352}{T}} f_{r,N}}{f^2 + {f_{r,N}}^2} + \frac{0.01278 e^{\frac{2239.1}{T}} f_{r,N}}{f^2 + {f_{r,O}}^2} \right) \right] \quad (2.1.4)$$

Where f is the sound frequency, T is the absolute temperature (in kelvin), T_0 is the reference temperature value of 293.15 K, p_s is atmospheric pressure, p_0 is the reference pressure of 101 325 Pa), while $f_{r,N}$ and $f_{r,O}$ are the respective relaxation frequencies of nitrogen and oxygen molecules. The mathematical relationship of these relaxation frequencies with humidity and air pressure is provided in page 5 of Kapoor et al. [82].

This gives the following log plot of sound attenuation:

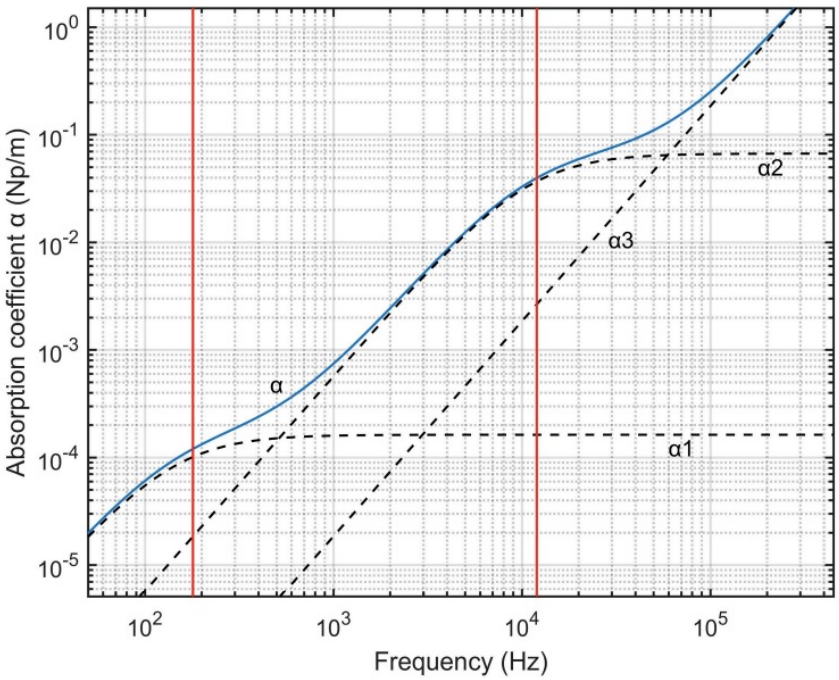

Figure 2.4: Sound attenuation with frequency and other atmospheric factors, taken from [82]. $\alpha 1$ (dashed line) plots the frequency-dependant attenuation dictated by the vibrational relaxation of atmospheric nitrogen. $\alpha 2$ (dashed line) plots the frequency-dependant attenuation dictated by the vibrational relaxation of atmospheric oxygen. $\alpha 3$ (dashed line) plots the frequency-dependant attenuation associated with the air's intrinsic bulk viscosity (due to molecular rotation) that dominates at higher-frequencies. α (blue line) plots the overall, observed absorption coefficient, combining the effects of $\alpha 1$, $\alpha 2$ and $\alpha 3$. The red lines divide the range of frequencies where attenuation is dominated by $\alpha 1$, $\alpha 2$ and $\alpha 3$ respectively, from left to right. Values are for frequency attenuation under standard atmospheric conditions 293.15 K, 1 atm and 20% relative humidity. Absorption coefficients along the y axis are measured in units of nepers per metre ($\mathrm{Np\,m^{-1}}$) and can be converted to decibels per metre by dividing by 0.1151.

Equation (2.1.4) and fig. 2.4 shows that the general trend in attenuation rate is proportional to the frequency squared, but with divergences in slope, principally due to the relaxation frequencies of nitrogen and oxygen.

To further complicate matters, sound interactions with objects between the source and receiver also have an effect, and these too can be frequency dependent. These

interactions include absorption, reflection/scattering, and refraction. For instance, high-frequency sounds, with short wavelengths, will reflect strongly from small objects, hence the use of ultrasound in echolocation by bats [82].

As higher frequencies attenuate faster over distance, this means deployments of BARs recording species with ultrasonic vocalisations will need to be closer to areas of activity. For instance, studies recording bats need to be well within the flight and feeding paths of these animals [26]. Furthermore, this difference in frequency attenuation should be taken into consideration when deploying grid arrays of BARs to determine the location and migration of animals passing through [6]. Section 2.2.5 discusses how the properties of the microphones can further influence the effective range of BARs.

Additional factors like environmental noise, absorptive/reflective surfaces, barriers and refraction can also alter the way sound intensity attenuates with distance. For instance, large water bodies tend to reflect sounds upwards, while large obstacles like foliage and boulders tend to leave acoustic shadows [83].

In terms of what precautions can be taken to overcome these challenges:

1. Attempts by researchers to calculate detection distances, localise sound with a grid array of devices, and other analyses requiring the speed of sound or spatial distribution of sound should take into account the above confounding factors and equations. Accurate measurement in air would require logging temperature, humidity, and air pressure and potential absorbent/reflective materials.
2. As a general practice, avoid placing recorders above large bodies of water or other large reflective surfaces without sufficient surrounding soft material/vegetation to absorb the reflected sound.
3. Undesirable background noise, like flowing water and human activity, can be mitigated by using natural barriers like soft vegetation in between and by facing the microphone away from these undesired sources and closer to desired sounds.

4. For species of animal calling at higher frequencies, recorders need to be placed closer to mitigate the higher level of attenuation. For example, when recording bats

5. When placing BARs in arrays, or in close proximity to each other, Metcalf et al. recommend spacing devices at least 250 m apart to avoid spatial "pseudo-replication" - two devices recording the same sound and these sounds being mislabelled as separate occurrences [3].

2.2 Sound Recording Technologies

The design and development of BARs encompass a range of electronic components and theory. Modern Bioacoustic Recorders (BARs) are typically battery-powered, microprocessor-based, and autonomous [84]–[89]. In the past decade, there have been significant advances in each of the underlying technologies used in BARs, which have allowed for greater performance, efficiency, functionality and falling costs [90].

The following sections break down the advances in BAR constituent components into:

1. **Microcontroller Units (MCUs)**. Discussing functionality, architecture and firmware.
2. **Single Board Computers (SBCs)**. Discussing common use and tradeoffs.
3. **The AudioMoth Developer board**. Introducing the SBC and the underlying circuitry.
4. **Power supply and management**. Discussing power regulation, device efficiency and battery power.
5. **Microphones**. Discussing impedance and the different types of microphones.
6. **On-device signal processing steps**. Discussing adjustable gain, ADC, sample rate and quantisation

7. **Sound data storage**. Discussing on-device SD card flash storage.

When developing electronic sensors for environmental research, Chan et al. recommend that hardware is considered in the context of the full deployment-to-analysis pipeline [91]. In the case of this project's device, this means considering aspects such as:

1. The device size and weight, for transportability.
2. The ease of use and maintenance by the intended user. With a simple interface, deployment process and data collection/management process.
3. The overall power capacity and efficiency. So that the required deployment time can be fulfilled.
4. The long-term durability of memory components through multiple read-write cycles, protecting against data loss and corruption.
5. The modularity and capacity to swap or add additional components for maintenance and improving functionality over time.
6. The robustness of component parts to extremes in outdoor environments. Particularly for exposed electronic components and when choosing enclosures.

2.2.1 Microcontroller Units (MCUs)

Microcontroller Units (MCUs) are compact Integrated Circuits (ICs) designed to govern specific operations within an embedded system. They act as a small computer within a single Metal-Oxide-Semiconductor (MOS) chip and with multiple other internal "peripherals" that serve particular functions. A typical MCU integrates one or more Central Processing Units (CPUs), memory, and programmable I/O ports, facilitating the execution of a wide range of operations. In addition, they can include program memory as ferroelectric RAM, NOR flash or One-Time-Programmable Read-Only Memory (OTP ROM), with a small amount of RAM [92].

MCUs are commonly used for reading and processing analogue sensor signals, such as a microphone in a BAR device, and implementing control laws on other components in an embedded system. As they handle data in a digital format, analogue signals must first be converted by an internal ADC peripheral to be processed, and any signal out intended to be analogue must pass through an internal Digital to Analogue Conversion (DAC) peripheral to be transformed [93].

The core components of a MCU consist of inputs, storage, processing control logic, and outputs [94]. These elements work in tandem to achieve the desired functionalities in embedded applications. Internal communication between these component parts of an MCU are achieved with data and address busses. I/O ports enable MCUs to communicate with external peripheral components and manage embedded systems [95].

RAM is another important consideration, especially in applications involving the continuous processing of large amounts of data. Most MCUs have built-in RAM for short-term data caching. However, in cases where data manipulation and signal processing are more complex, larger temporary storage may be required [96]. In BAR devices, where real-time filtering of audio can be necessary, a larger Static Random Access Memory (SRAM) chip may be integrated to serve as an additional buffer. This additional caching mechanism allows for more refined data processing before the sound files are stored to flash memory [97].

MCUs represent a class of Very Large Scale Integrated circuit (VLSI) circuits that have seen substantial advancements due to the continuous improvement of logic IC technology. Two technologies/logics that can be used to create logic ICs are Transistor-Transistor Logic (TTL) circuits and Complementary Metal-Oxide Semiconductor (CMOS) circuits. The use of one technology over the other is based on the required voltage, power constraints, noise tolerance and speed [98]. For example, CMOS circuits typically consume less power than TTL, but TTL circuits are more suited to higher speeds. That said, CMOS circuits are more commonly used for MCUs and have mostly superseded TTL. This is due to the power savings and the

smaller footprint, as modern CMOS circuits can now be manufactured at less than 22 nm for processors and internal flash memory like RAM [99]. Figure 2.5 shows the CMOS NAND gate, which forms the foundational component of CMOS logic. CMOS NAND gates are functionally complete, allowing them to be combined to construct other common logical gates such as AND and OR. They are also more efficient than NOR gates, as they connect the slower charge mobility p-MOSFETs (Q1 and Q2 in fig. 2.5B) in parallel rather than in series [98].

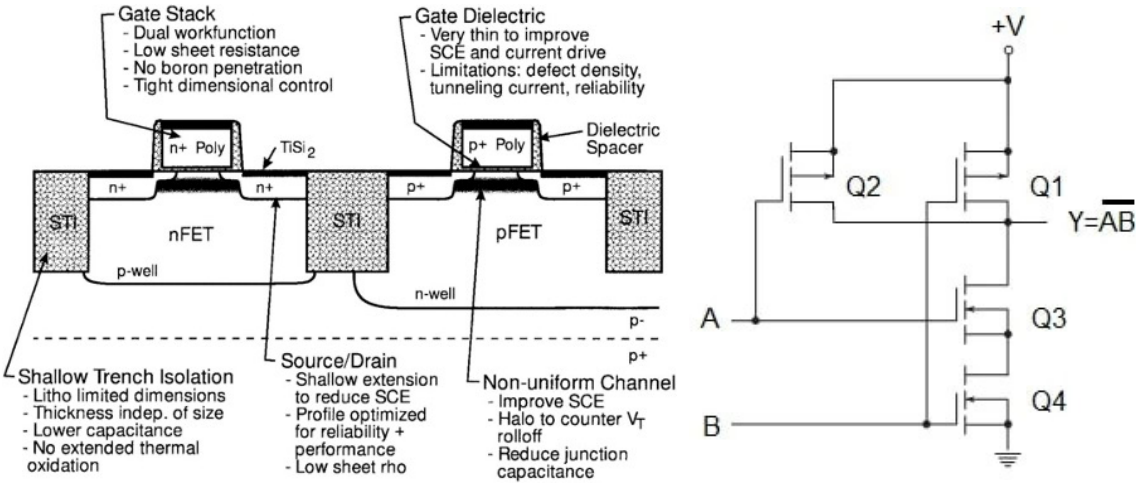

(A) A cross-section of a CMOS, with key features labelled.

(B) The circuit schematic of a CMOS NAND Gate.

Figure 2.5: Schematics of a CMOS NAND gate, the technology and logic underpinning CMOS logic in modern MCUs. Taken from [98].

Recent advancements in CMOS technology can be attributed to breakthroughs in semiconductor manufacturing techniques, such as in UV lithography, which has enabled the scaling down of CMOS transistors to nanometre dimensions [100]. The miniaturisation of CMOS transistors has allowed for the integration of a greater number of transistors per unit area, and consequently more complex logic gates, onto a single chip die. This reduction in CMOS transistor size has also enabled greater power efficiency, since smaller transistors reduce the parasitic capacitance when switching and so reduce the dynamic power consumption of the circuit as a whole [101]. This relationship can be expressed as:

The Dynamic Power Consumption of a CMOS Transistor

$$P_{dynamic} = C_L {V_{DD}}^2 f \tag{2.2.1}$$

Where C_L is the load capacitance, V_{DD} is the supply voltage, and f is the switching frequency. Taken from [102].

The two values that determine the power consumption in a CMOS circuit are the static power consumption and the dynamic power consumption. Static power consumption in CMOS transistors is very low and is the result of leakage current when the inputs are held at one logic level and not in charging states. Dynamic power consumption increases with high-frequency switching of transistors and forms the most significant contribution to overall power consumption. The charging and draining of a capacitive output load also significantly adds to dynamic power consumption [102]. Therefore, gains in efficiency of dynamic power through the miniaturisation of CMOS circuits have had a profound impact on the power consumption of MCUs.

In addition, improvements in MCU architectures have enhanced data processing capabilities while maintaining power efficiency. Modern MCUs implement advanced power management techniques, such as Dynamic Voltage and Frequency Scaling (DVFS), which adjusts V_{DD} and f dynamically based on the computational workload, further optimising energy usage [103]. The incorporation of Advanced RISC Machine (ARM) architectures into MCU design has further improved their power efficiency. ARM's Reduced Instruction Set Computer (RISC) architecture allows for simpler instruction execution, allowing MCUs to perform tasks more efficiently with fewer transistors compared to traditional Complex Instruction Set Computing (CISC) architectures. ARM-based MCUs also make use of DVFS as well as various power-saving modes, such as sleep and deep sleep states, which reduce quiescent power consumption when full processing power is not required [104].

These technological advancements have facilitated the deployment of more sophisticated and energy-efficient devices that can operate for extended periods on minimal power, enabling long-term data collection in remote or resource-constrained environ-

ments. In remotely deployed sensors, like BAR devices, the MCU handles power distribution, controls communication with other Printed Circuit Board (PCB) components, sets the clock frequency, schedules recordings, and handles sleep modes. Additionally, the MCU handles signal processing tasks (discussed in section 2.2.6) and the transmission of data to longer-term flash storage mediums like SD cards (discussed in section 2.2.7) [105]. Further power efficiency in MCUs is achieved by writing firmware to minimise consumption and strategically regulating the power supply of device modules, such as deactivating the ADC and other modules when not in use [106]. For instance, fig. 2.6 shows a block diagram of the EFM32WG "Gecko" series MCU from Silicon Labs, with colours indicating the internal blocks/modules that can be turned on and off in accordance with different power needs during audio sampling or when idle.

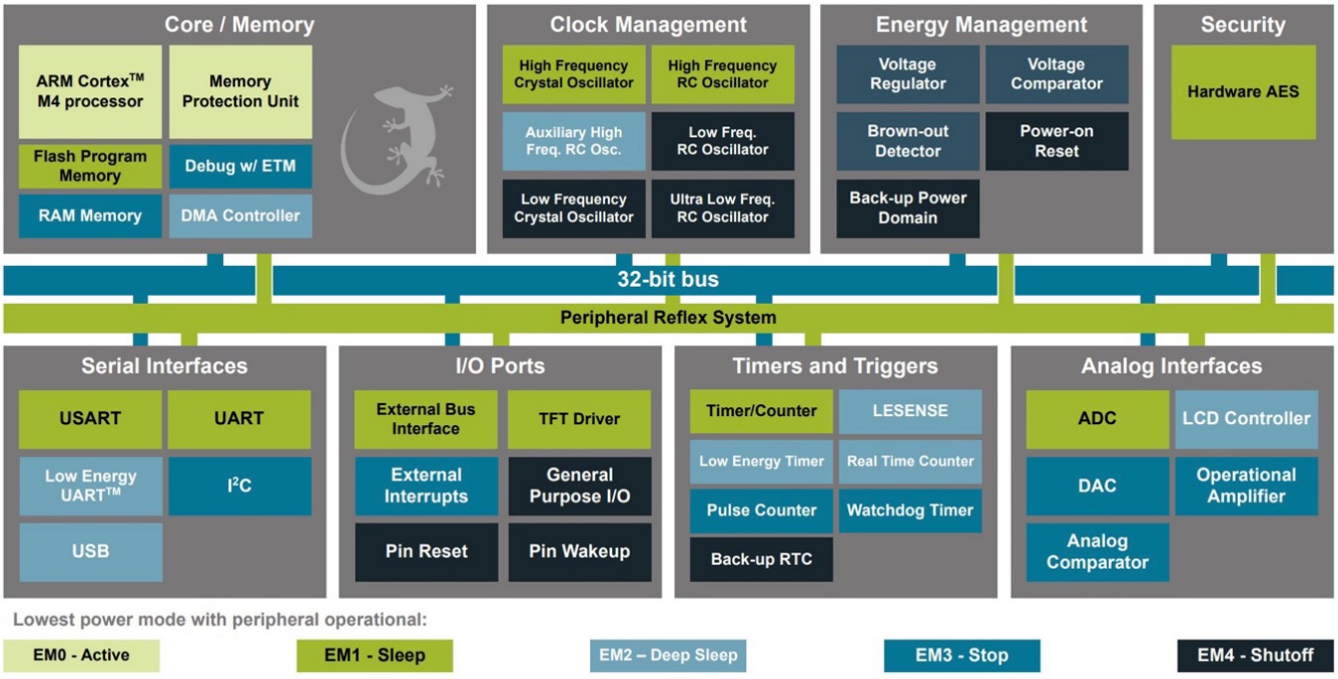

Figure 2.6: A MCU Block Diagram, for the EFM32WG "Gecko" series MCU. Taken from [107]. The colours of the boxes represent different power modes where these blocks can be operations, shown as EM0 - EM4 in the bar at the bottom. Light green represents the greatest power consumption peripherals, while dark blue represents the lowest power consumption peripherals.

2.2.2 Single Board Computers (SBCs)

Low-cost, Single Board Computers (SBCs) have played a growing role in modern remote monitoring projects for wildlife and conservation [4]. For instance, the rising popularity of the Raspberry Pi [108], [109] and Arduino [110] platforms have formed the basis of many of these amateur electronics. As a specific example, the SOLO device uses the Raspberry Pi A+ board as the foundation for its Bioacoustic Recorder [109]. The downside to using these platforms is that there are redundant firmware and hardware built in, outside the need of a BAR device. The redundant firmware occupies space in the external flash storage, or in the MCU's Read-Only Memory (ROM)/Electrically Erasable Programmable Read-Only Memory (EEPROM). The redundant firmware and hardware can also unnecessarily drain power when recording and idle. For instance, the Linux-based Raspbian Operating System (OS) occupies 8GB on the external microSD card, and additional installed software can run regular "daemon" calls to wake up the processor or subsystems unnecessarily when idle [108].

Some gains can be made by reducing power consumption programmatically by switching off these calls to the processor, as well as the USB controller, the High-Definition Multimedia Interface (HDMI) controller, Light-Emitting Diodes (LEDs), Wi-Fi/Bluetooth and using a higher-level and "Turing Complete" compiled language like C [108]. Even so, there remain intractable inefficiencies. Having said that, the Raspberry Pi and Arduino provide a useful point of reference when building a BAR device. Furthermore, the demand for these and the numerous of BAR devices built with these SBCs to date, shows the need in the scientific and citizen science communities for user-friendly, extensible, and low-cost solutions that can meet the specific functional needs of a study/site and the available budget.

More bespoke commercial SBCs have their advantages in terms of being able to make a more efficient device and power only what's strictly necessary. Thus, commercial makers of BARs devices have previously developed their own custom hardware and analysis software, and sold at a high price point. For instance, Frontier Lab's BAR

LT is costed at £463.95 per device [111], which is within budget for small-scale scientific studies, but can be out of reach for wildlife conservation Non-Governmental Organisations (NGOs) or citizen science projects when looking to deploy in greater numbers.

In summary, when choosing an SBC platform for a BAR device, there are a series of trade-offs to be made in terms of power efficiency, cost, extensibility, and user-friendliness for those lacking electronic expertise. The challenge for this project was to identify a SBC platform to best meet these requirements and build on these.

2.2.3 The AudioMoth Developer SBC

After investigation and consideration of the factors discussed before and after this section in this literature review, it was decided that the AudioMoth SBC represented the best platform on which to build the Biophone BAR device of this project.

This was principally for the following reasons:

1. The power efficiency, particularly its low-power ARM Cortex-M4F-based MCU. As the MCU processing and base power consumption can represent a significant part of the overall power consumption of a BAR device when recording and idle, this was a key consideration [112]. In addition, the lack of unessential aspects included in the Raspberry Pi and Arduino firmware/hardware, discussed in section 2.2.2, was appealing. Reducing these power-consuming elements would enable devices to be deployed in the field for longer periods and collect more data.

2. The high raw sampling rate and flat frequency response of the microphone across the audible and ultrasound range. This allowed for the potential collection of ultrasonic calls from bats, insects and small mammals [112].

3. The bespoke, but extendable design. With options for connecting additional peripheral electronic components, as well as options for modifying its underly-

ing open-source circuitry design, firmware and configuration software [113].

4. The relatively low cost of £71.74 GBP per SBC [114]. This represented a significant difference from comparable commercial options at the beginning of this project, like Frontier Lab's BAR LT at £463.95 GBP [111] or Wildlife Acoustics' Song Meter Micro at £400.81 GBP [115]. All reported prices were taken in taken from the manufacturer's website in February 2022 and converted from United States Dollar (USD) or Australian Dollar (AUD) using the Google Finance conversion tool [116], [117].

The AudioMoth SBC was developed by Open Acoustic Devices (OAD) in 2017, with the first iteration being fully open-source. The device is programmable, allowing users to customise recording settings and schedule recordings for specific time intervals and audio frequencies with a simple desktop application. Users can adjust recording parameters such as sample rate, gain, and trigger conditions, providing flexibility for different recording scenarios [112].

The hardware of the AudioMoth consists of:

1. An EFM32 Gecko processor, MCU.
2. A low-power, omnidirectional Micro-Electromechanical Systems (MEMS) microphone.
3. A micro SD card slot for the storage of audio data.
4. A micro Universal Serial Bus (USB) port for configuration and flashing new firmware.

The MEMS microphone used in the AudioMoth Developer board is omnidirectional, with a sensitivity of $-38\,\mathrm{dB\,V\,Pa^{-1}}$, 63 dBA Signal-to-Noise Ratio (SNR), and a dynamic range of 10 Hz to 192 kHz [113].

In terms of power management, the AudioMoth is designed to operate on low power to enable extended monitoring periods. The EFM32WG380F256-QFP100 MCU has low-power sleep modes to conserve energy when not actively recording, shown in

fig. 2.6. The device can be powered by standard AA batteries or external power sources, allowing for flexibility in field deployments [112].

The basic AudioMoth SBC version has been widely used in various ecological studies and citizen-science wildlife monitoring projects, with >30,000 units sold in the first four years after its release [118]. The studies investigated in this literature review all used the basic version of the AudioMoths. This version comes with a battery holder for three AA alkaline batteries attached and Surface-Mount Technology (SMT) solder-able points to attach an external microphone, externals switches, external power sources and for General Purpose Input/Output (GPIO) communication. In the studies investigated, these SBCs were housed in a bespoke Ingress Protection Rating 7 (IPX7) polycarbonate injection-moulded case [119]–[121], sold separately by OAD [122], a ziplock sandwich bag [119], [123], [124], or a simple custom casing, such as a modified lunch box [125] or gutter pipe [85]. One of the larger studies investigated involving the use of these SBCs was the "The Soundscapes to Landscapes Project", documented by Snyder et al. This study used 259 volunteer citizen scientists to deploy, collect, curate and analyse audio data recorded with AudioMoth SBCs over 5 years [126]. Over this time, the group deployed the devices at 281 sites, collected 12,431 hours of audio and labelled 230,066 audio clips with identified breeding bird species [126]. The authors noted their study's need to limit continuous recording, opting for a one-in-every-ten-minutes recording schedule, due to the limited battery life of the default three alkaline batteries [126]. Another academic study by Barber-Meyer et al. used a transect of AudioMoth recorders to monitor wolf detection distance in the Superior National Forest, Minnesota, recording continuously for ≈25 days [119]. The Authors placed AudioMoths at set intervals from a captive wolf pack, and found that on-site AudioMoth captures 100% of both "solo" and "chorus" howls, while the next closest device (at ≈500 m) captured significantly less, only 37% of chorus howls and 8.9% of solo howls [119]. Based on these findings, the authors concluded that the future use of AudioMoths would be useful in a large passive sampling arrays for occupancy studies and for tracking populations during seasons when the target animal stick to a limited range. In the case of wolves, this

would be home sites in late spring and summer or winter kill sites. The authors also noted the logistical challenge of having to replace the batteries every 14 days for continuous recording, especially when deploying at remote locations with multiple devices. They suggest that a larger external battery attached to extend battery life "could significantly alter the ease of remote field deployments of multiple units".

Instead of the basic AudioMoth board used in previous studies, this project set out to build upon the AudioMoth Developer version of the board. This version has the components discussed above, but differs from the basic version by having pluggable Japan Solderless Terminal (JST) ports for connecting external components to. These include ports for as alternative power supplies, an external on/off switch, LED output, GPIO ports and an external microphone mini-jack port already affixed. Using the Developer SBC therefore allowed for the straightforward connection and testing of a larger battery supply, a higher quality external microphone, and an external switch/LED. Thus, this project set out to investigate of the usefulness of this extended functionality in a BAR device for ecologists/citizen scientists and the impact these peripheral electronic components would have on the performance of the device, discussed further in section 2.3. Figure 2.7 to fig. 2.9 show the AudioMoth Developer SBC viewed from above and schematics of the audio and power circuitry, which are discussed in greater depth in the next sections of this literature review.

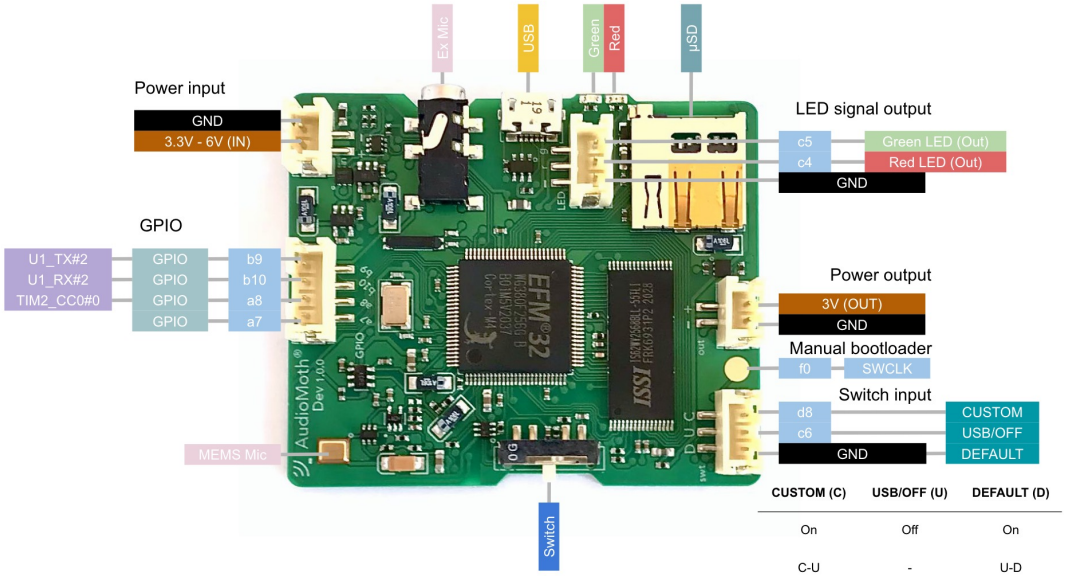

Figure 2.7: The AudioMoth Dev SBC, view from above, taken from [113].

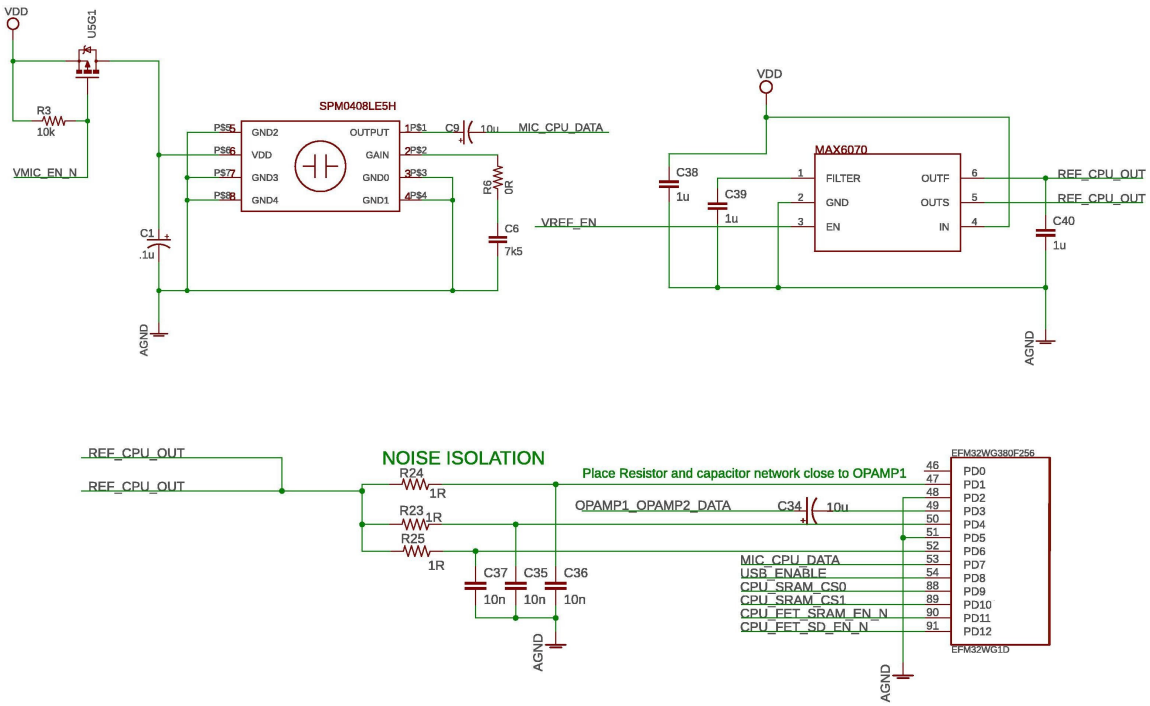

(a) Audio circuitry schematics

(a) Audio circuitry schematics

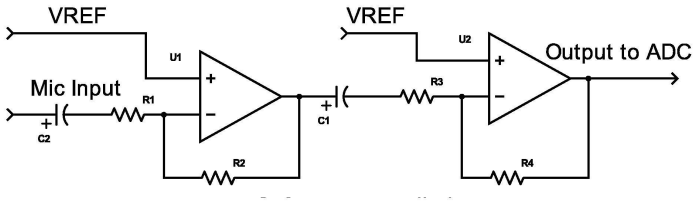

(b) Microphone cascaded inverting operational amplifier

Figure 2.8: The AudioMoth's audio circuitry. Taken from [85]. Key labelled components for **(a)** include:

1. *SPM0408LE5H*: The MEMS microphone. This is turned on via a switch (*U5D1*), triggered by the MCU (*VMIC_EN_N* line). The microphone's analogue output is labelled as *MIC_CPU_DATA*.
2. *MAX6070*: A low noise, low-drift voltage reference IC, used in the MCU-based Operational Amplifier (Op-Amp) Pre Amplifier (Preamp) circuit (shown in (b)) via the *REF_CPU_OUT* line.
3. *EFM32WG380F256*: The MCU, where Preamp and Analogue to Digital Conversion (ADC) take place. Once converted, the 12-bit digital data is temporarily stored to a buffer located in the external SRAM chip (*SRAM* lines), minimising the use of the energy-demanding MCU processor. Once the SRAM buffer is full, the processor is switched on and audio samples are saved to the micro SD card via a Serial Peripheral Interface (SPI) bus (not shown).

(b) shows the AudioMoth microphone-to-ADC Preamp configuration. A cascaded Op-Amp configuration is used to invert, amplify and buffer the signal. This Op-Amp configuration is internal to the MCU, making use of the on-board Op-Amp circuitry in the analogue peripheral pre-amp block. The level of gain is firmware-controlled via the *OPAMP1_OPAMP2_DATA line* in (a), connecting to pin 40 of the MCU (not shown).

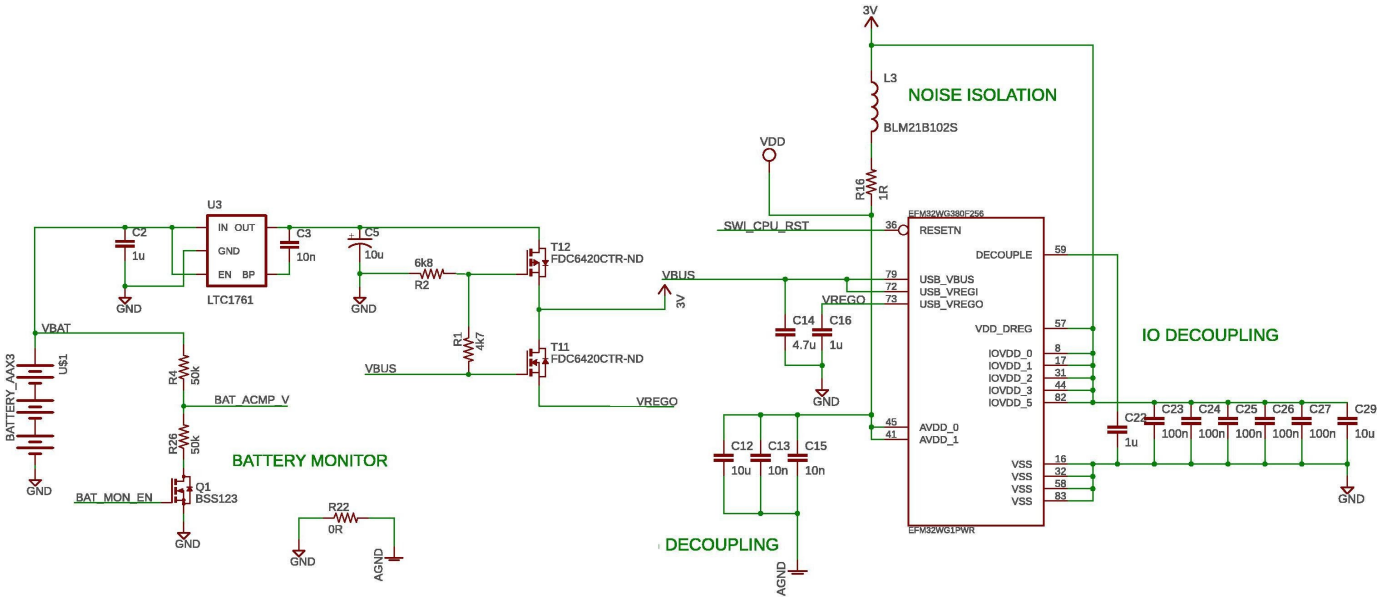

Figure 2.9: The AudioMoth's power management circuitry. Taken from [85]. Key labelled components include:

1. *BATTERY_AAX3*: This represents the 3 AA batteries used in the basic version of the AudioMoth SBC.
2. *LTC1761*: The power supply voltage regulator which converts the DC supply from the batteries to a stable 3.3 V. Alternatively, a 5 V USB power supply (*VBUS*) can be used, connecting instead to the MCU's internal voltage regulator (*VREGO*). The Battery's voltage is also regularly measured by the MCU, using the *BAT_MON_EN* line to trigger current to flow via *BAT_ACMP_V*. These lines connect to the MCU pins 21 and 18 respectively (not shown). Ground and artificial ground, used by the audio circuitry, are connected via a 0Ω resistor.
3. *EFM32WG380F256*: The MCU, where power is decoupled with an array of capacitors for the MCU's own use (*IO DECOUPLING*). This *IO DECOUPLING* is to facilitate rapid spikes in power, such as periods of heavy computational load in the processor block. Furthermore the MCU redistributes the 3.3 V power to the other components of the SBC (as *VDD*), such as the microphone.

2.2.4 Power Consumption and Power Electronics

Deployment time is a key aspect for a BAR device. While longer deployments for more power-hungry devices are possible by multiple rotating and recharging cycles, reducing the frequency of rotations cuts down on man-hours, travel time, and the cost of a monitoring operation.

Maximising deployment time requires considering the DC power supply, power management circuitry and the overall efficiency of a device. In the literature, SBC MCUs used for BAR devices operate in the range of 3 to 5 volts, consuming tens of milliamps whilst recording, and so consuming several hundred milli-watts. For instance, the SOLO device, based on the Raspberry Pi A+ board, consumes 350 mW while recording at 48 kHz [109]. Because of the limited sleep capacity on the Raspberry Pi MCU, the SOLO device continuously runs a Linux OS during operation, even while idle [109]. The 2018 paper by Hill et al. observed that the many of the available Raspberry Pi-based devices and commercially available BARs devices consumed between 400 mW to 1000 mW when idle; making this a major contributor to overall power consumption in between scheduled recordings [112]. By contrast, Hill et al. state that the AudioMoth consumes approximately 30 µA while sleeping and consumes 10 mA 40 mA when recording to a SanDisk Extreme 32 GB microSD card [85].

For today's available BAR devices, both commercially and in the academic literature, some of the reported largest power consumption steps include start-up processes, writing data to the SD card flash memory and onboard signal processing. [87], [109], [112]. Figure 2.10 Shows commercial devices, Raspberry Pis and the AudioMoth when recording at 48 kHz.

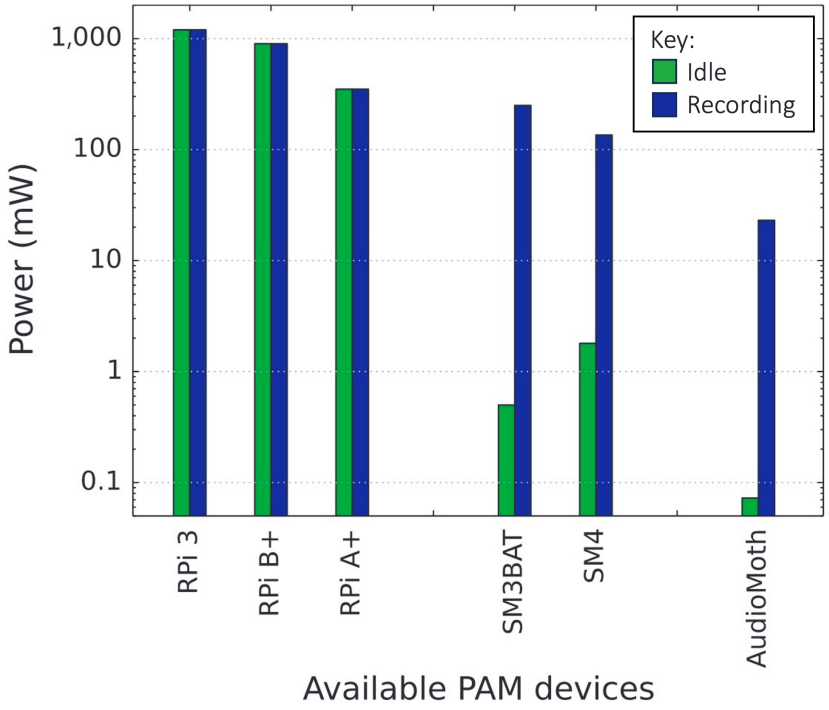

Figure 2.10: Power consumption comparison of the BARS when recording and idle. Taken from [112]

DC power supply for most BAR devices comes from batteries, with possibly some trickle charge from solar, due to the need for an independent power supply when deploying in remote locations [87], [112], [127]. Since a battery's capacity, voltage and chemistry can vary significantly, and since the discharge curve means the voltage will vary over time, supply voltage control components are a necessity. For instance, AudioMoth Dev uses two 3 V regulators for digital circuitry and analogue circuitry. These regulators can take input voltages of 3.3 V to 6 V and outputs a steady 3 V v_{cc} to the board components (see fig. 2.9) [113].

2.2.5 Microphones

In the literature, most modern BARs either use ECM or surface-mounted MEMS mics, as these are small in size, have a low operating voltage and low power con-

sumption [124].

When choosing microphones, the output impedance of the microphone through the cable/trace and the input impedance of the downstream audio circuitry (hence referred to as the "load impedance") should be considered [46]. Load impedance is subject to downstream circuitry, such as Preamp, ADC or filtering (discussed in section 2.2.6) before or within an MCU. Typically, the first component the microphone signal reaches is Preamp, which provides the main source of load impedance.

Microphone output impedance itself is not a constant value but changes with the frequency of the output analogue signal. For simplicity, a single value of 'nominal output impedance' is typically used. Standard practice recommends that the microphone's load impedance should be at least four times that of the nominal output impedance [128]. Due to the wide variability of potential load impedances, commercial microphones are grouped into three categories:

1. Low-impedance microphones: $< 600\Omega$ [128].
2. Medium-impedance microphones: $600\Omega - 10000\Omega$ [128].
3. High-impedance microphones: $> 10000\Omega$ [128].

Higher-impedance microphones are cheaper to manufacture but suffer from degrading audio quality with a long cable. The cable material's characteristic impedance and cable length increase the overall output impedance. This, in effect, creates a low-pass filter and degrades the audio quality, particularly at lower frequencies, as cable length increases. In the case of BAR devices, this means that for external plug-in microphones, more expensive, lower-impedance microphones and low-impedance preamps are required where there is significant cable length. In addition, any external long cables in an outside environment must also be shielded from Electromagnetic Interference (EMI) induced noise.

The relationship between the Preamp input voltage, load impedance and output impedance can be expressed as:

The Effect of Output and Load Impedance on a Microphone Signal

$$V_L = \frac{Z_L \times V_S}{Z_L + Z_S} \tag{2.2.2}$$

Where V_L is voltage at the preamp input, Z_L is the load impedance at preamp, V_S is the initial voltage at the microphone output and Z_S is the microphone output impedance. Taken from [128].

2.2.5.1 MEMS Microphones

MEMS microphones are the more power-efficient option, with a high dynamic range and small form factor. They are also typically supplied with a second semiconductor die for pre-amplification and can contain their own ADC for providing a direct digital output [129]. Both designs make use of a pressure-sensitive diaphragm attached to a conductive plate that forms a variable capacitor, where the gap between the plates gives the capacitance. This change in capacitance results in a varying voltage as an analogue output [129].

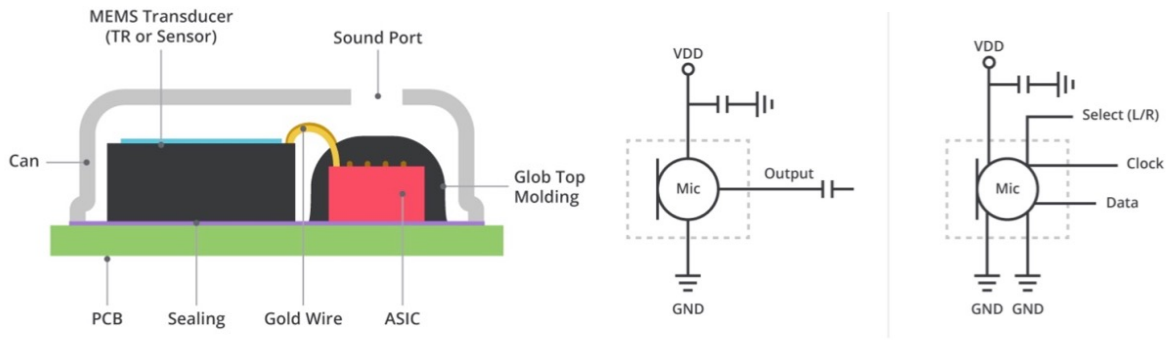

(A) MEMS microphone cross-section, with key components labelled

(B) MEMS microphone circuitry.

Figure 2.11: MEMS microphone schematics. Taken from [130]. For **(A)**, The sound port can be either in the diagram as shown (top-ported) or channel through the PCB (bottom ported) [129]. **(B) left** represents circuitry for an analogue output, while **(B) right** is for digital output.

2.2.5.2 ECM Microphones

ECM microphones are an older technology than MEMS microphones. They require a small charge supplied near-permanently to an electret material to work, referred to as "phantom power". Hence, they are commercially referred to as a member of the Plug In Power (PIP) microphones. The value of the output voltage changes as sound pressure waves move a capacitive electret diaphragm [129]. This can be understood as:

The Voltage and Capacitance relationship in an ECM

$$\Delta V = \frac{Q}{\Delta C} \tag{2.2.3}$$

Where ΔV represents the change in voltage out of the microphone, Q represents the charge held, ΔC represents the change in capacitance with the moving microphone diaphragm.

Figure 2.12 shows a cross section and wiring of a typical ECM microphone. The analogue voltage signal is first buffered and amplified by an internal Junction-gate Field-Effect Transistor (JFET) within the microphone housing. Typically, a common-source amplifier configuration JFET is used inside the microphone, and an external load resistor and DC blocking capacitor are connected [129].

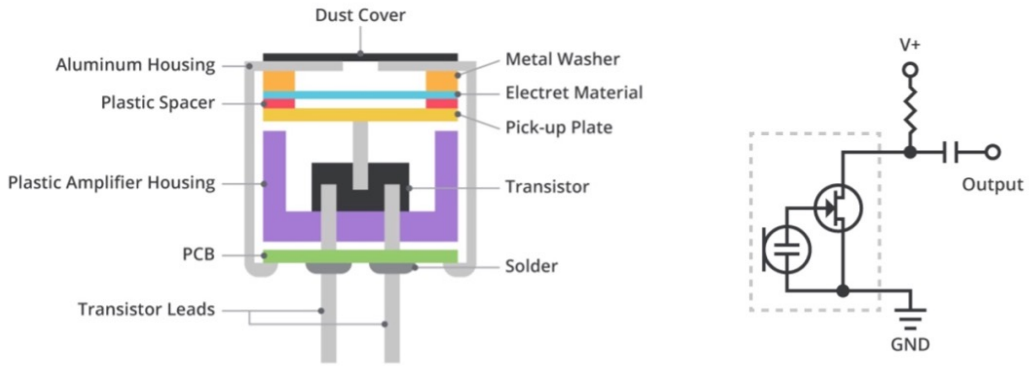

(A) ECM microphone cross-section, with key components labelled

(B) ECM microphone circuitry

Figure 2.12: ECM Mic Schematics. Taken from [130].

A disadvantage of ECMs is that their membranes are mechanically delicate and hence require a bulky metal housing. Their response across frequencies is also sensitive to humidity, which can create noise in humid deployment locations [131]. Having said that, off-the-shelf PIP ECM microphones can be purchased with better sensitivity and SNR compared to MEMS microphones relatively easily and cheaply [131].

The built-in microphone the AudioMoth Developer SBC uses is the SPM0408LE5H-TB MEMS microphone [132]. But the SBC also has a minijack socket for receiving a PIP microphone. OAD, the designers of the AudioMoth recommend using the Primo EM258 microphone as a cheaper option [133].

In terms of the directionality of microphones within a BAR device, Lapp et al. found that the AudioMoth MEMS mic had "a generally omnidirectional response that suffers from attenuation behind the recorder, an effect that is accentuated when it is mounted on a tree" [124]. Therefore, there will be some inherent directionality to any deployed BAR device based on the AudioMoth SBC, as the board, casing and tree the device is mounted to will attenuate sounds. This can be somewhat alleviated by having a microphone protruding from the box, but as has been pointed out by Metcalf et al. before, this puts the microphone at risk of damage from humans, animals and the environment [3].

2.2.6 On-Device Signal Processing Steps

Once sound pressure waves have been converted to an analogue audio signal by a microphone, there are several steps required to record audio in a BAR device. Continuous, analogue signals undergo multiple transformations and processing steps before being saved to a SD card or equivalent. Each of these transformations has some unavoidable loss of resolution and tradeoffs. The key steps discussed in this section include amplification and digitisation.

2.2.6.1 Preamp and Adjustable Gain

Pre Amplifiers (Preamps) are an Op-Amp-based circuit used to uniformly amplify an analogue signal from a microphone, as a full spectrum boost. As the initial microphone signal is relatively weak, ranging from −30 decibel to −60 decibel, some Preamp is required to produce a signal large enough to be electrical-noise-tolerant and for further processing. Many sound recording circuits include an "adjustable gain" feature in the Preamp, which can be a stand-alone Op-Amp IC, or are based within a block of the MCU and controlled with input from the firmware [134]. The latter is the case with the AudioMoth SBC, with a schematic of the cascaded inverting amplification schematic shown in fig. 2.8. Adjustable gain allows the end user to increase the recorded volume in environments that are particularly quiet and vice versa. However, there is a tradeoff with amplifying audio signals, as, in noisy environments, it will increase the likelihood of amplitudes that exceed a maximum range (referred to as "clipping") that can compromise interpretation [135]. Therefore, when deploying a BAR device with adjustable gain, a nominal gain level should be set with enough headroom to avoid excessive noise, clipping or distortions. That said, the initial gain should be set high enough before entering the ADC unit, so that there is not the requirement for additional amplification post-recording, as this will also amplify artificial noise, known as the "noise floor" of a recording.

2.2.6.2 Analogue to Digital Conversion

Analogue to Digital Conversion (ADC) involves the conversion of a continuous analogue waveform into a set of discrete sampled values, a process known as quantisation. The quantisation interval represents the smallest distinguishable difference between two discrete levels, while the bit depth refers to the number of digital bits used to represent each sample. These factors together determine the dynamic range and resolution of a digitised signal [136]. A larger quantisation interval and higher bit depth result in a more accurate representation of the higher frequency components

of an analogue signal. But a higher bit depth requires more storage space, consumes more power and must be catered for in MCU design. Most recordings from BAR devices are therefore capped at 16-bit [135], [136], as with Compact Discs (CDs). Typically, the ADC circuitry exists as a block within an MCU, as is the case for the AudioMoth's EFM32 microcontroller [107].

2.2.6.3 Audio Sampling

Raw sampling rate, or samples per second, within a BAR device can be understood as the frequency that the ADC itself samples, while the recorded sample rate of the final audio is the frequency of these measurements that are transformed and saved to an audio file. The raw sample rate can be higher or equal to this value. The sampling rate determines the number of samples taken per unit of time and is typically measured in samples per second or Hertz (Hz) [137].

The Nyquist–Shannon sampling theorem states that the recorded sampling rate should be at least twice the maximum intended frequency to properly reconstruct an acoustic signal. Frequencies above this threshold will be biased by aliasing and so should be band-limited [138]. In limited systems that require a lower than optimal sampling rate, a more complicated analogue Anti-Aliasing Filter (AAF) is required to prevent aliasing of high-frequency components [139]. Any AAF would be connected to the input of the ADC block. In practice, because of the tradeoffs with reducing bandwidth, AAFs permit some aliasing in frequencies close to the Nyquist limit. And thus, it is recommended that practitioners oversample to make sure all frequencies of interest are captured; this also allows for a simpler, analogue filter, which is less costly and more robust. The need to oversample has meant that audio is typically recorded at a sampling rate of 44.1 kHz (for CDs), to 48 kHz, allowing all frequencies up to the maximum of human hearing, of roughly 20 kHz, to be captured [139]. That said, if in a study of a target species, the maximum vocalisation frequency is significantly lower than 20 kHz then savings can be made in power con-

sumption and file size by setting a BAR to a lower sampling rate. The potential lower power consumption comes from the lower number of SD card writes, and the file size is proportional to the number of samples. "Downsampling" can also be useful post-recording to reduce file size while still retaining signals of interest. For instance, as birds do not normally vocalise above 11.025 kHz [140], audio can be downsampled to 24 kHz to still capture the signal while saving on storage space [141].

2.2.7 Data Storage Components

Some frequently cited memory storage components for microprocessor-based logging projects in the literature include: dedicated EEPROM ICs, USB flash drives and Secure Digital (SD) cards [142]. Each of these storage methods represents a form of NAND flash memory, but with different architectures, regulating components and data transmission protocols. Dedicated EEPROM ICs have low current consumption but are also limited in memory, confined to the MB range. USB drives have a much larger capacity, in the hundreds of GB, but consume more power, between 20 mA to 40 mA when idle [143]. By comparison, SD cards are broadly able to meet both power and capacity needs, with GB capacities and low power consumption, in the mA range when recording. And, they can further reduce this power consumption to µA levels when idle [143]. Hence, these are the preferred option in the literature for remotely deployed devices like BARs [87], [109], [112], [144].

Some further benefits of SD cards include:

1. Fast read/write times, in the hundreds of MHz range [145].
2. They have a more compact size and typically of lower cost than USBs of similar capacity [145].
3. They are resilient to dust, water/humidity, knocks and vibration, and temperature extremes [145].
4. They are replaceable once the maximum number of read/write cycles has been

reached [145].

Modern SD cards have also benefitted from many decades of improvements in NAND flash memory and Metal–Oxide–Semiconductor Field-Effect Transistor (MOSFET) technology. Figure 2.13A shows a single Floating Gate Metal-Oxide Semiconductor (FGMOS) cross-section that makes up one bit of stored data. Memory is achieved by controlling voltages at the control and source to create a path for electrons to flow between the source, allowing some of these electrons to pass into the island and be captured there via Fowler-Nordheim electron tunnelling [98].

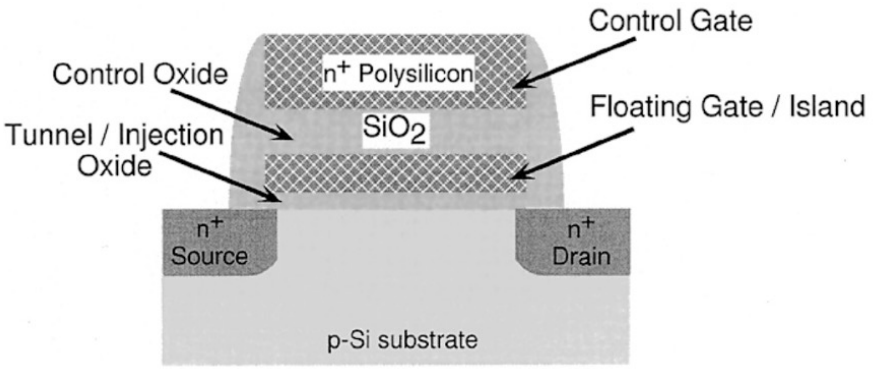

(A) A cross-section of a conventional FLASH storage FGMOS, representing one bit of data. Taken from [98].

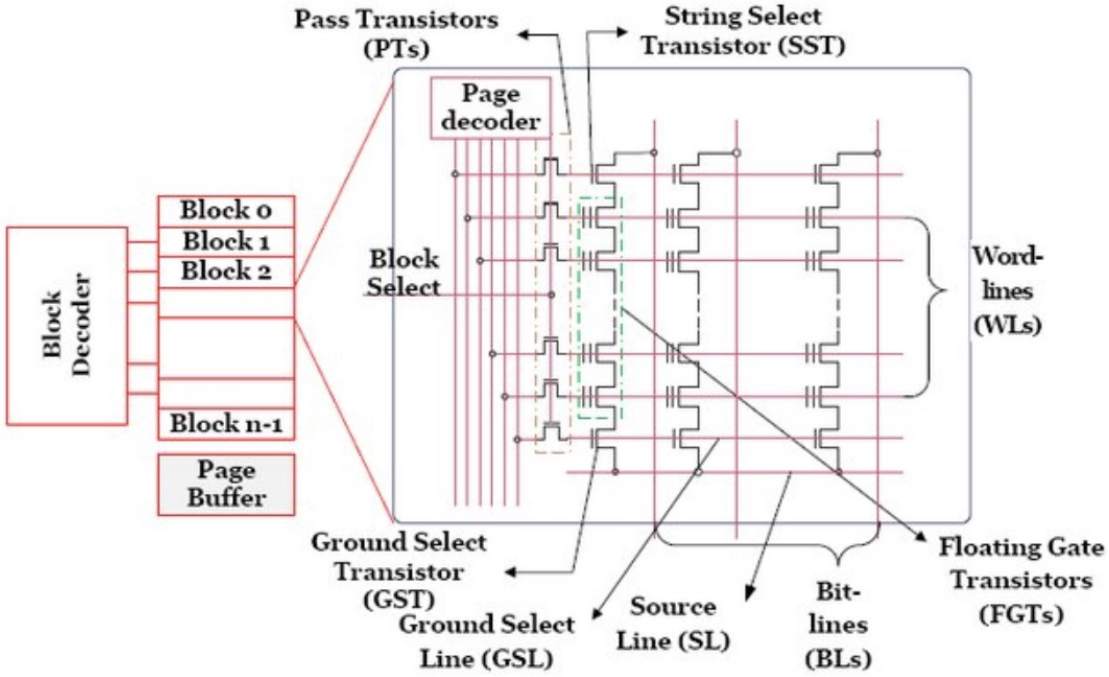

(B) A block diagram for the NAND FLASH memory array. Taken from [146].

Figure 2.13: Flash Memory Schematics.

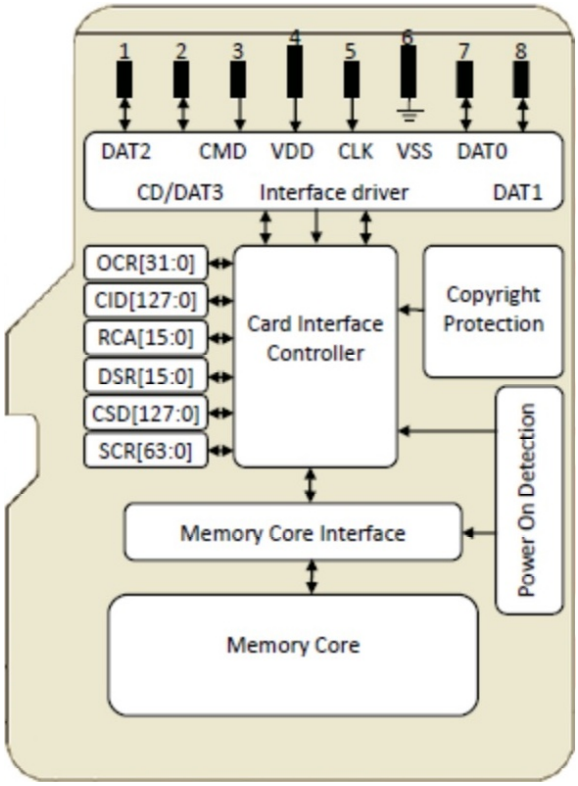

Figure 2.14: The architecture of a micro SD card by Silicon Power, 3.0 SD330 series. Taken from [147]. Shorthands include:

1. *DAT2*: Data line (Bit 2).
2. *CMD*: Command/Response line.
3. *VDD*: Supply Voltage.
4. *CLK*: Internal Clock signal.
5. *VSS*: Supply voltage ground.
6. *DAT0*: Data Line (Bit 0), serves as the SPI data pin.
7. *CD/DAT3*: Card Detect/Data Line (Bit 3).
8. *DAT1*: Data Line (Bit 1).
9. The *OCR*, *CID*, *RCA*, *CSD* and *SCR* are all different types of status registers, typically only required in the initialisation process of the SD card.

2.3 Research Gap

The literature review articulates the underlying technologies and details the common use of BAR devices by practitioners. In particular, the guidance for researchers, detailed in section 2.1.3.1 provides a useful starting point for design considerations. Furthermore, while conducting this literature review, some additional common themes from bioacoustic studies were observed on important requirements for a novel BAR device:

1. The cost of the device and ease of use have played a large role in uptake [118].
2. Extensibility and customisation are also valued in a BAR device so as to meet the particular needs of a study. This requires modularity and sufficient headers/ports to add new features [51].
3. Devices should be robust and deploy without error for long periods. This requires efficient use of power by components and robust signal processing [51].
4. There is value in capturing a full spectrum of biological audio data given the broad range of frequencies terrestrial animals will use [73].
5. There is also value in long-term continuous recording, facilitated by a large DC supply, rather than relying on triggered or scheduled recordings, as these may miss key vocal events [53].

Already, there exists a series of BARs available on the market, with either their own custom SBC, or building off more accessible SBCs like the Raspberry Pi and Arduino. Some of the robust commercial versions designed for long-term continuous recording cost upwards of £500 GBP [111], [115]. The devices discussed in section 2.2.2 that build off the Raspberry Pi provide a cheaper option, but these are less power efficient and are not inherently able to sample audio in the ultrasound range, thereby missing a wide range of animal taxa that use these frequencies.

The basic AudioMoth SBC is able to achieve these three key aspects of low cost,

low power consumption and up to 384 kHz raw ADC sampling rate, but this too has some limitations. These limitations include:

1. A small battery pack, consisting of three AA batteries [85]. For surveys where limited sample time is required, this may be sufficient, but more continuous recording requires a significantly larger battery capacity.
2. The built-in MEMS microphone has a wide dynamic range [85] but also has a lower SNR than some cheap, commercially available PIP microphones in the audible range. Thus, there is value in exploring the use of high-quality external microphones.
3. AudioMoths can only be configured to record at one sample rate and on one schedule at a time [85]. Therefore, switching between sample rates in a more comprehensive survey, one that records birds during the day and bats at dusk, is not currently feasible with one board alone.

As of yet, there has not yet been a complete published device that builds off the AudioMoth Developer SBC platform to fulfil the needs listed above. Hence, this project proposes to build such a device and test its usefulness to researchers and non-expert practitioners.

3. Hardware Design

3.1 First version design (version 1.0)

The original Biophone device, version 1.0, was developed using off-the-shelf components and custom 3D-printed parts. Figure fig. 3.1 shows the internals and external view of the device.

The key electronics components for this design included:

1. Two AudioMoth SBCs, in a parallel circuit, for recording at different sample rates and/or schedules simultaneously. These were labelled "A" for audible range recording and "UI" for ultrasound or infrasound recording (see fig. 3.2).
2. A 10Ah NiMH battery pack, made up of four D-cell batteries and supplying both PCBs.
3. A IP40-rated external push-button switch with a built-in LED. This switch was connected to both AudioMoth SBCs so these could be turned on and off simultaneously. The switch's LED was powered by the "A" AudioMoth SBCs and would flash in accordance with the green LED built into the board.
4. A durable and waterproof IP65-rated polycarbonate enclosure, with a clear lid to view LEDs and fixing points.
5. A Primo EM258 Plug In Power (PIP) microphone [148] for higher quality audio within the audible range, connected to the "A" AudioMoth SBC. Waterproof microphone membranes were also affixed to cover each of the microphone holes.
6. A set of 3D-printed components. These were created in .stl form in Fusion 360, v.2.0.19941 [149] (see fig. 3.3), and printed using the PrusaSlicer software, version 2.7.0 [150]. The filament material used was Prusament Polycarbonate [151]. These components were designed to fix the SBCs and external micro-

phone to the inside of the enclosure lid, as well as "acoustic horns" on the outside of the lid, to protect the microphone membranes from abrasion.

7. An IP68-rated condensation and pressure release valve to prevent the buildup of condensation within the enclosure with changing temperature.

The cost of the v1.0 device components came to £304.04 GBP per device, containing 39 unique parts. The full lists all components and costs can be found in the appendix of this document, in table A.1. The most components expensive for this version were the two AudioMoth SBCs at £71.74 GBP each, the microSD cards at £24.89 for the 256 GB card and £59.99 for the 512 GB card, the Primo EM258 microphone at £22.68 GBP and the four D-cell NiMH batteries at £21.33GBP. These together made up 89.6% of the cost.

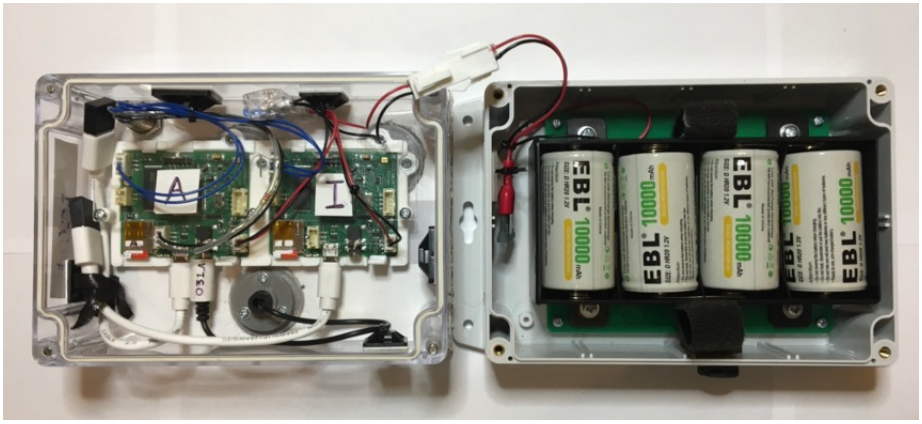

(A) Biophone V1.0 internals

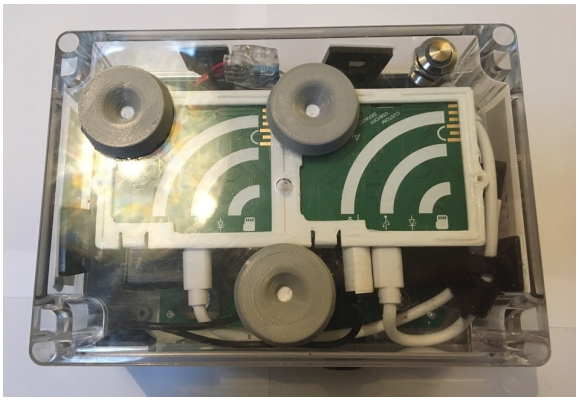

(B) Biophone V1.0 externals

Figure 3.1: The Biophone v1.0, internals and externals.

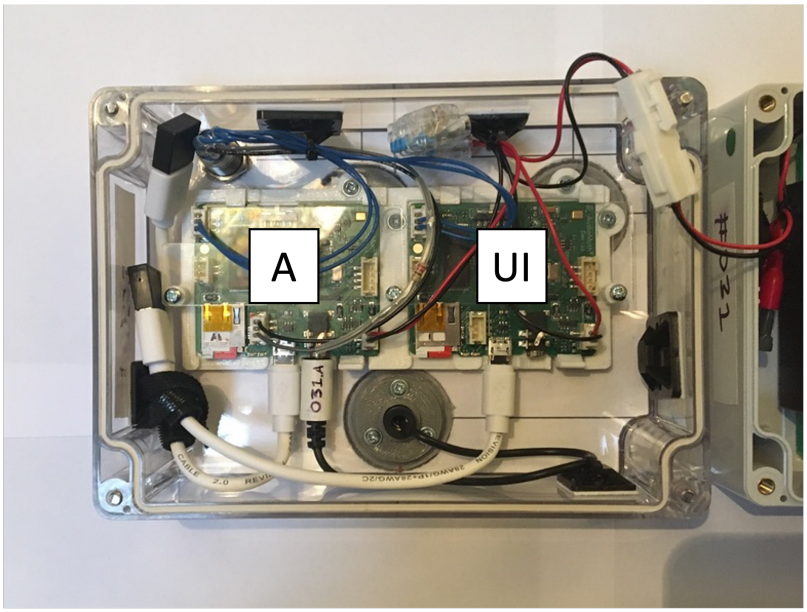

Figure 3.2: Close-up of the Biophone v1.0 lid internals. The two AudioMoths SBCs were labelled based on their expected captured frequency range when being used in the field. The first board is labelled "A" for recording audible frequency range (20 Hz to 20 kHz). The second board is labelled "UI" for recording ultrasound (20 kHz to 192 kHz) and/or infrasound (0 Hz to 20 Hz).

During deployments, the A board would record audible animal sounds, such as birds, with a higher-quality Primo EM258 PIP microphone on a schedule appropriate for bird activity. Meanwhile, the UI board would record at a higher sampling rate, above 48 kHz, for ultrasonic or infrasonic calls, such as from bats or elephants, with a more restricted and bespoke schedule due to the higher anticipated energy consumption and file size on the SD card for ultrasound. The UI board made use of the default MEMS microphone built into the board, the SPM0408LE5H-TB, as this was observed to have a better response at these frequencies. These two boards together would allow users to capture a vast range of animal vocalisations simultaneously, as part of a full soundscape survey.

Modifications were made to select components during the build process, such as the cutting and drilling of holes in the enclosure to fit the external switch, the 3D printed parts, the condensation release valve and the microphone membranes. In addition, acrylic/polycarbonate plates for mounting the battery holder and SBC baffle were laser cut using .svg files generated in Fusion 360 (see fig. 3.3). 3D-printed parts were

also waterproofed with CT1 silicone before being screwed together. All modifications are also detailed in table A.1.

After the initial prototype, thirty v1.0 Biophones were assembled in 2022, with the assistance of staff and students from CYC, as part of an extracurricular workshop. The cost of materials for this workshop was covered by educational funds from local industry and the college. Follow-up troubleshooting and repairs were then made, before deploying devices for the field test at the Cwm Hesgyn site (see section 4.1). Feedback was also taken after this first build to inform future assembly.

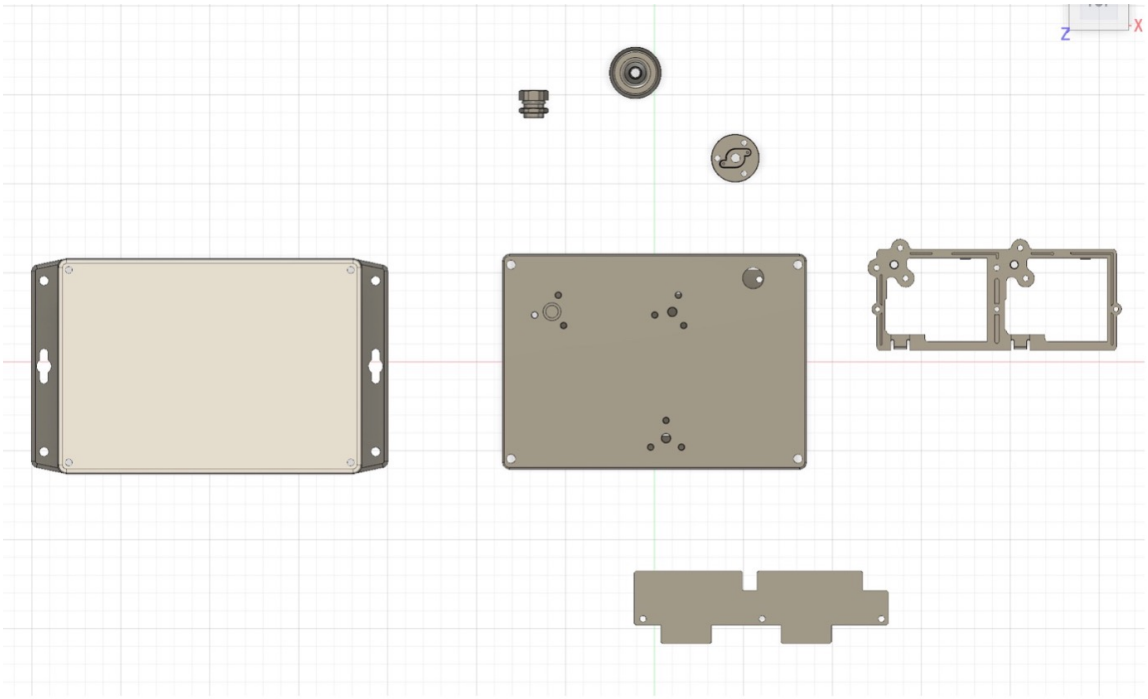

Figure 3.3: A 3D model of the Biophone v1.0 with enclosure, 3D printed parts and components like the vent and microphone membranes separated. Fusion 360 was used to create and modify Computer-Aided design (CAD) models and generate .stl/.svg files of components were used for 3D printing, laser cutting of and the design of drilling jigs for en masse assembly

3.2 Redesign (version 1.1)

Following the feedback from the first build and the field test, several improvements were made to this original design, with the purpose of:

1. Removing difficult-to-assemble parts. Connectors that required crimping were replaced with soldered connectors or pre-made parts. This included upgrading the external microphone to one with a larger capsule, the Primo EM272, for easier resoldering.

2. Avoiding 3D printer defects. Prusament polycarbonate filament was substituted with Prusament Acrylonitrile Styrene Acrylate (ASA) [152], which proved much less prone to defects during printing while retaining material durability.

3. Adding a switch protector. It was discovered that the device could accidentally be triggered on and off with minimal contact in the field. In version 1.0 this was addressed by keeping the foam packing stuck to the lid during deployments. In version 1.1, a new baffle component was 3D-printed and added to prevent this.

4. Increasing the battery life. The original 10Ah NiMH batteries were substituted for a custom 30Ah Li-ion battery pack. This battery pack was custom made by Floreat Energies, using 6 Samsung 21700 cells in parallel, with Battery Management System (BMS) safety/charging circuitry.

5. Increasing plug-and-play. The power and switch wiring were linked to Japan Solderless Terminal (JST) plugs, and a new, cutom PCB was designed for connecting both the power and switch wires (see section 3.3).

Figure fig. 3.4 shows the v1.1 design internals and externals.

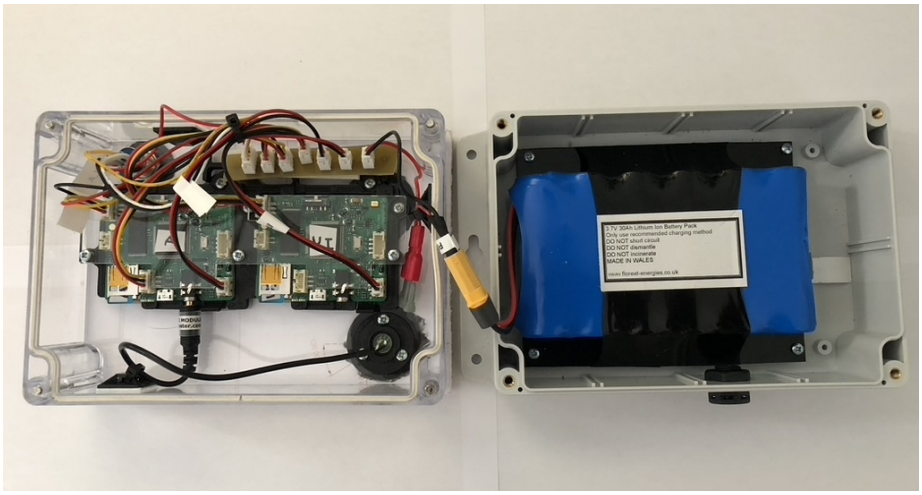

(A) Biophone v1.1 internals

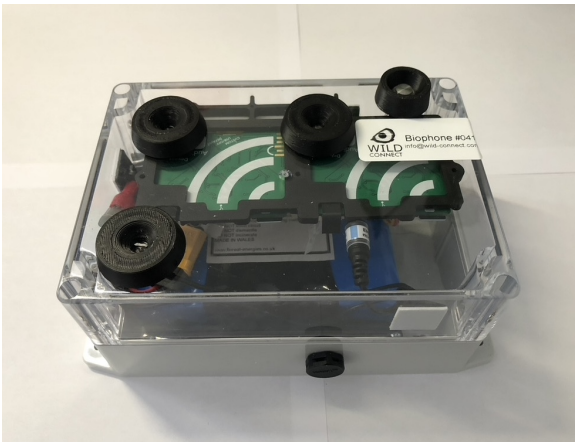

(B) Biophone v1.1 externals

Figure 3.4: The Biophone v1.1, internals and externals.

This version had a material cost of £301.43 per device and was made up of 34 unique parts. For further details on the cost breakdown and differences between v1.0 and v1.1, see table A.1. After the initial prototype, thirty v1.1 Biophones were made at CYC via another extracurricular workshop in 2024. The cost of materials for this workshop was covered by a Knowledge Transfer Fund from the Welsh Government.

3.3 Custom Connector PCB Design

The Custom Connector PCB for v1.1 followed a simple, compact design that could fit in within the lid and allow for the straightforward plugging in of wired components. The connections made were designed to distribute power, allow for switching of both AudioMoths boards simultaneously, and connect the external switch's LED to the first AudioMoth board's red LED; which would be active when recording. The PCB also include a 200 mA fuse built in to replace the previous, more bulky 2 A car fuse. Designs were done in the free circuit design software KiCAD [153]. Once designed, .gbr files were generated and sent to PCBWay for assembly and shipment. Figure 3.5 shows the board design from start to finish.

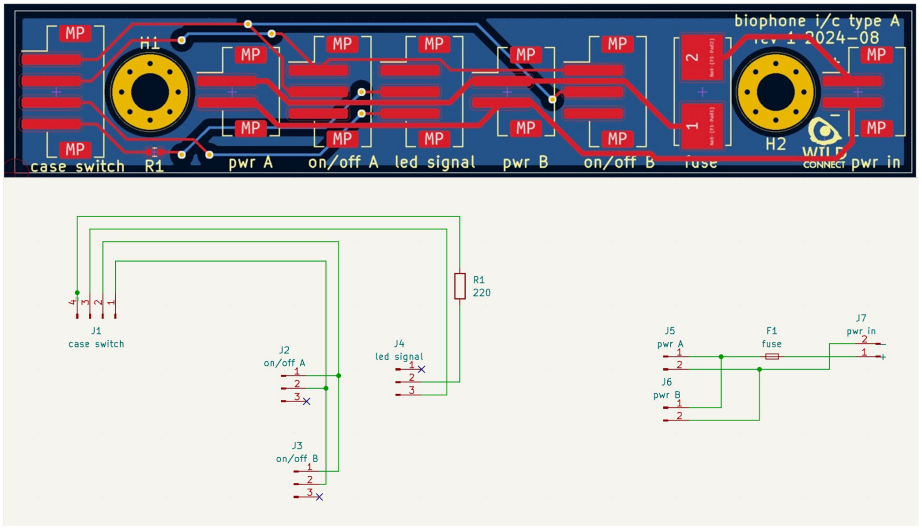

(A) Traces and footprints of and wiring of board components, developed in KiCAD.

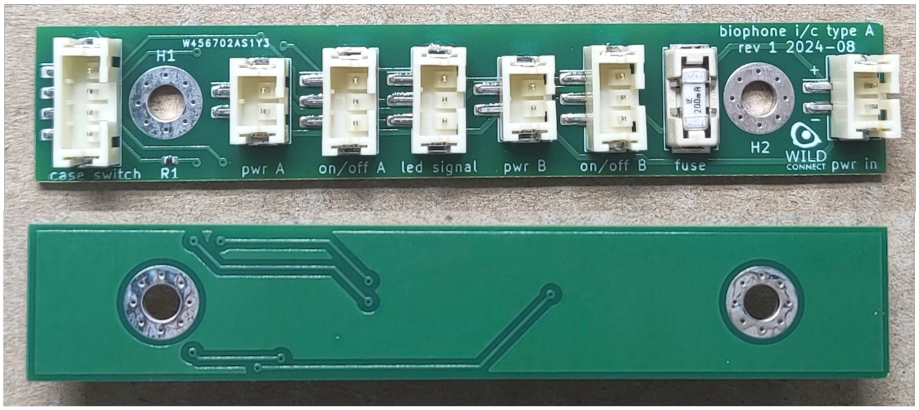

(B) The final assembly from PCBWay, front and back.

Figure 3.5: The custom connector PCB layout. For **(A)**, traces on the top of the PCB are coloured in red, while those on the bottom of the PCB are blue.

4. Methods

4.1 Field Tests Methodology

This study was undertaken in Cwm Hesgyn, part of the Rhiwlas Estate, near Bala, North Wales, in June 2022. Cwm Hesgyn is a listed Site of Special Scientific Interest (SSSI), designated by Natural Resources Wales (NRW). This field study was part of a larger "Upland Ecosystem Research Project", undertaken by the Holistic Restoration LLP research group and overseen by the North Wales Moorland Partnership (NWMP). Researchers on the site were documenting the effect of grazing sheep during summer period, on livestock health and the local flora and fauna. The deployment and collection of the Biophone devices was facilitated by the use of local volunteers and workers on the estate. The findings from the greater study can be found here: Rhiwlas Grazing Study [154].

For the purposes of this study, Biophone v.1.0 devices were deployed on the 31st of May 2022 and collected on the 10th of July 2022. Five sites within Cwm Hesgyn were chosen for their corresponding microhabitat, based on the dominant plant coverage and soil, each of which had been documented in a previous survey of the site by NRW. The microhabitats on each site were Blanket Bog, Upland Flush, Acid Grassland, Bracken and Upland Dry Heath. Table 4.1 shows an overview of these microhabitats. A habitat map of the Rhiwlas Estate and the locations of deployed Biophones are shown in fig. 4.1. As well as the habitat type, sites were chosen for the presence of existing wooden posts to fix devices to (put in place by Holistic Restoration beforehand), the ease of accessibility on foot and ensuring the devices were space >250 m apart to avoid the pseudo-replication of vocalisations captured.

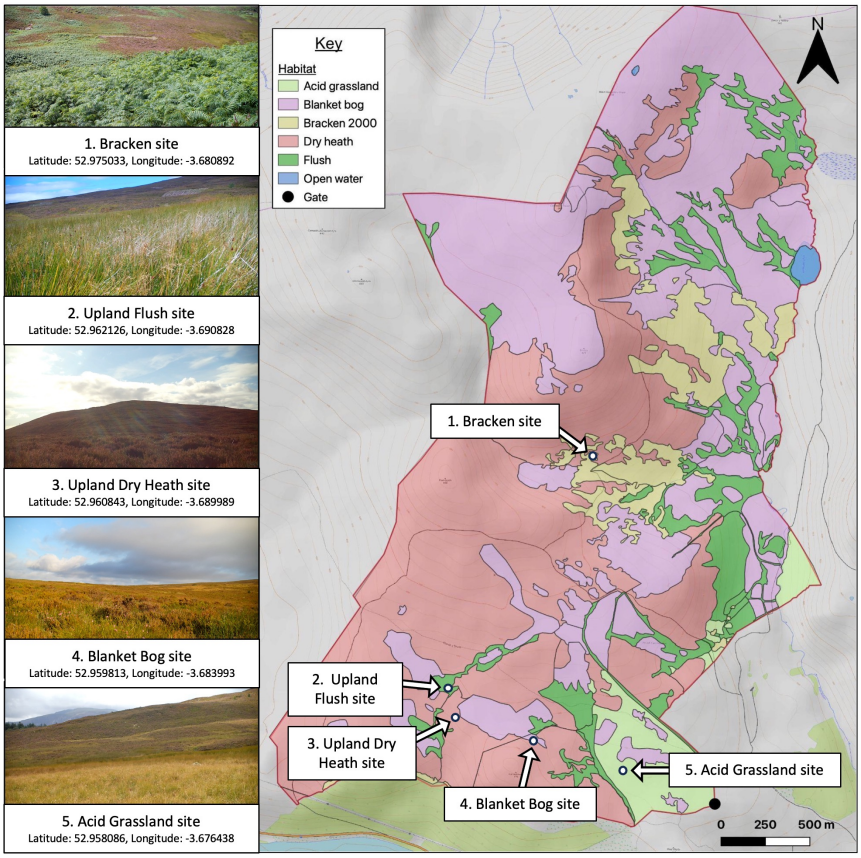

Figure 4.1: Cwm Hesgyn Biophone Deployment Map. Modified from [154]. Photos of each deployment site and coordinates are shown on the left. Within the map, different habitat types are coloured based on a 2020 ecological survey (Terrestrial Phase 1 Habitat Survey) by Natural Resources Wales (NRW).

Table 4.1: A Summary of the Field Study Site Microhabitats.

	Sites				
	Blanket Bog	**Upland Flush**	**Acid Grassland**	**Bracken**	**Upland Dry Heath**
Description*	Wet peatland (>0.5m deep peat) with Sphagnum Moss, Purple-moor and Cotton Grass. Form at the top of river catchments, where rainfall is frequent and heavy, and drainage is poor.	Waterlogged areas with flowing water, supplied by groundwater, where peat does not form. Vegetation dominated by small sedge fens and thickets of Purple-moor Grass.	With a rich mix of grasses and herbs, which livestock tend to favour for grazing. Usually on well-drained, acid, mineral soils, or drained peat. With a pH of 5.5 or less.	An area where bracken dominates, at >95% canopy cover in the height of growing season.	Made up of Heathers, Bilberry and other dwarf shrubs. Freely draining acidic or neutral soil.

* All descriptions adapted from The UK Habitat Classification Working Group 2018 Report [155].

Each of the Biophone v1.0 devices had the following deployment parameters set for each of the two internal AudioMoth SBCs:

1. **A (Audible) boards**. Set to record for 10 minutes and sleep for 10 minutes, 24 hours a day. A sampling rate of 48 kHz was used. A 200 Hz high-pass filter was applied to block excessive wind noise. Daily power consumption was estimated at 150 mA h. Daily data produced was estimated at 4.2 GB.
2. **UI (Ultrasound/Infrasound) boards**. Set to record for 15 minutes and sleep for 45 minutes, 24 hours a day. A sampling rate of 250 kHz was used. The 48 Hz DC noise-blocking filter was disabled. Daily power consumption was estimated at 130 mA h. Daily data produced was estimated at 9 GB.
3. **Other common settings**. Estimations of power consumption and bytes of data produced were made using the AudioMoth Configuration Application [156]. Based on the power calculations, the boards were expected to last for 35.7 days and thus produce 149.9 GB of data on the A board and 321.3 GB of data on the UI board; well within the limit of the respective 256 GB and 512 GB SD cards. The AudioMoth firmware version used was 1.8.0 for all boards. Low-voltage cut-off was enabled. All LEDs were enabled. The NiMH/Li-ion voltage range setting was enabled. All other settings were default.

The purpose of this field testing was to see how the Biophone handled real-world deployments. In particular, to identify vulnerabilities to breakage, data corruption, key aspects of the user experience and the usefulness to ecology. Physical breakages were reported by users and documented during the course of the studies. An initial test run was conducted in the months before, where the setup, deployment and data transfer processes were demonstrated.

As well as the Biophones, a maintenance kit was provided to the group containing:

1. Custom-made furry hat covers for the Biophones to mitigate wind buffering on the microphone membrane, observed in previous test runs.
2. Foam padding, initially for stacking the Biophones on top of each other. But

it was observed in test runs that the switch could be triggered by the furry hat in wind, so this was fixed on as a barrier during deployments.

3. A reel of garden wire for fixing boxes to posts.
4. BONAI Universal Battery chargers for the D-Cell NiMH batteries.
5. A Western Digital 18 TB external HDD drive for data storage.
6. SanDisk MobileMate micro SD card readers, for transferring data to the external hard drive with a personal laptop.
7. Microfibre cloths for cleaning the SD cards, as it was observed that dust on the pins could interfere with recording.
8. micro USB leads for configuring recording schedules.
9. A permanent marker pen and white electrical tape for marking boxes.
10. Screwdrivers, an antistatic brush set, cable ties and pliers for opening up the box and basic cleaning and maintenance.
11. Small items were held in a basic fishing tackle box, and all items fit into a 35 L Really Usefull Storage Box.

For the deployment process, sites were walked to on foot by volunteers/workers, carrying devices in a rucksack. Boxes were affixed to wooden stakes in the ground with garden wire and screws, with a screwdriver. Figure 4.2 shows a deployed Biophone device in the Upland Heath site.

Data corruption, both within recordings and the breakdown of SD cards, was reported by users and investigated by manually looking at the audio spectrogram, using the software Audacity (Version 3.7.0) [157] and AudioMoth-generated metadata in the .wav file "comment", following the completion of the study. From the .wav file metadata, values for why recording stopped were noted. Feedback on user experience was collected via an in-person debrief at the end of the study. Freely available software was used to identify bird species present and calculate acoustic indices as a proxy for biodiversity. For the species identification list in the audible

range, the BirdNET algorithm and desktop app [158] were used. Some rudimentary validation of these identified birds was done by manually comparing audio/spectrograms against those recorded on the Xeno-Canto database [159]. That said, no chartered ecologist expertise was used to confirm identifications, so further validation with such an expert would be required for greater confidence on the species identified and the ecological implications. For the UI board data, potential bat recordings were screened with Kaleidoscope Pro Software, version 5.5.2 [160]. Curation of this BirdNET data and the calculation of acoustic indices were done on audible range frequencies using packages in the statistical program R [161]. The packages used included dplyr [162], stringr [163], seewave [164] and soundecology [165].

Figure 4.2: A Biophone Deployment. This shows deployment of the v1.0 device on the Cwm Hesgyn site with a furry hat cover over the top. Boxes were affixed to stakes in the ground with garden wire and screws and set to record.

4.2 Laboratory Tests and Methodology

In order to track the power consumption of the Biophones, the following preparation, assembly and experiments were undertaken:

1. A current-sense intermediary circuit was simulated and then built to measure current to the two AudioMoth SBCs used in each device. Biophone devices of both version 1.0 and 1.1 were modified to accommodate this experiment.
2. The current draw with AudioMoths at different sampling rates and internal states was tracked via this intermediary circuit and viewed on an oscilloscope.
3. The device's power consumption over a continuous recording period was tracked using the intermediary circuit and using a Graphtec voltage logger.

4.2.1 Power Tests: Building the Current Sense Circuit

The high-side current sense circuit made use of an INA138 [166] as the principal current sense amplifier. Measurements for the initial oscilloscope readings were taken at the output of this Op-Amp. For the continuous logging over multiple days, measurements were taken after feeding the signal through a buffer OPA340PA Dual In-line Package (DIP) Op-Amp [167], with unity negative feedback, thereby reducing the load from the logger on the INA138. In addition, a low-pass filter, consisting of a 130Ω resistor and a 10 µF electrolytic capacitor, was used to dampen the larger and more frequent spikes observed in the initial tests. Figure 4.3 shows the circuit layout simulated in National Instruments (NI) MultiSim [168]. In this simulation, a current source was used to represent the variable current draw of the AudioMoths SBCs' load and the corresponding voltage gain across the sense resistor. A 0.1Ω shunt resistor was used to minimise voltage drop preceding the load, while producing enough voltage drop to be sufficiently amplified by Op-Amps and detected by the logger and oscilloscope.

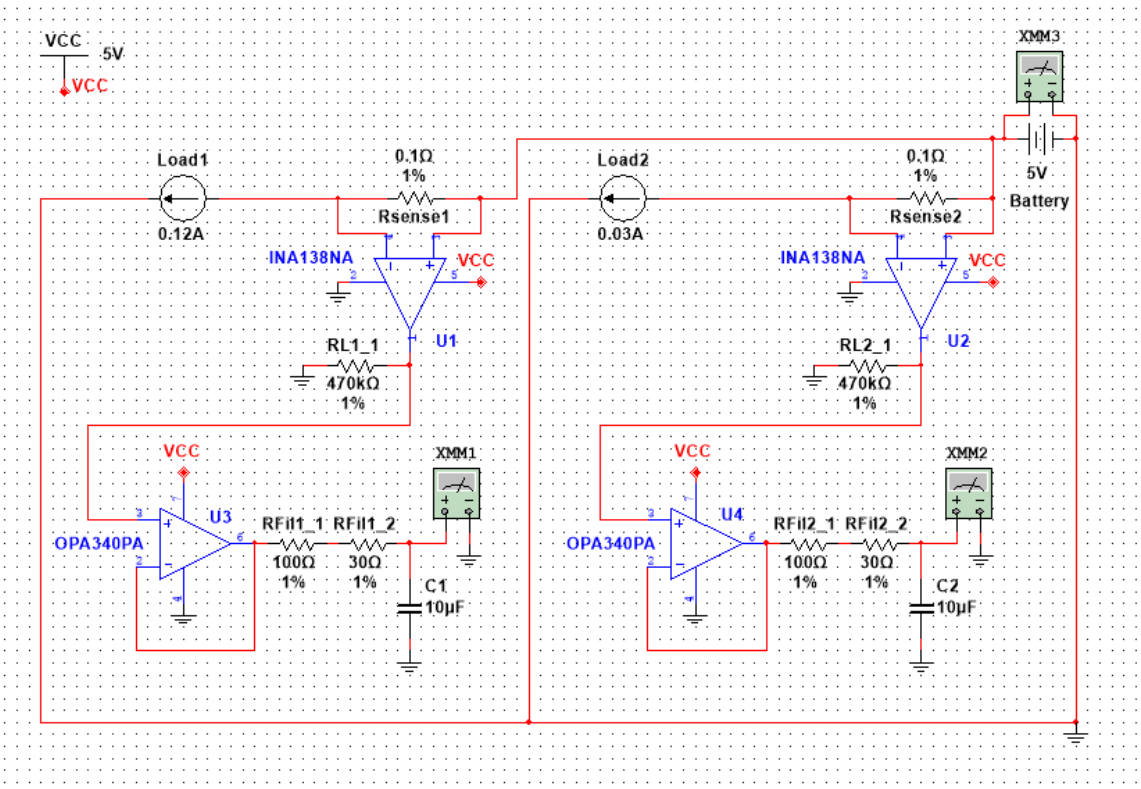

Figure 4.3: Intermediary current sense circuit, simulated schematic. Made using Multi-Sim by NI. The symbols XMM 1-3 represent points of measurement for the voltage logger tests described in section 4.2.3. For oscilloscope readings, detailed in section 4.2.2, V_o was measured before the buffer Op-Amp, at the output of U1 and U2.

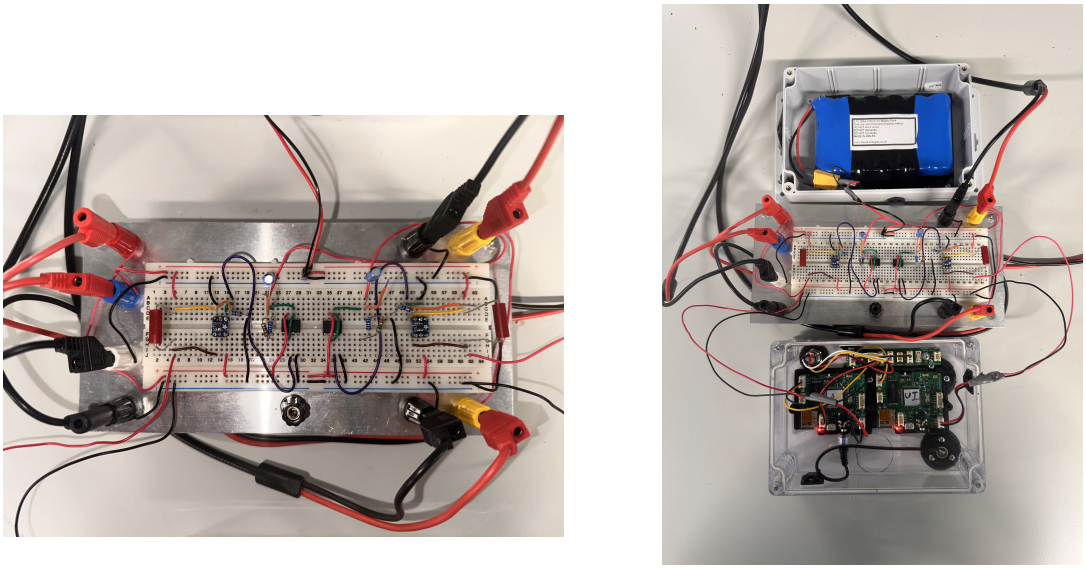

(A) Intermediary Current Sense Circuit Breadboard

(B) Intermediary Current Sense Circuit Breadboard, connected to Battery and PCBs

Figure 4.4: Intermediary Current Sense Circuit Breadboard

The voltage-voltage gain from the sense resitor, as well as the correct functioning of the circuit, was confirmed using a Tektronix DPO 2014B Digital Phosphor Oscilloscope [169] and a Tektronix AFG1022 Arbitrary Function Generator [170]. The Arbitrary Function Generator was programmed to produce a pulsed 50 ms square wave every 340 ms (duty cycle: 14.7%). The square wave's peak voltage was 2.5 V, and 47Ω resistors were used for the two parallel loads, giving a current of ~116 mA. No visible effects of the Op-Amp circuit's amplification, such as slew rate or ripple, were observed. Via this test, the voltage-voltage gain of the current sense circuit was confirmed to be at 94, within a ±1% error, for each of the INA138 Op-Amps, concurring with the datasheet [166]. Once connected inline between the battery and the two AudioMoth SBCs (see fig. 4.4), current drawn through the sense resistor was calculated with the following rearranged equation from the INA138 datasheet:

The current across a shunt/sense resistor with gain from the INA138 Op-Amp

$$I_{sense} = \frac{V_o \times 5000}{R_{sense} \times R_L} \tag{4.2.1}$$

Where I_{sense} represents the current across the shunt/sense resistor, V_o represents the output voltage measured, R_{sense} represents the resitance of the shunt/sense resitor, R_L represents the load resitor attached and the value of 5000 comes from the built-in 5kΩ resistors of the Op-Amp inputs.

The practical implementation of this intermediary circuit involved connecting components on a breadboard, with seperate voltage rails for the battery power and V_{CC}, powering the Op-Amps. The power supply for V_{CC} was supplied with a Keithley 2230-30-1 Triple Channel DC Power Supply [171]. Connecting wires were solid-core and 22 American Wire Gauge (AWG).

4.2.2 Power Tests: Current Sense Oscilloscope Measurements

The Tektronix DPO 2014B Digital Phosphor Oscilloscope was used to probe the INA138 Op-Amp output pins in the intermediary circuit. The intention of these tests was to identify key aspects within the waveforms of the AudioMoth PCB in different states (recording with a 48 kHz to 384 kHz sampling rate) and with the different peripheral components of the biophone attached (such as the external switch LED and external microphone). Screenshots were then taken and saved to a USB stick. AudioMoths sampling rates were configured using the AudioMoth Configuration Desktop app and a micro-USB cable.

4.2.3 Power Tests: Current Sense Continuous Recording

The Graphtec GL900 Ver3.03 midi logger [172] was used, with Bayonet Neill–Concelman (BNC) cables used to connect to the intermediary circuit. The sampling rate for logging was one sample every 50 ms. For generating the voltage displays, data was

loaded into the GL900-APS Ver.2.06 Desktop Application. This app was also used to calculate the RMS, maximum and minimum values for each channel's voltage, which was converted into amperes and power consumption using eq. (4.2.1) and $P = V \times I$, using the AudioMoth SBC's internally regulated voltage of 3.3 V.

5. Results

5.1 Field Test Results

5.1.1 Performance of Biophone Devices in the Field

For deployments, devices were successfully deployed, affixed to posts and collected by the volunteer members at each of the five sites, during the month period. Upon collection, the boxes were observed to be intact. Once opened up, the devices were also observed to have not suffered from any water ingress into the box, despite significant rainfall and stormy weather during the period. Once returned and recharged, the devices and SD cards were observed to function as normal. That said, one of the device A boards (on the Bracken site) did not record, due to human error in not setting the internal clock beforehand. So this data was supplemented from the UI board of the device. This audio was first downsampled to 48 kHz and a 200 Hz filter was applied (to match the A board configuration) using the SOX command line tool, before acoustic indices were calculated. Hence, the values for this site in the plots are more sparse, as the UI board had 45-minute gaps between recordings.

In the field, the minimum number of days the devices were able to record complete and uncorrupted .wav files with the schedule described in section 4.1, was 23.97 days, which was 11.73 days before the deployment time predicted on the AudioMoth Configuration App. The maximum successful recording time was 26.88 days. Days beyond this successful recording period, the sound files were observed to have one of three errors in a steady progression:

1. The AudioMoth SBC would attempt to record, but the sound file would contain an artificial “drumming” sound appearing and eventually dominating the other sounds. files would cite “recording stopped due to low voltage” in the file

metadata. This is shown in fig. 5.1.

2. The AudioMoth SBC would attempt to record, but cut the recording short, after a few seconds, also citing "recording stopped due to low voltage" in the file metadata.

3. The AudioMoth SBC would not record, but would create an empty .wav file.

Apart from low voltage, no other additional errors were observed in the .wav file metadata.

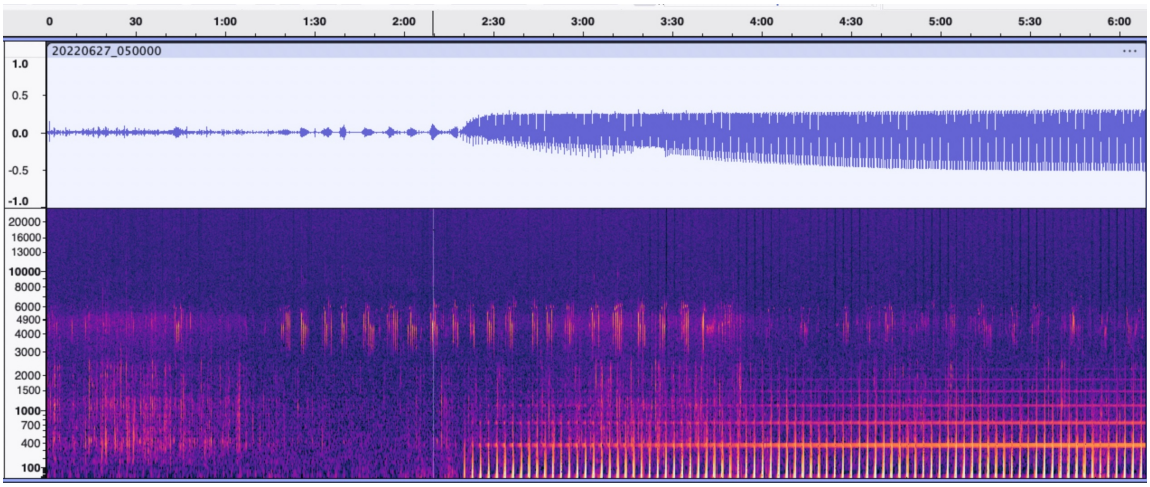

Figure 5.1: Artificial "drumming" noise observed in the field study. Picture taken in Audacity. Amplitude sits in the blue bar above the spectrogram. The noise consists of regular beats at low frequency as a well as pure tones. This occurred in later files where the.wav file cited low voltage in the file metadata. Bird calls were still being recorded as the artificial noise progressed, in the 3 kHz to 6 kHz range on the y axis. This noise was observed to repeat every 340 ms.

5.1.2 Sound Data Analysis

Figure 5.3 shows the aggregated mean acoustic index values for Acoustic Complexity Index (ACI), Bioacoustic Index (BI), Normalised Difference Soundscape Index (NDSI) and Acoustic Entropy Index (H) over an average 24 hours. In the ACI, BI and NDSI charts, there's a large peak between 04:00 am and 06:00 am, correlating with sunrise [173]. There is also an observable separation between the different

sites/colour bands where devices were deployed, particularly in NDSI and H. The observed overall pattern in ACI and BI is the same across sites, indicating a similar daily acoustic pattern between sites in the features these indexes measure.

Table 5.1 shows the bird species identified from all the collected audio data using BirdNET. A total of 26 unique species of birds were identified on the BirdNET Desktop app. Precise latitude and longitude values (shown in fig. 4.1 previously) were used in the app to provide a location-specific species list for analysis. Furthermore, bird identifications were filtered for a minimum threshold of >80% confidence, based on the recommendations of Sethi et al. that a minimum of 0.7–0.8 was appropriate for most studies [34]. It is noteworthy that a significant number of the species listed are rare elsewhere in the UK. With 9 species on the Birds of Conservation Concern 5 (BOCC5) red list and 11 on the amber list, making up 77% of the identified species. Figure 5.2A shows a spectrogram view of one of the identified birds, the Eurasian Skylark, which sits on the red list of conservation concern in table 5.1.

No bat identifications were successfully made from the UI board data using Kaleidoscope Pro Software. That said, some unidentified ultrasound calls were found in the .wav file spectrograms. One is shown in fig. 5.2B.

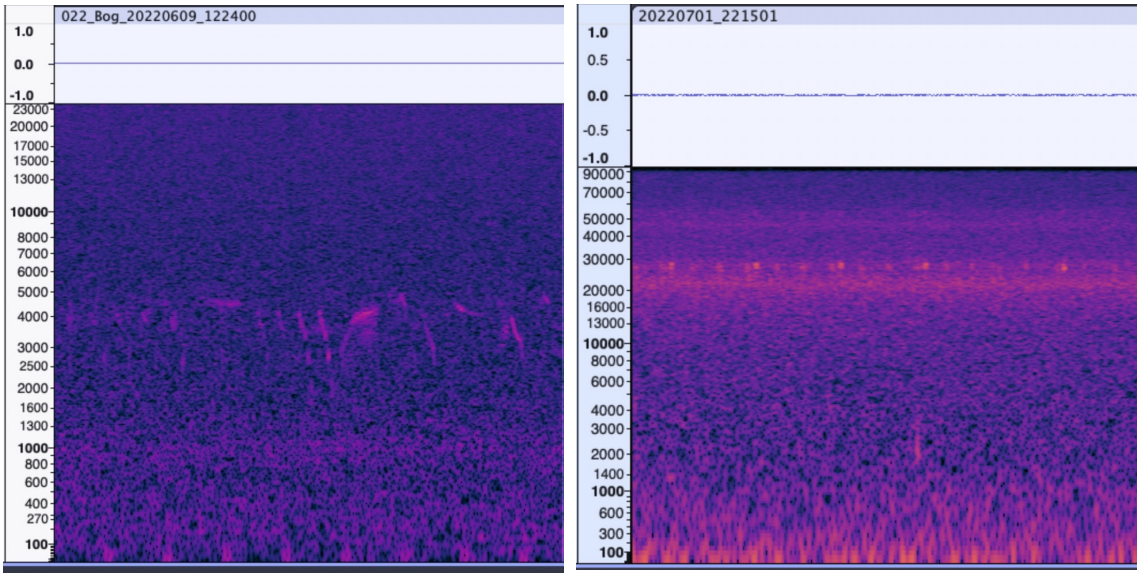

(A) A spectrogram of an identified bird from the field, a Eurasian Skylark

(B) An unidentified ultrasonic signature

Figure 5.2: Spectrograms of animal calls from the field study. Amplitude sits in the blue bar above the spectrogram and shows the overall sound is very faint. Picture taken in Audacity. **(A)** shows an Eurasian Skylark identified using BirdNET, this species signature can be seen as a swooping pattern between 2.5 kHz and 5 kHz on the y axis. **(B)** shows an unidentified ultrasonic call, which can be heard as a chirping-like noise when slowed down by 4 times. This species signature can be seen as a small dots pattern between 20 kHz and 30 kHz on the y axis.

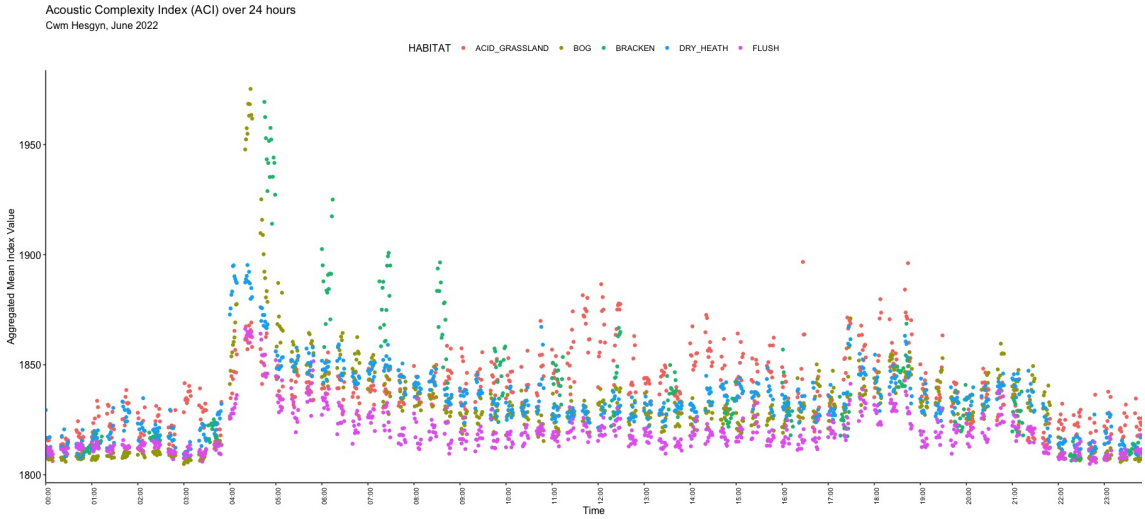

(A) Cwm Hesgyn, Acoustic Complexity Index (ACI) over an aggregated 24 hours.

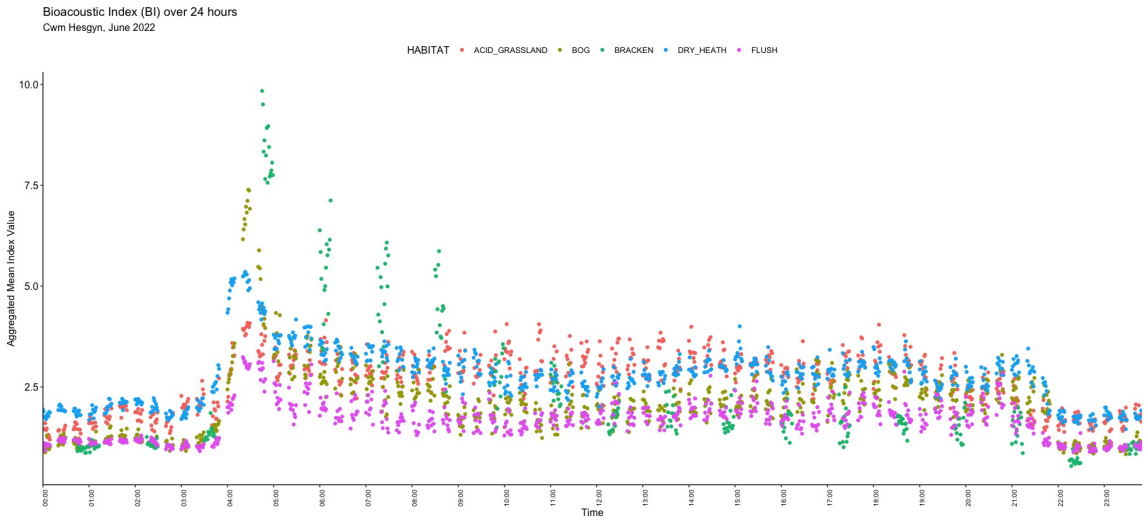

(B) Cwm Hesgyn, Bioacoustic Index (BI) over an aggregated 24 hours.

Continues to next page

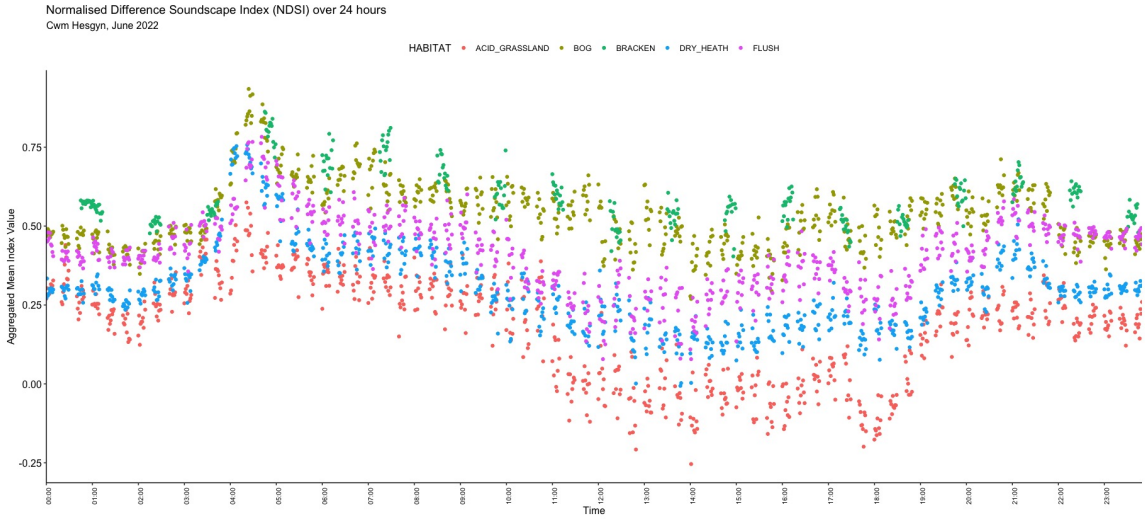

(C) Cwm Hesgyn, Normalised Difference Soundscape Index (NDSI) over an aggregated 24 hours.

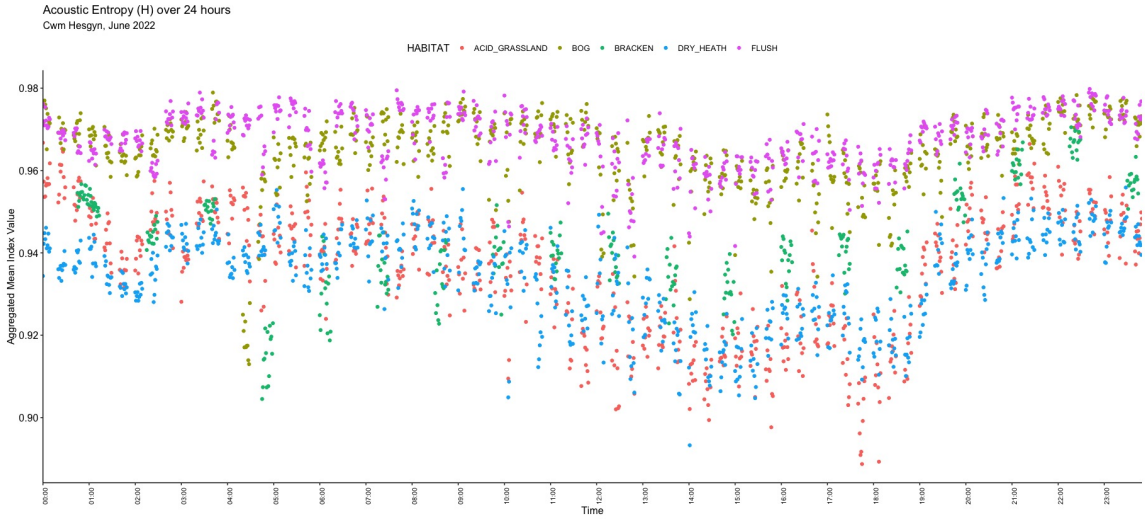

(D) Cwm Hesgyn, Acoustic Entropy Index (H) over an aggregated 24 hours.

Figure 5.3: Acoustic indices plots for the Cwm Hesgyn field test. Colouring of points based on site/micro-habitat.
Colour key:
Acid Grassland site: red
Upland Bog site: yellow green
Bracken: green
Dry Heath: blue
Upland Flush: pink

Table 5.1: The Cwm Hesgyn field study BirdNET results.

Common Name	Scientific Name	Conservation * Concern	Number of Calls Identified	Confidence Mean	First Call Occurrence	Last Call Occurrence
Black-headed Gull	*Chroicocephalus ridibundus*	Amber list	3	0.93	23/06/2022 00:23	23/06/2022 00:23
Carrion Crow	*Corvus corone*	Least concern	4	0.86	22/06/2022 09:25	23/06/2022 07:03
Common Buzzard	*Buteo buteo*	Least concern	26	0.87	11/06/2022 07:20	25/06/2022 07:47
Common Cuckoo	*Cuculus canorus*	Red list	1	0.98	14/06/2022 06:28	14/06/2022 06:28
Common Greenshank	*Tringa nebularia*	Amber list	3	0.90	14/06/2022 22:03	16/06/2022 06:04
Common Raven	*Corvus corax*	Least concern	15	0.86	13/06/2022 05:40	25/06/2022 09:03
Common Sandpiper	*Actitis hypoleucos*	Amber list	5	0.83	10/06/2022 20:23	22/06/2022 10:27
Common Shelduck	*Tadorna tadorna*	Amber list	1	0.83	25/06/2022 13:22	25/06/2022 13:22
Common Snipe	*Gallinago gallinago*	Amber list	1	0.83	17/06/2022 19:27	17/06/2022 19:27
Common Swift	*Apus apus*	Red list	2	0.93	22/06/2022 18:07	22/06/2022 18:07
Dunnock	*Prunella modularis*	Amber list	7	0.86	09/06/2022 13:01	19/06/2022 03:43
Eurasian Curlew	*Numenius arquata*	Red list	1	0.86	15/06/2022 01:01	15/06/2022 01:01
Eurasian Moorhen	*Gallinula chloropus*	Amber list	4	0.87	18/06/2022 16:49	24/06/2022 13:00
Eurasian Siskin	*Spinus spinus*	Least concern	10	0.90	09/06/2022 12:23	21/06/2022 10:23
Eurasian Skylark	*Alauda arvensis*	Red list	15	0.85	16/06/2022 08:03	23/06/2022 16:46
Eurasian Wren	*Troglodytes troglodytes*	Amber list	81	0.90	09/06/2022 16:45	24/06/2022 10:20
European Stonechat	*Saxicola rubicola*	Least concern	1434	0.94	09/06/2022 15:22	25/06/2022 14:08
Gray Heron	*Ardea cinerea*	Least concern	1	0.92	16/06/2022 05:23	16/06/2022 05:23
Lesser Redpoll	*Acanthis cabaret*	Red list	10	0.84	13/06/2022 20:43	24/06/2022 15:03
Meadow Pipit	*Anthus pratensis*	Amber list	7846	0.90	09/06/2022 12:44	25/06/2022 20:45
Northern Wheatear	*Oenanthe oenanthe*	Amber list	2	0.94	21/06/2022 06:27	22/06/2022 18:27
Reed Bunting	*Emberiza schoeniclus*	Amber list	6	0.91	10/06/2022 10:09	23/06/2022 05:47
Tree Pipit	*Anthus trivialis*	Red list	7	0.83	15/06/2022 05:27	25/06/2022 18:27
Western Yellow Wagtail	*Motacilla flava*	Red list	1	0.82	15/06/2022 05:47	15/06/2022 05:47
Yellowhammer	*Emberiza citrinella*	Red list	1	0.82	20/06/2022 06:03	20/06/2022 06:03

* Conservation concern assignments taken from the 2021 BOCC5 report [174].

5.2 Lab Tests Results

5.2.1 Current Sense Oscilloscope Measurements

Figure 5.4 Shows the current sense readings from one of the AudioMoth SBCs within the Biophone in different states. Follow-up calculations were made using the oscilloscope to get the Root Mean Square (RMS) V_o values that were converted to I_{sense} with eq. (4.2.1) and power with $P = V \times I$, using the AudioMoth SBC's internally regulated voltage of 3.3 V. Figure 5.4A, shows two large current spikes before recording begins. These peak at 127.65 mA or 421.25 mW of instantaneous power consumption. These peaks are likely the initial powering up and initialisation of the AudioMoth MCU and SD card microcontroller, which is discussed in section 6.2.2.

Figure 5.4B-D has several features of interest. For instance, the small, frequent waveforms that repeat every ~2.7 ms consuming 8.72 mA of RMS current, or 28.7 mW RMS power. These waveforms have been magnified in fig. 5.4E and do not visibly change between sample rates. While the larger square wave in Figure 5.4B, repeats every 341 ms in (duty cycle: 16.42%), consumes 31.28 mA RMS current, or 103.2 mW RMS power.

Figure 5.4C and fig. 5.4D show a clear increase in frequency of the larger square waveform when the configured sample rate is increased to 192 kHz and 384 kHz. The period for these waveforms is 82.1 ms (duty cycle: 70.65%) for 192 kHz and 42.66 ms (duty cycle: 93.76%) for 384 kHz. The pulse width of the square wave shortens slightly once up to 384 kHz in sample rate, with a width of at 56 ms long for 48 kHz and 192 kHz, to 40 ms long at 384 kHz. That said, the power consumed by these square wave pulses works out similarly to ~30 mA RMS current, or ~99 mW RMS power. This increasing frequency in the square waveform is likely due to a greater number of writes to the SD card per second, which is discussed in section 6.2.2.

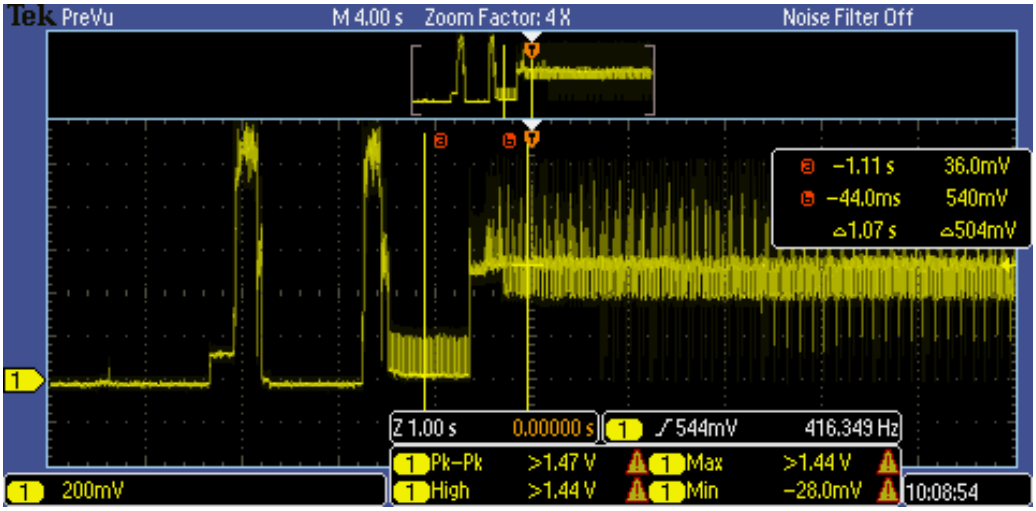

(A) AudioMoth SBC boot up before recording.

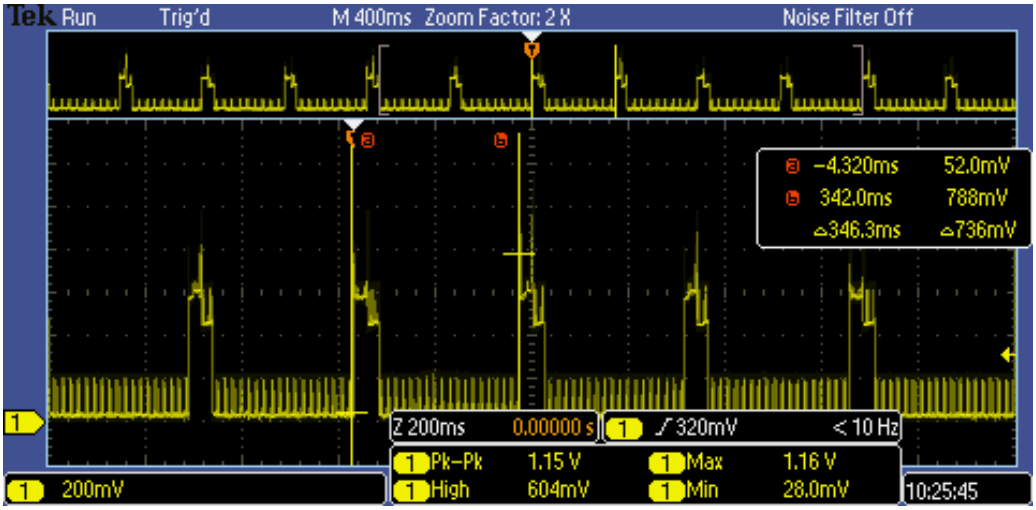

(B) AudioMoth SBC in recording state at a 48 kHz sampling rate.

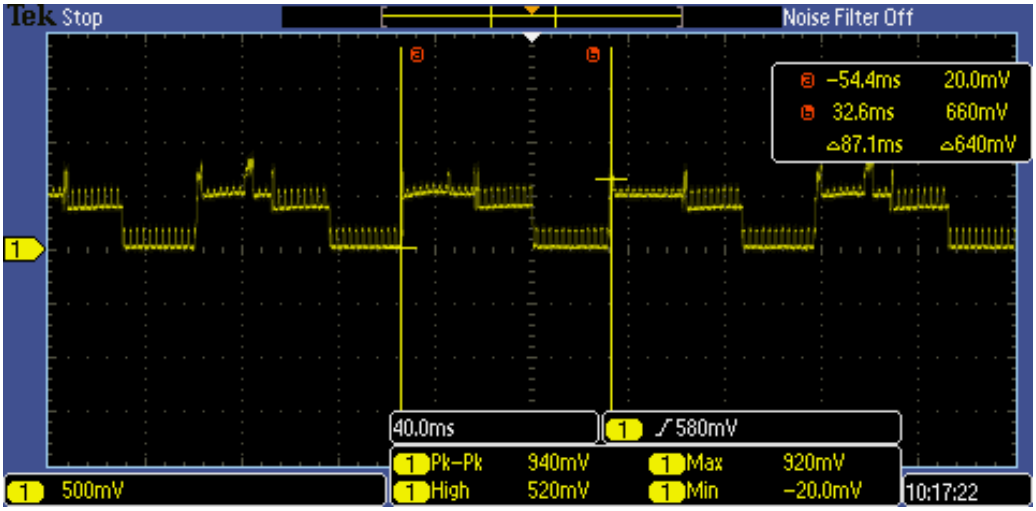

(C) AudioMoth SBC in recording state at a 192 kHz sampling rate.

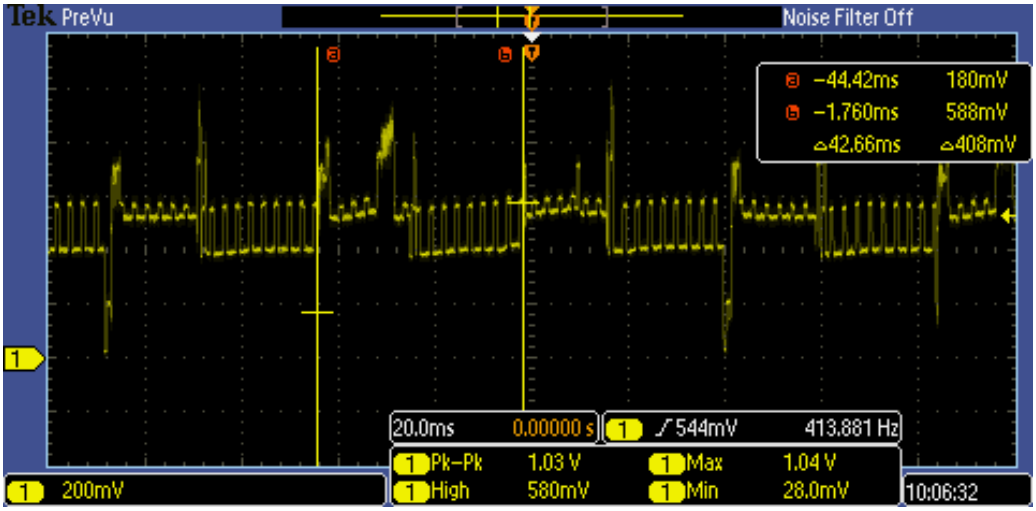

(D) AudioMoth SBC in recording state at a 384 kHz sampling rate.

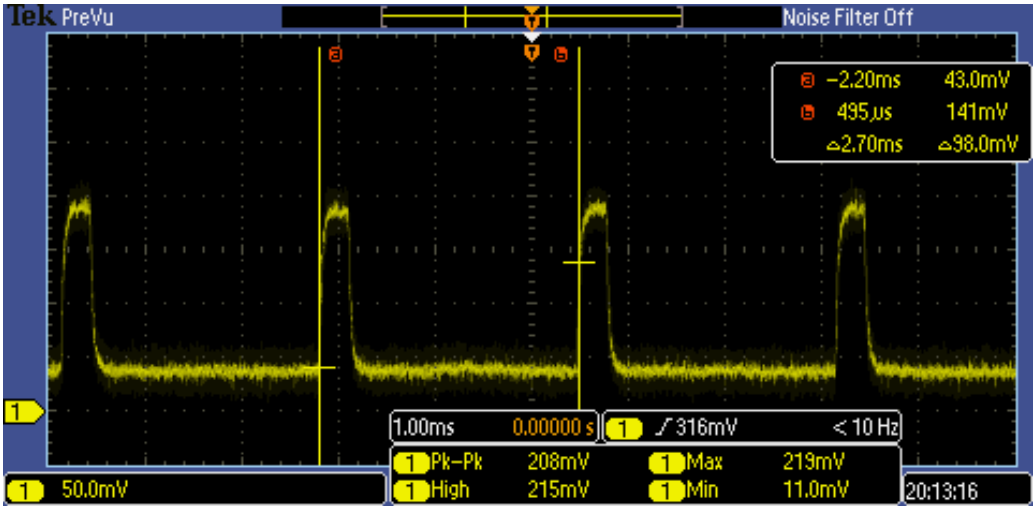

(E) AudioMoth PCB in recording state, close up on recurring frequent peaks.

Figure 5.4: Current sense oscilloscope measurements.

5.2.2 Current Sense Continuous Recording Test

Table 5.2: Biophone v1.0 and v1.1 PCB current consumption metrics.

Parameter	**v1.0 (NiMH, 10Ah)**		**v1.1 (Li-ion, 30Ah)**	
	A board	**UI board**	**A board**	**UI board**
Maximum Amperes (mA)*	181.49	130.43	178.76	138.85
Maximum Instantaneous Power Consumption (mW)†	598.91	430.40	589.90	458.19
Minimum Amperes (mA)*	-0.11	0.32	1.17	-2.13
Minimum Instantaneous Power Consumption (mW)†	-0.35	1.05	3.86	-7.02
Average Amperes (mA)*	23.51	61.06	22.13	60.23
Average Power Consumption (mW)†	77.59	201.51	73.02	198.75
Root Mean Squared Amps (mA)*	34.15	61.70	31.28	60.83
Root Mean Squared Power Consumption (mW)†	112.69	203.62	103.21	200.73
Recording duration (day hour minute second)‡	04d 16h 43m 28s	04d 20h 37m 37s	25d 00h 52m 51s	07d 16h 25m 23s
Total amp-hours consumed§	11.98		30.16	
Total watt-hours consumed§	57.26		127.60	
Stated reason for the end of recording‖	Low voltage cutoff	Low voltage cutoff	Low voltage cutoff	Insufficient storage space on SD card

* Values were calculated using the GL900APS desktop application and converted to current using eq. (4.2.1).
† Calculated using $P = V \times I$, where V is the AudioMoth SBC's internal regulated voltage of 3.3 V.
‡ Values from visual inspection of the data in the GL900APS desktop application.
§ Calculated using the sum of root mean square values of each A/UI board multiplied by its recording time.
‖ Paraphrased from the .wav file metadata "comment" parameter.

Table 5.3: Biophone v1.0 and v1.1 battery voltages over time.

Parameter	v1.0 (NiMH, 10Ah)	v1.1 (Li-ion, 30Ah)
Voltage at start, before recording (V)*	5.405	4.188
Voltage minimum, at end of recording (V)*	3.110	3.150
Time elapsed (day hour minute second)†	04d 20h 37m 37s	25d 00h 52m 51s

* Values were calculated using the GL900APS desktop application.
† Values from visual inspection of the data in the GL900APS desktop application.

Table 5.2 shows the metrics for current consumption by the AudioMoth SBCs over time. The final calculated consumed watt-hour values closely resemble those expected of the 10 A h and 30 A h ratings for the batteries of v1.0 and v1.1 respectively. In both versions, the A boards have the higher maximum amperes, reflecting the large spike around the square waves in the oscilloscope readings. But in both designs, the UI boards have the higher average current/power and RMS values, reflecting the more frequent power-consuming square waves shown in the oscilloscope readings. In this configuration, the UI board represented ~65% of the watt-hour power-consuming load (using RMS values). Or, put another way, the UI board consumed ~2 times the power.

Table 5.3 shows the battery voltage metrics over time. The recording time for v1.1 (30 A h Li-ion battery) was ~5 times the length of the recording time for v1.0 (10 A h NiMH battery) running for ~25 days versus ~4.8 days. This significant increase over the ratio of amp-hour capacity between the batteries can be explained by the fact that the higher-consuming UI board, sampling at 384 kHz, switched off to standby mode due to insufficient SD card storage after 7.7 days, thereby removing what constituted a significant portion of the load. That said, similar to what was observed in the field study, a portion of the audio collected had artificial noise and recordings were cut short, making the actual useful recording time for the devices as **3.91 days** and **24.73 days** for the v1.0 and v1.1 respectively. Figure 5.5 shows the "drumming" artificial noise appearing again in the lab. Upon visual inspection, the noise appears

to repeat every 340 ms, as with the square waves when sampling at 48 kHz in fig. 5.4, which was the sampling rate of this recording.

The final battery voltages as recordings cut off in table 5.3 were similar for both versions; around 3.1 V. This is noticeably 0.2 V below the stated operating voltage of the AudioMoth board and LT1761 voltage regulator. This indicates that the cutoff voltage, set by the MCU, has some tolerance/inaccuracy.

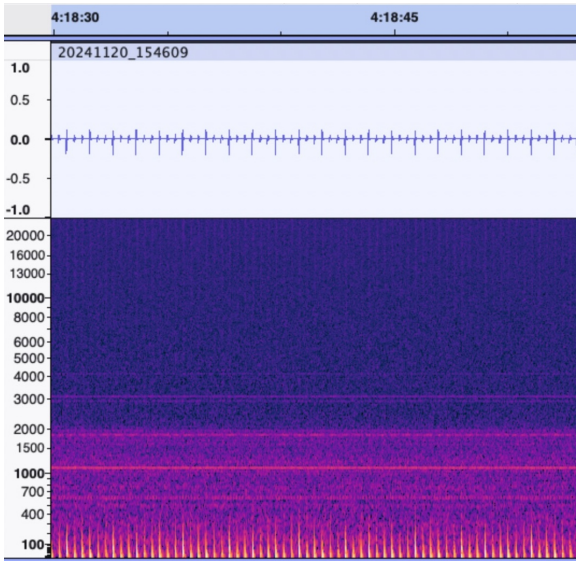

Figure 5.5: Artificial "drumming" noise observed during the continuous recording test.

Figure 5.6 shows the key moments of activity of the v1.0 and v1.1 devices over the recording period. These include booting up, the A board of the v1.0 stopping recording, the UI board of the v1.0 stopping recording, and the UI board of v1.1 stopping recording. The reasons cited for the v1.0 boards stopping in the metadata is low voltage, while the UI board of v1.1 stopped due to a full microSD card. There are some noticeable dips throughout the recording period in the battery voltage of v1.0, corresponding with the larger peaks of the consuming boards, particularly the peaks in the A board, which were shown to have a higher maximum current in table 5.2. There are smaller, but also noticeable dips in the v1.0 battery voltage, also corresponding to the larger current peaks.

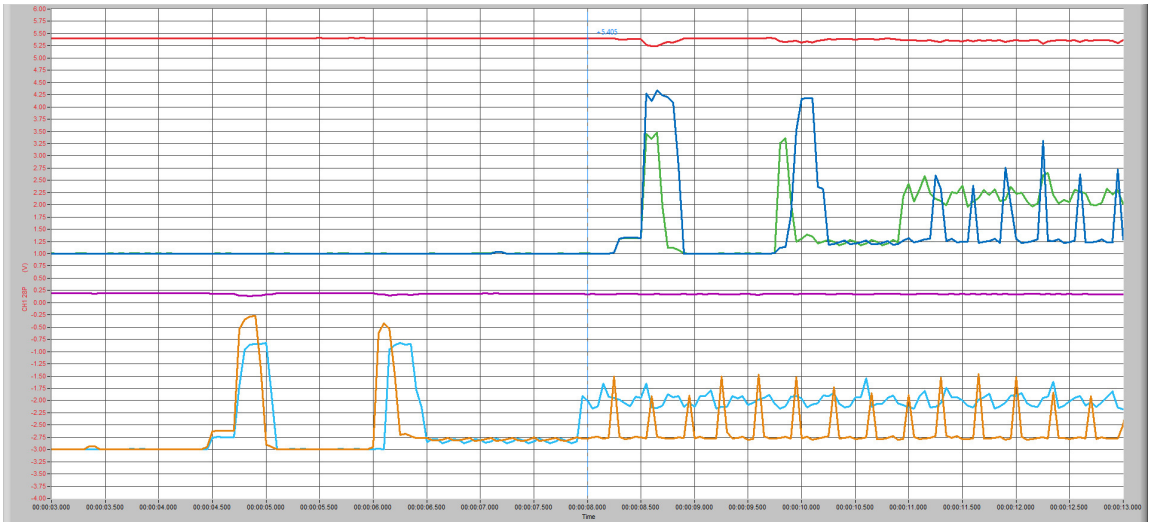

(A) Current measurements of the preconfigured V1.0 and v1.1 device boards starting up.

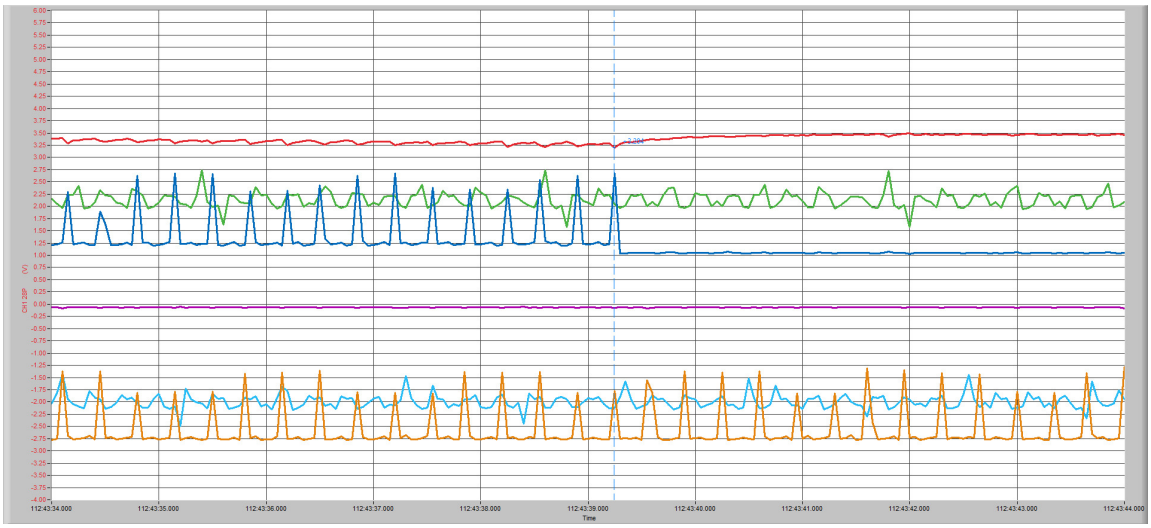

(B) Current measurements of v1.0 A board low voltage cutoff.

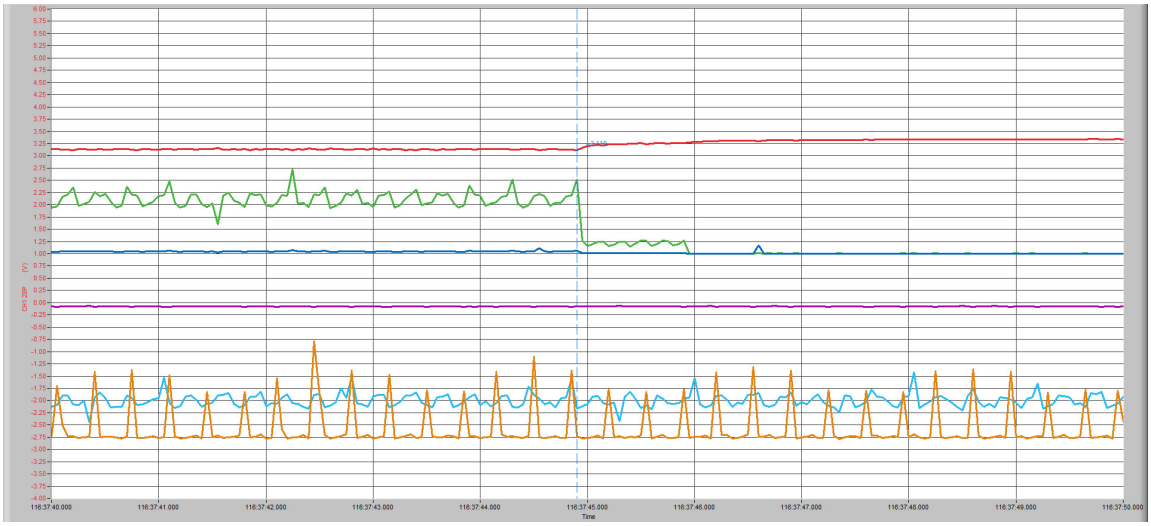

(C) Current measurements of v1.0 UI board low voltage cutoff.

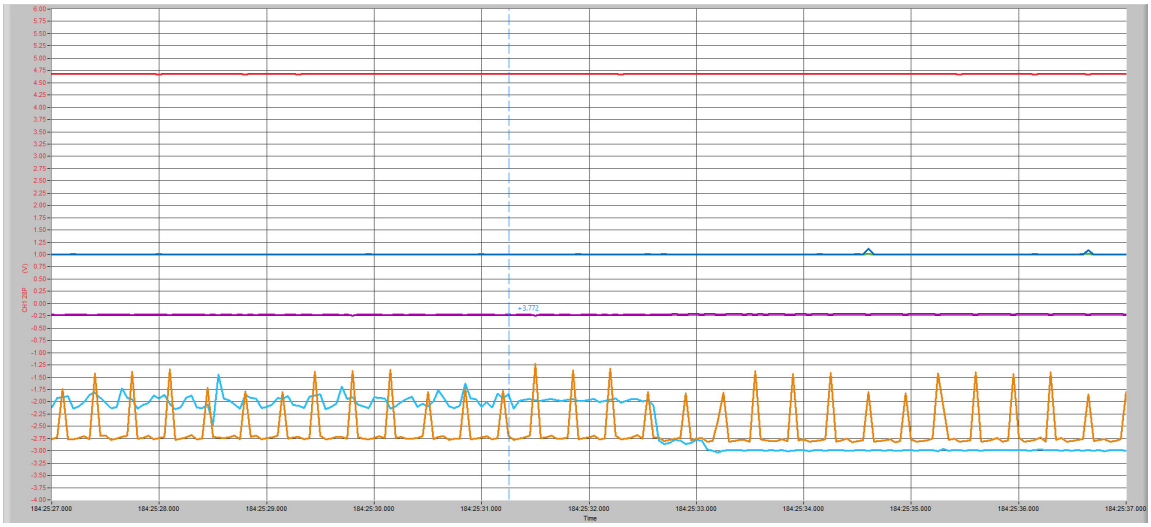

(D) Current measurements of v1.1 UI board running out of storage space.

Figure 5.6: The current cense logger measurements.
Colours key:
v.1.0 device (10Ah NiMH battery):
Red: Battery Voltage, Dark Blue: A board current, Green: UI board current.
v.1.0 device (30Ah Li-Ion battery):
Purple: Battery Voltage, Orange: A board current, Light Blue: UI board current.

6. Discussion

6.1 Field Study Discussion

6.1.1 Field Study Deployment Time

During this deployment of v1.0 devices, the minimum real deployment time of 23 days was significantly less than the expected 35 days calculated with the AudioMoth Configuration App. Based on this observation, v1.1 was proposed and built for future deployments, with a larger 30 A h Li-ion battery pack (see section 3.2). As for this particular deployment, several factors could have played a part in this observed difference. The most likely candidate is the intrinsic increased power consumption of the Samsung Evo Select SD cards over the Sandisk Extreme values that the AudioMoth Configuration Application calculations are based on [85]; this and other power-consuming components are discussed in section 6.2. In terms of environmental effects on the hardware, it has been observed that higher temperatures, as one would expect in the deployment month of June, can increase the self-discharge rate. That said, Sato and Yagi argue that this is likely negligible for most applications, due to commercial NiMH batteries' inherently low self-discharge rate [175].

As for the observed drumming noise cut-short .wav files, there are a few potential causes. These are discussed in greater depth in section 6.2.3

6.1.2 Field Study Acoustic Data Analysis

In terms of the acoustic data analysis, the number of rare and endangered bird species is noteworthy. This could suggest that the Rhiwlas Estate provides a positive example of low-impact livestock grazing of land, without the detrimental effects on

biodiversity. This is in contrast to more intensive farming practices that would remove these microhabitats in favour of traditional grass or mono-crop. Having said that, the vocalisations identified in BirdNET, and the corresponding species list generated, were not validated with a chartered ornithologist, so it is uncertain that 100% of these species were true positives. Thus, future research should seek to fully validate this data. For those rare birds that were correctly identified, it should be reiterated that the UK's current biodiversity intactness is particularly poor, as noted in the global analysis by Newbold et al. [18]. So, once common species that may have been present in higher numbers in the past 50 years are now on the amber and red list.

Regarding the lack of identified bats, this could be attributed to the fact that all sites consisted of low grassland, shrub or bracken and were far from any typical roosts of bats, such as caves, buildings, cliffs, or tree hollows. This coincides with Fuller et al.'s findings when mapping this particular area of Wales and defining this area as low in suitable bat habitats [176]. In terms of the unidentified ultrasonic call, there are a few possible candidates. First, it could be a missed identification of a bat by Kaleidoscope. Alternatively, the ultrasonic signatures could be from another taxa group not identified by Kaleidoscope's classifier. For instance, several species of bush crickets in the UK have been observed to routinely stridulate from 20 kHz to 40 kHz [177]. To determine the true answer, an expert in identifying these taxa should examine the data. As this ultrasonic signature was not found in the lab test ultrasound recordings, electrical noise was deemed less likely to be the cause, but further research would be required to fully rule this out.

As for the acoustic indices plots, the visual separation of values for each site could suggest that there is a discernible acoustic difference between microhabitats when data is aggregated in this format. This may be a useful indicator of habitat type, restoration levels or reference for biodiversity levels between sites. However, as noted in section 2.1.3.3, sound can travel differently dependant on the surrounding environment, and this could have skewed acoustic indices values for each site. For instance,

the denser and taller surrounding vegetation naturally present in certain microhabitats (such as Bracken) can absorb more sound reduce index values. Alternatively, the sites with greater exposure to wind, such as the Acid Grassland site, could have had skewed data due to more regular masking by wind. A more comprehensive study would be required to investigate this, with the potential need to ground-truth indices with an ecological survey of each sites' fauna, as recommended by Alcocer et al. [37]. Regarding the peaks between 04:00 am and 06:00 am in the ACI and BI and NDSI plots, these do correlate with the anticipated time of the "dawn chorus", when many UK species of bird have been observed to be most actively vocalising [173]. The stronger dawn chorus in the bracken and bog habitats suggests a potential greater bird diversity in these sites [178], but again, this would require further study.

6.2 Lab Tests Discussion

6.2.1 Current Sense Circuit Discussion

Since the intermediary circuit was built on a breadboard, it is, by nature, prone to resistance, inductive losses, stray capacitance and noise. Bryant points out that any length of conductor will have resistance, inductance, and capacitance wherever two conductors are separated by a dielectric, such as between adjacent columns or protruding wires. This is especially important to consider when switching high-frequency analogue signals, and specialist breadboards or PCBs are recommended in this case [179].

In terms of resistance, Bryant calculates that 10 cm of 1 mm copper track has 45mΩ of resistance at 25°C and points out that this is even higher at high frequencies due to impedance and the "skin effect"[179]. For this circuit, the resistance may have meant a slightly uneven power supply and differences between ground return paths, due to a voltage drop across the conductor, but given the much higher resistance of

the load, it is likely to have had a small effect.

In the case of inductance, this would increase with a longer conductive path travelled through the components and breadboard terminal strips/power rails. This would be particularly obvious in the longer routes taken by the power rails, connecting the battery to the AudioMoth SBC and connecting the power supply to the Op-Amps. This may explain some of the dips in voltage when more significant current was being drawn in table 5.2. Thus, future designs would benefit in accuracy by being built with components packed more closely together, as a bespoke PCB, with minimal trace length between components.

That said, any potential crosstalk, caused by capacitive and inductive coupling from parallel wires, or between adjacent columns, should also be considered when designing a future current sense PCB or improved breadboard design. A PCB solution should observe proper grounding techniques, may require extra spacing, should avoiding adjacent signal layers, and may require Faraday shields to be put in place. Some crosstalk was observed by this author when testing with INA138 Op-Amp signal lines to the buffer closer together on the breadboard in section 4.2.1 and was avoided by spacing these out.

In terms of the skin effect or impedance, the switching frequency observed in oscilloscope readings was relatively low, with the most frequent regular 2.7 ms signal lasting 800 µs, or switching at ~1.250 kHz. So, the inherent resistivity of copper (ρ) and the corresponding voltage drop across the breadboard terminal strips/power with length are likely to play more of a role. Similarly to before, a bespoke PCB considering all these factors would be a possible solution, but for this project the losses were within the margin of error.

6.2.2 Current Sense Oscilloscope Measurements Discussion

Having personally communicated with A. Rogers from Open Acoustic Devices (OAD) (the creators of the AudioMoth SBC) he was able to point to the origin of the visible peaks in current in these tests [180].

For the small peaks every ~2.7 ms, shown in fig. 5.4, these signal the MCU processor powering up at the end of each DMA transfer. The frequency of this signal, at ~370 Hz, is related to the steps taken in the MCU. The AudioMoth's ADC samples at the maximum device sample rate of 384 kHz, irrespective of the configured sample rate. There are 1024 samples then sent to a buffer, via the MCU, in the PCB's SRAM, while the MCU processor is asleep. When this buffer is full, another buffer is automatically switched to by the DMA interrupt. This switch triggers the processor to wake up and handle the data. The processor activating and performing computational operations draws more significant current and so leads to these regular peaks [180]. Since the ADC is sampling at 384 kHz and will switch buffers every 1024 samples this can be calculated as:

The AudioMoth Processor ADC DMA cycle

$$\frac{1024\,\mathrm{S}}{384\,000\,\mathrm{S\,s^{-1}}} \approx 0.0027\,\mathrm{s} \tag{6.2.1}$$

Where S is samples and $\mathrm{S\,s^{-1}}$ is samples per second [180]

As for the larger square waves, according to Rogers, these represent the current drawn to write data from the SRAM to the SD card flash memory. For each DMA interrupt, the raw ADC samples are averaged, filtered and copied to one of eight 32 kB buffers within a circular buffer. Once each 32 kB buffer is full, a SD card write is triggered [180]. This works out as:

AudioMoth Write to SD Card Timing Calculation

$$\frac{\frac{32\times1024\,\mathrm{B}}{2\,\mathrm{B\,S^{-1}}}}{48\,000\,\mathrm{S\,s^{-1}}} = 341\,\mathrm{ms} \tag{6.2.2}$$

Where B represents bytes, $\mathrm{B\,S^{-1}}$ represents bytes per sample and $\mathrm{S\,s^{-1}}$ represents samples per second

In previous literature, it has been noted that energy consumption during microSD card writes can vary drastically between brands, as is shown in fig. 6.1. Hill et al. also write that the SD card represents the highest power-consuming step of the device recording [112]. It might be assumed that the brand used in this study, the Samsung Evo Select SD card range, would behave similarly to the Samsung Evo Plus range in fig. 6.1, although comprehensive datasheets are not publicly available. However, based on the RMS mA values in table 5.2 it seems the performance of the SD cards is more towards the bottom of this table, with an averaged RMS current of 32.72 mA (107.98 mW) consumed at 48 kHz and 61.27 mA (202.2 mW) consumed at 384 kHz. This meant that together the boards consumed 310.17 mW of power at maximum load. Thus, even with an external microphone and switch LED, was still more efficient than the Raspberry Pi-based SOLO BAR that consumed 350 mW while recording at 48 kHz [109].

Some of the additional power consumption on the A board can be attributed to the PIP microphone. But, according to the product datasheets, this would contribute a negligible additional amount, consuming 550 µA [148]. Instead, the attached switch LED may be consuming more power, at ~13 mA per flash. In the oscilloscope readings, this may be contributing to the large spikes in the square wave, as the LED flashes with every SD card write. No other increase in the height of the square wave or waveform more generally was observed between SBCs with the switch LED plugged in or not. This may go some way to explaining the higher power consumption of the A board sampling at 48 kHz, of 32.72 mA, versus the Evo Plus value of 21.1 mA in fig. 6.1, an increase of 55%, although further investigation is required. Future designs of the Biophone could avoid this additional power consumption by removing

the switch LED or using a larger resistor to reduce current from the 3 V output header. Another option would be to develop some custom firmware that switches off all LEDs after 15 minutes, allowing observation by the user of the correct flashing to indicate the device is recording, but reducing the power consumed over time.

For the UI board, the majority of the power consumption can be attributed to the Evo Select 512 GB SD card, as no additional microphone or LED was plugged in. This value of 61.27 mA consumed at 384 kHz represents a 91% increase in power consumption over the Evo Plus, of 32 mA in fig. 6.1. It has also been observed by Hill et al. that different GB of SD cards of the same brand can vary in their power efficiency during, so could be an additional cause, on top of differences between the Evo Plus and Evo Select [112]. A future study could investigate these differences. But, for the purposes of this device, using a more efficient brand of SD card, such as the SanDisk Extreme cards, might be the best course of action in in future deployments.

	Average consumption (mA)			
	16kHz	48kHz	192kHz	384kHz
SanDisk Extreme 32GB	9.8	12.3	24.1	38.5
ADATA Premier Pro 64GB	9.9	12.7	26.3	39.8
SanDisk Extreme 64GB	10.6	14.5	33.7	43.5
Lexar Professional 64GB	10.8	15.7	37.5	55.0
SanDisk Extreme 128GB	11.4	16.9	45.4	55.1
Samsung Evo Plus 64GB	21.1	22.2	26.3	32.0
Kingston CANVAS Go! Plus 64GB	41.0	42.0	47.1	52.3
SanDisk Ultra 256GB	55.5	57.1	67.6	70.7

Figure 6.1: The power consumption of different brands of SD cards in the AudioMoth. Taken from [181].

In his communications, Rogers speculates that the effect of the different SD cards on oscilloscope reading could result in a higher base current consumption, moving the whole waveform up, as well as a higher square wave with SD card writes. In addition, he notes that between SD writes the card is still powered on, but in a standby mode, where the power consumption of this standby mode can vary from card to card. Furthermore, the different write speeds and write currents could result in square

waves of differing height and widths. Given that the SD cards have internal load balancing protocols and delete and write pages autonomously, this might provide another explanation for the large spikes around the square wave. The AudioMoth MCU continues to send data in 512 B chunks during this time, but the SD card microcontroller does a significant amount of internal work upon receiving this data, which can make them non-determininistic [180].

6.2.3 Current Sense Continuous Recording Measurements Discussion

As would be expected, the amp-hour capacities for the 10 A h v1.0 NiMH battery and 30 A h v1.1 Li-ion battery had a significant effect on the recording time: **3.91 days** for the v1.0 and **24.73 days** for v1.1 respectively. That said, it's clear in both versions of the Biophone that having the UI board record continuously at a 384 kHz sampling rate is impractical for most real-world deployments. This is both because of how rapidly the power is consumed, at 2 times the power, and the size of the data generated (a 512 GB in ~7 days). For future in-the-field deployments, it would be sensible to limit ultrasonic recording as much as possible, relying on a more restrictive and bespoke schedule, or using the frequency or amplitude trigger configurations available in the configuration app. Hill notes that, for many environments, the spectrum above 16 kHz is typically quiet [7], so using the amplitude/frequency trigger that the AudioMoth Configuration App offers might be the best configuration.

In addition, the observed dips in battery voltage that correspond with the larger peaks of the consuming A and UI boards suggest that greater power decoupling capacitors prior to the linear regulators of the Audiomoth boards might be required. This would be to avoid the voltage unnecessarily dropping below the 3.6 V threshold required by the LT1761 regulator (V_{cc} of 3.3 V plus the dropout voltage of +0.3 V [182]), with the large current peaks from the boards. Rogers has also stated that future versions of the AudioMoth may substitute the linear regulator with a voltage

booster IC chip to get the maximum capacity out of the batteries [183]. The power decoupling and voltage booster IC chip should be explored in future research to further extend effective deployment time.

6.2.4 Artificial Noise, the Probable Cause

In forum posts on this topic on the OAD website, Rogers says that the SD cards can create mechanical noise when writing, which then gets transmitted through the microphone via the board and casing. The previously observed behaviour is that this noise becomes more apparent as the battery voltage gets close to the minimum voltage required by the SD card and other components in the board. This would explain why the frequency of the noise matches that of the square waveforms every 340 m sec, corresponding to the SD writes. In the OAD team's observations, the brand of SD card used also has an impact on the amount of mechanical noise generated, with SanDisk Extreme cards being less prone to this issue. This noise is both electrical and mechanical and is due to the high write currents used by SD cards, which requires internal capacitors that physically expand and contract with the write current [183], [184]. Physically separating this noise from the microphone might go some way to alleviate this problem in a future design. This could be achieved using acoustic foam inside the box, to shield from sound and rubber matting underneath the AudioMoth SBCs to absorb vibrations. That said, as this noise only occurs towards the end of the battery life, the gains in additional recording time would be unlikely to be worth the cost.

7. Conclusion

7.1 Key Takeaways

The purpose of this research project was to design and develop a BARs device using cheap and low-powered components that could be assembled and deployed by experts and non-experts alike. It also aimed to investigate the power-consumption characteristics of the device and how it would handle real-world deployments.

The project undertook a literature review to explore the underlying theory and technologies behind BARs and was able to identify a market/research gap based on the literature and current commercially available BAR devices. The review supported the rationale of building off the AudioMoth Developer SBC and building in modular additional features that could be added to improve functionality and usability. These included additional battery capacity using two parallel AudioMoth SBCs (labelled "A" and "UI") for multiple sample rates/schedules, a higher quality microphone, an external switch, and a durable enclosure. This device, the Biophone, was then built and tested.

The product development of the prototype Biophone involved 3D printing of fixings, waterproofing, wiring, drilling, soldering and assembly that was then replicated en masse in a workshop with students from Coleg y Cymoedd (CYC), demonstrating the potential for non-expert assembly. Two versions of the biophone were built and tested. V1.0 used a 10 A h NiMH battery. V1.1 built off of feedback from the assembly workshop and the field test. It had a 30 A h Li-ion battery for longer deployments, a custom PCB for easier assembly and maintenance, and a larger microphone capsule for easier soldering. Both versions had a material cost of ~£300.

The field deployments of v1.0 showed the device could be used in an outdoor environment by non-experts for species and biodiversity surveys. During this deployment,

the Biophone V1.0 was able to record for 23 days on a bespoke schedule for each of the boards. 26 species of birds were identified on site, many of which were rare or endangered. Also, an unique unidentified ultrasonic signature was captured. However, further research is required to determine if this was of biological origin and, thus, determine the Biophone's effectiveness at capturing ultrasonic vocalisations. Evaluation of acoustic indices of the site showed a strong "dawn chorus" of birds in each site and visible differences of acoustics between sites.

Both V1.0 and V1.1 were tested in the laboratory. These tests demonstrated the power consumed by the Biophone when boards were continuously recording at audible and ultrasonic sampling rates; the maximum power consumption levels that could be expected. Under these conditions, the v1.0 has a useful recording time of 3.91 days, and the v1.1 lasted 24.73 days. A mean Root Mean Square (RMS) of 32.72 mA (107.98 mW) was consumed at 48 kHz on the A board and 61.27 mA (202.19 mW) was consumed at 384 kHz on the UI board. The total RMS consumption of the device was therefore 139.78 mA (310.17 mW). This was at the higher end of the SD card consumption table by AudioMoth in fig. 6.1 [181]. Thus, the tests highlighted the importance of microSD card choice, both in terms of power consumption and a mechanical noise that was observed at the end of the recording period. Having said that, even with an external microphone switch, LED and two boards consuming at maximum power, the device was more efficient than a Raspberry Pi-based BAR device, the SOLO, which consumes 350 mW while recording at 48 kHz[109]. Furthermore, the total device consumption at the maximum power consumption levels are close to this value for the SOLO, while recording on two separate boards. That said, these results show the necessity of strictly limiting recordings at the ultrasound level with more bespoke scheduling or using an amplitude/frequency trigger for initiating ultrasonic recordings.

In summary, the tests show that the Biophone is suitable for recording wildlife by experts and non-experts with the considerations above. The devices were able to record for long periods with considered scheduling. This device design can continue

to be updated and improved (see section 7.4) but was able to fulfil its intended use case and can be used for further wildlife monitoring.

7.2 Contribution

This project demonstrates methods, key considerations and trade-offs for building and deploying a BAR with non-expert end-users. All designs, insights and components are available for other researchers to use, with a list of components provided in table A.1, in the appendix. This project also demonstrated the applicability of building off of the AudioMoth Developer SBC with peripheral hardware, leaving room for further add-on features to be explored.

7.3 Limitations

This study worked within the confines of limited resources and time. There were additional tests into aspects of the devices that were not able to be undertaken due to these constraints that might otherwise have been achievable with a larger team of researchers. These are discussed more in section 7.4.

The sample size for both the field test and the lab tests are limited to 2 and 5 devices, respectively. This could be improved on by undertaking multiple recordings on multiple devices with multiple controlled and logged environmental parameters in the future.

The power tests RMS calculations were limited by the USB stick memory when plugged into the GL900 voltage logger, which was restricted to a minimum 50 µs sample rate in order to record over 11 days. This meant the waveforms had a lower resolution than the oscilloscope readings.

The field tests were limited in the number of man-hours that could be expended by

the deploying groups. In addition, there were elements of human error, with one of the A boards not recording (due to the internal clock not being set beforehand), and this had to be supplemented in the analysis data.

Analysis of the data with acoustic indices also carries a margin of error, due to the effects of other non-biological sounds, which require additional work to filter out. BirdNET itself does not account for all the different calls some species of bird with a larger vocal repertoire can make, such as the blackbird and song thrush, which have also been known to mimic and blend other birdsong, so false positives/negatives remain possible without scrutiny from bird experts.

7.4 Future Works

On top of suggestions made in the discussion, further research and iteration could be done to optimise the Biophone's design and functionality. These would be necessary to further scale up deployments and meet the needs of academics and non-expert practitioners. Such future works could include:

1. Further reducing size and cost. While having two AudioMoth PCBs was necessary for this study to have independent schedules and sampling rates, an improved device would make use of one PCB, with custom firmware to switch between sampling rates and microphones.

2. Building in remote communication capability. This can include local connectivity, such as Bluetooth and Wi-Fi, or long-range communications, such as Long Range (LoRa) radio or cellular. This could enable remote control of the device, reporting of device diagnostics, or streaming of audio/highlights from a distance, avoiding unnecessary visits to deployment sites. While this has been done in other BAR devices, it has not yet been done for the AudioMoth Dev platform. Though any attempt to do so should seek to not undermine the AudioMoth PCB's key strengths in power efficiency and cost. In addition,

many sites have limited cellular coverage, so bandwidth of data transmission may have to be limited.

3. Further improving user-friendliness. An Organic Light-Emitting Diode (OLED) screen or phone application to show the recording status, battery life and storage space of the device would help understanding and avoid some potential human errors. Some common mistakes observed in test runs being: not syncing the clock, not charging batteries, or replacing SD cards. This would require developing custom firmware hardware and software.

4. Linking GPS and building for synced arrays. OAD have recently released a GPS unit that allows for this, and the investigation of the communication protocol used for this add-on should be investigated when adding additional components.

5. Building in additional sensors to link climate and animal behaviour. In particular, temperature, light, pressure and humidity have been shown to play a key role in triggering hatching, feeding, migration, breeding of several species, as well as their vocalisations. For instance, crickets will stridulate according to these factors [185]. Having these sensors might also enable more accurate localisation and distance prediction of sounds, as discussed in section 2.1.3.3.

6. Building in the capability to power devices with renewable power, like solar panels, to extend deployment time in the field. This is only possible in locations with unobstructed and regular sunlight, so it may not be suitable in certain deployments, such as on the forest floor.

A. Appendix

A.1 Biophone Components

Table A.1: A component list of Biophones v1.0 and v1.1.
Where CNPD is Component Number Per Device and TC is Total Cost. All prices are in GBP, according to date of last purchase in December 2023. Modifications made to components during the build process are also detailed. The overall device cost and number of components are listed in the last two rows.

#	Description	Purpose	Manufacturer	Part Number	Part Cost	Modifications	v1.0		v1.1	
							CNPD	TC	CNPD	TC
1	PVC A1 foam board, (0.041 m2)	Packing foam for stacking and holding lid when device is open	The Range, artstudio	823571	£0.16	Cut into 17x12mm rectangles, doubled up and holes drilled to accommodate acoustic horns	1	£0.16	1	£0.16
2	Polycarbonate enclosure	Enclosure	Multicomp Pro	MC001109	£12.62	Drilled holes in lid to accommodate screws from 3D printed board holders and acoustic horns, as well as external swicth. Drilled hole in base for pressure/ condensation release valve.	1	£12.62	1	£12.62
3	Micro SD card, 512GB.	MicroSD card for, AudioMoth UI board data storage	Samsung	Evo Select, MB-ME512KA/ EU	£59.99	NA	1	£59.99	0	£0.00
4	Micro SD card, 256GB.	MicroSD card for, AudioMoth A board data storage	Samsung	Evo Select, MB-ME256SA/ EU	£24.89	NA	1	£24.89	1	£24.89
5	Pressure/ condensation release valve	Releasing internal pressure and humidity	Selectronix Onboard	SEL-3404BN	£2.48	NA	1	£2.48	1	£2.48

Continued on next page

Table A.1 – continued from previous page

#	Description	Purpose	Manufacturer	Part Number	Part Cost	Modifications	v1.0		v1.1	
							CNPD	TC	CNPD	TC
6	Acoustic vents/water-proof membranes	Micorphone hole waterproof cover	Huizhou Sinri Technology Company Limited	SEL-3391-10/7	£0.16	NA	9	£1.44	9	£1.44
7	External on/off switch with LED	External On/off switch	RS PRO	111-6518	£3.42	NA	1	£3.42	1	£3.42
8	Fuse, 2A	Fuse for battery power	Littelfuse	0287002. PXCN	£0.20	NA	1	£0.20	1	£0.20
9	Fuse connectors, female Quick Disconnects	Fuse connectors	Heschen	NA	£0.15	NA	2	£0.30	2	£0.30
10	Resistor, 220 Ohm	Resistor For switch LED	KOA	CFS1/ 2CT52A221J	£0.04	Soldered to wires	1	£0.04	1	£0.04
11	Heat Shrink Tube (0.06 m)	Heat shrink wrapping	RS PRO	399-912	£0.02	Cut to size, shrunk to wires	5	£0.12	0	£0.00
12	Cable Tie Base, Black, 19x19mm	For cable-tying wires to the inside of the box	PRO POWER	PP01523	£0.40	NA	4	£1.60	4	£1.60
13	Cable ties, 100mm x 2.5mm, Black Nylon	For cable-tying wires to the inside of the box	RS PRO	233-455	£0.03	Excess cut off	5	£0.16	5	£0.16
14	Screws, Panhead, 10mm. 3.0	For screwing components together	Utility Fsteners	6031030010	£0.02	NA	2	£0.04	7	£0.14
15	Screws, Panhead, 6mm. 3.0	For screwing components together	Utility Fsteners	6031030006	£0.02	NA	7	£0.14	7	£0.14
16	Screws, countersunk, 10mm	For screwing components together	Utility Fsteners	06035030010	£0.02	NA	2	£0.04	2	£0.04
17	Screws, panhead, 9.5mm	For screwing components together	RS PRO	546-5654	£0.02	NA	4	£0.08	4	£0.08
18	Washer, M3	For screwing components together	RS PRO	560-338	£0.03	NA	4	£0.12	4	£0.12
19	Acrylic 3mm sheet for fixing battery holder (0.014 m2)	Plastic plate for fixing the NiMH battery holder to	Sheet Plastics	6923CTS	£0.39	Laser cut	1	£0.39	1	£0.39

Continued on next page

Table A.1 – continued from previous page

#	Description	Purpose	Manufacturer	Part Number	Part Cost	Modifications	v1.0		v1.1	
							CNPD	TC	CNPD	TC
20	3mm polycarbonate baffle for PCBs (0.008 m2)	See through plastic baffle for protecting the AudioMoth SBCs from touch	Sheet Plastics	PCC3CTS	£0.58	Laser cut	1	£0.58	1	£0.58
21	Red wire (0.10 m)	For wiring power components together	Alpha Wire	3251 RD005	£0.01	Cut to size and crimped/soldered	2	£0.02	0	£0.00
22	Black wire (0.10 m)	For wiring power components together	Alpha Wire	3251 BK005	£0.01	Cut to size and crimped/soldered	1	£0.01	0	£0.00
23	Blue wire (0.40 m)	For wiring switch components together	Alpha Wire	3251 BL005	£0.01	Cut to size and crimped/soldered	1	£0.01	0	£0.00
24	Pre-made circuit board connectors, PH2, only one end	For plugging into custom PCB	Shappy	NA	£0.06	Crimped	0	£0.00	1	£0.06
25	3 port lever wire connector	3 port lever wire connector	Ideal industries	4198G	£0.10	NA	2	£0.20	0	£0.00
27	Crimps for power leads, female	Crimps for power leads	Wurth Elektronik	6490071 3722DEC	£0.06	Crimped	2	£0.11	0	£0.00
28	Crimps for JST PH headers	Crimps for JST headers	JST	BPH-002T-P0.5S	£0.02	Crimped	10	£0.22	0	£0.00
29	Crimps for 3 way connectors, male	Crimps for 4 way connectors	RS PRO	458-689	£0.05	Crimped	6	£0.30	0	£0.00
30	JST PH2 plugs female	JST PH2 plugs	JST	PHR-2	£0.02	NA	2	£0.04	0	£0.00
31	JST PH3 plugs female	JST PH3 plugs	JST	PHR-3	£0.05	NA	3	£0.14	0	£0.00
32	Pre-made circuit board connectors, JST PH2	For plugging into custom PCB	Shenzhen Holy Electronic Co., Ltd.	NA	£0.15	NA	0	£0.00	2	£0.30
33	Pre-made circuit board connector wires, JST PH3	For plugging into custom PCB	Shenzhen Holy Electronic Co., Ltd.	NA	£0.15	NA	0	£0.00	3	£0.45

Continued on next page

Table A.1 – continued from previous page

#	Description	Purpose	Manufacturer	Part Number	Part Cost	Modifications	v1.0		v1.1	
							CNPD	TC	CNPD	TC
34	Pre-made circuit board connector wires, PH4, only one end	For plugging into custom PCB	Winwill	NA	£0.21	Soldered to switch	0	£0.00	1	£0.21
35	Solderable power lead connectors, XT60 and coloured heatshrink	For connecting battery and power cales	RUNCCI-YUN	NA	£0.30	Soldered to wires	0	£0.00	1	£0.30
36	CT1 TRIBRID Silicone (20 ml, per device).	Waterproofing externals 3D printed components against lid	CT1	NA	£0.89	Spread to waterprood lid components	3	£2.68	3	£2.68
37	AudioMoth Developer board SBC	Principal recording SBC	Open Acoustic Devices	NA	£71.74	NA	2	£143.48	2	£143.48
	NiMH D cells batteries, 10Ah	NiMH Batteries for V1.0 device	EBL	NA	£5.33	NA	4	£21.33	0	£0.00
	D cell battery holder, coil spring contact	Battery holder for v1.0 device	RS PRO	185-4714	£2.37	NA	1	£2.37	0	£0.00
33	Bespoke Lithium power packs 30Ah	Li-ion batteries for v1.1 Biophones	Floreat Energies	NA	£44.20	NA	0	£0.00	1	£44.20
34	Bespoke Battery pack charger for Lithium power packs	Li-ion battery charger for v1.1 Biophones	Floreat Energies	NA	£18.70	NA	0	£0.00	1	£18.70
35	External miccrophone for v1.0. mono module, with 3.5mm plug, 1.5m	Higher quality microphone, connected to A board	Primo	EM258	£22.68	NA	1	£22.68	0	£0.00
36	External miccrophone for v1.1. premade.	Higher quality microphone, connected to A board	Primo	EM272	£29.20	NA	0	£0.00	1	£29.20
37	Rubber sleeve holder 6mm.	Holding the microphone capsule in place, butted up against the microphone hole	FEL	NA	£1.44	NA	1	£1.44	0	£0.00

Continued on next page

Table A.1 – continued from previous page

#	Description	Purpose	Manufacturer	Part Number	Part Cost	Modifications	v1.0		v1.1	
							CNPD	TC	CNPD	TC
	Rubber sleeve holder 10mm.	Holding the microphone capsule in place, butted up against the microphone hole	FEL	NA	£1.32	NA	0	£0.00	1	£1.32
38	Custom power/switch PCB	To distribute power and switching for v1.1	PCBWay	NA	£11.72	NA	0	£0.00	1	£11.72
39	3D printed component PC blend: Plastic acoustic horns (0.015 kg)	To hold components in plcae to lid of enclosure	Prusa	NA	£0.01	3D printed on site	3	£0.03	0	£0.00
40	3D printed component PC blend: Plastic acoustic horn fixing point (0.001 kg)	To hold components in plcae to lid of enclosure	Prusa	NA	£0.01	3D printed on site	1	£0.01	0	£0.00
41	3D printed component PC blend: Plastic PCB-holding bracket (0.009 kg)	To hold components in plcae to lid of enclosure	Prusa	NA	£0.01	3D printed on site	1	£0.01	0	£0.00
43	3D printed component ASA: Plastic acoustic horns (0.015 kg)	To hold components in plcae to lid of enclosure	Prusa	NA	£0.01	3D printed on site	0	£0.00	3	£0.03
44	3D printed component ASA: Plastic acoustic horn fixing point (0.001 kg)	To hold components in plcae to lid of enclosure	Prusa	NA	£0.01	3D printed on site	0	£0.00	1	£0.01
45	3D printed component ASA: Plastic PCB-holding bracket (0.009 kg)	To hold components in plcae to lid of enclosure	Prusa	NA	£0.01	3D printed on site	0	£0.00	1	£0.01
46	3D printed component ASA: Plastic switch cover (0.005 kg)	To hold components in plcae to lid of enclosure	Prusa	NA	£0.01	3D printed on site	0	£0.00	1	£0.01

Continued on next page

Table A.1 – continued from previous page

#	Description	Purpose	Manufacturer	Part Number	Part Cost	Modifications	v1.0		v1.1	
							CNPD	TC	CNPD	TC
						Total number of components	100		75	
						Total cost		£304.04		£301.43

A.2 Bill of Materials For Laboratory Tests

Table A.2: A bill of materials for the intermediary current sense circuit

Item	Part Number	Manufacturer	Number bought (number used)	Symbol in Simulation Figure	Cost* (GBP)
Op-amp (current sense)	INA138	Texas Instruments, Provided by Swansea University	0 (2)	U1 & U2	£0.00
Op-amp (buffer)	OPA340PA	Texas Instruments	5 (2)	U3 & U4	£22.96
0.1Ω resistor	146-9511	RS PRO	5 (2)	Rsense 1 & 2	£20.93
Coloured Wires	NA	Provided by Swansea University	0 (24)	NA	£0.00
Breadboards	NA	Provided by Swansea University	0 (2)	NA	£0.00
				Total costs incurred:	£43.89

* Cost at time of purchase.

Bibliography

[1] J. Artiola, I. Pepper, and M. Brusseau, "Monitoring and Characterization of the Environment", in *Environmental Monitoring and Characterization*, Elsevier, 2004, pp. 1–9, [Online]. Available: https://linkinghub.elsevier.com/retrieve/pii/B9780120644773500035.

[2] J. J. Lahoz-Monfort and M. J. L. Magrath, "A Comprehensive Overview of Technologies for Species and Habitat Monitoring and Conservation", *BioScience*, vol. 71, no. 10, pp. 1038–1062, Oct. 2021, [Online]. Available: https://doi.org/10.1093/biosci/biab073.

[3] O. Metcalf, C. Abrahams, B. Ashington, *et al.*, "Good practice guidelines for long-term ecoacoustic monitoring in the UK", The UK Acoustics Network, Report, Feb. 2023, pp. 1–82, [Online]. Available: https://www.britishecologicalsociety.org/applied-ecology-resources/document/20230136742/.

[4] O. Berger-Tal and J. J. Lahoz-Monfort, "Conservation technology: The next generation", *Conservation Letters*, vol. 11, no. 6, e12458, 2018, [Online]. Available: https://onlinelibrary.wiley.com/doi/abs/10.1111/conl.12458.

[5] C. P. Elemans, K. Heeck, and M. Muller, "Spectrogram Analysis of Animal Sound Production", *Bioacoustics*, vol. 18, no. 2, pp. 183–212, Jan. 2008, [Online]. Available: https://www.tandfonline.com/doi/full/10.1080/09524622.2008.9753599.

[6] S. R. P.-J. Ross, D. P. O'Connell, J. L. Deichmann, *et al.*, "Passive acoustic monitoring provides a fresh perspective on fundamental ecological questions", *Functional Ecology*, vol. 37, no. 4, pp. 959–975, Apr. 2023, [Online]. Available: https://besjournals.onlinelibrary.wiley.com/doi/10.1111/1365-2435.14275.

[7] A. Hill, "Low-cost, open source acoustic sensors for conservation", *University of Southampton*, Jul. 2020, [Online]. Available: https://eprints.soton.ac.uk/452458/1/Final_thesis_unsigned.pdf.

[8] J. Papán, M. Jurečka, and J. Púchyová, "WSN for forest monitoring to prevent illegal logging", IEEE, 2012, pp. 809–812, [Online]. Available: https://ieeexplore.ieee.org/abstract/document/6354360?casa_token=H-I4sLxyKsoAAAAA:N0Bk_9VNwZv6QiSLIwp6yEaUrRsQrvuodQ1kDz229sisgxhwUH4w9a0f532lxxObyrOouyc.

[9] M. A. Bee and E. M. Swanson, "Auditory masking of anuran advertisement calls by road traffic noise", *Animal Behaviour*, vol. 74, no. 6, pp. 1765–1776, Dec. 2007, [Online]. Available: https://www.sciencedirect.com/science/article/pii/S0003347207003314.

[10] N. Alvarez-Berríos, M. Campos-Cerqueira, A. Hernández-Serna, C. Amanda Delgado, F. Román-Dañobeytia, and T. M. Aide, "Impacts of Small-Scale Gold Mining on Birds and Anurans Near the Tambopata Natural Reserve, Peru, Assessed Using Passive Acoustic Monitoring", *Tropical Conservation Science*, vol. 9, no. 2, pp. 832–851, Jun. 2016, [Online]. Available: https://doi.org/10.1177/194008291600900216.

[11] C. Astaras, J. M. Linder, P. Wrege, R. D. Orume, and D. W. Macdonald, *Passive acoustic monitoring as a law enforcement tool for Afrotropical rainforests. | EBSCOhost*, Jun. 2017, [Online]. Available: https://openurl.ebsco.com/contentitem/doi:10.1002%2Ffee.1495?sid=ebsco:plink:crawler&id=ebsco:doi:10.1002%2Ffee.1495.

[12] Verified Market Research, *Wildlife Tracking System Market Size, Share, Trends & Forecast*, Jan. 2023, [Online]. Available: https://www.verifiedmarketresearch.com/product/wildlife-tracking-system-market/.

[13] WWF, *Living planet report 2020* (Living planet report 2020). Gland, Switzerland: WWF, Sep. 2020, [Online]. Available: https://www.wwf.org.uk/sites/default/files/2020-09/LPR20_Full_report.pdf.

[14] D. U. Hooper, E. C. Adair, B. J. Cardinale, *et al.*, "A global synthesis reveals biodiversity loss as a major driver of ecosystem change", *Nature*, vol. 486, no. 7401, pp. 105–108, Jun. 2012, [Online]. Available: https://www.nature.com/articles/nature11118.

[15] C. Perrings, C. Folke, C. S. Holling, and B.-O. Jansson, *Biodiversity Loss: Economic and Ecological Issues*. Cambridge University Press, Jan. 1997, [Online]. Available: https://books.google.co.uk/books?hl=en&lr=&id=fd5z_LGBU7MC&oi=fnd&pg=PR7&dq=Biodiversity+Loss:+Economic+and+Ecological+Issues&ots=Je_51YO2fb&sig=xjXXK4lN8jgLmAyMsardwQjC1h8#v=onepage&q=Biodiversity%20Loss%3A%20Economic%20and%20Ecological%20Issues&f=false.

[16] B. J. Cardinale, J. E. Duffy, A. Gonzalez, *et al.*, "Biodiversity loss and its impact on humanity", *Nature*, vol. 486, no. 7401, pp. 59–67, Jun. 2012, [Online]. Available: https://www.nature.com/articles/nature11148.

[17] V. Beckmann, *Transitioning to Sustainable Life on Land*. MDPI, Nov. 2021, [Online]. Available: http://www.mdpi.com/books/pdfview/edition/1406.

[18] T. Newbold, L. N. Hudson, A. P. Arnell, *et al.*, "Has land use pushed terrestrial biodiversity beyond the planetary boundary? A global assessment", *Science*, vol. 353, no. 6296, pp. 288–291, Jul. 2016, [Online]. Available: https://www.science.org/doi/full/10.1126/science.aaf2201.

[19] M. Cardwell, "The Environmental Land Management Scheme: Public goods and levels of ambition", *Environmental Law Review*, vol. 26, no. 3, pp. 223–232, Sep. 2024, [Online]. Available: https://doi.org/10.1177/14614529241272293.

[20] A. Stuart, A. Bond, A. Franco, *et al.*, *How England got to Mandatory Biodiversity Net Gain: A Timeline*, SSRN Scholarly Paper, Rochester, NY, Jul. 2024, [Online]. Available: https://papers.ssrn.com/abstract=4883170.

[21] L. S. M. Sugai, T. S. F. Silva, J. W. Ribeiro Jr, and D. Llusia, "Terrestrial Passive Acoustic Monitoring: Review and Perspectives", *BioScience*, vol. 69, no. 1, pp. 15–25, Jan. 2019, [Online]. Available: https://doi.org/10.1093/biosci/biy147.

[22] J. A. Zwerts, P. J. Stephenson, F. Maisels, *et al.*, "Methods for wildlife monitoring in tropical forests: Comparing human observations, camera traps, and passive acoustic sensors", *Conservation Science and Practice*, vol. 3, no. 12, e568, Dec. 2021, [Online]. Available: https://research.wur.nl/en/publications/methods-for-wildlife-monitoring-in-tropical-forests-comparing-hum.

[23] B. J. Furnas and R. L. Callas, "Using automated recorders and occupancy models to monitor common forest birds across a large geographic region", *The Journal of Wildlife Management*, vol. 79, no. 2, pp. 325–337, 2015, [Online]. Available: https://onlinelibrary.wiley.com/doi/abs/10.1002/jwmg.821.

[24] J. C. Montgomery and C. A. Radford, "Marine bioacoustics", *Current Biology*, vol. 27, no. 11, R502–R507, Jun. 2017, [Online]. Available: https://www.cell.com/current-biology/abstract/S0960-9822(17)30074-X.

[25] R. P. Schoeman, C. Erbe, G. Pavan, R. Righini, and J. A. Thomas, "Analysis of Soundscapes as an Ecological Tool", in *Exploring Animal Behavior Through Sound: Volume 1: Methods*, C. Erbe and J. A. Thomas, Eds., Cham: Springer International Publishing, 2022, pp. 217–267, [Online]. Available: https://doi.org/10.1007/978-3-030-97540-1_7.

[26] A. C. Hughes, C. Satasook, P. J. J. Bates, *et al.*, "Using Echolocation Calls to Identify Thai Bat Species: Vespertilionidae, Emballonuridae, Nycteridae and Megadermatidae", *Acta Chiropterologica*, vol. 13, no. 2, pp. 447–455, Dec.

2011, [Online]. Available: http://www.bioone.org/doi/abs/10.3161/150811011X624938.

[27] R. Burnham, "Animal Calling Behaviours and What This Can Tell Us about the Effects of Changing Soundscapes", *Acoustics*, vol. 5, no. 3, pp. 631–652, Sep. 2023, [Online]. Available: https://www.mdpi.com/2624-599X/5/3/39.

[28] J. F. Gillooly and A. G. Ophir, "The energetic basis of acoustic communication", *Proceedings of the Royal Society B: Biological Sciences*, vol. 277, no. 1686, pp. 1325–1331, Jan. 2010, [Online]. Available: https://royalsocietypublishing.org/doi/full/10.1098/rspb.2009.2134.

[29] D. Stowell, "Computational bioacoustics with deep learning: A review and roadmap", *PeerJ*, vol. 10, e13152, Mar. 2022, [Online]. Available: https://peerj.com/articles/13152.

[30] D. Nieto-Mora, S. Rodríguez-Buritica, P. Rodríguez-Marín, J. Martínez-Vargaz, and C. Isaza-Narváez, "Systematic review of machine learning methods applied to ecoacoustics and soundscape monitoring", *Heliyon*, vol. 9, no. 10, e20275, Oct. 2023, [Online]. Available: https://linkinghub.elsevier.com/retrieve/pii/S2405844023074832.

[31] A. Napoli, P. R. White, and T. Blumensath, "Quantity Over Quality? Investigating the Effects of Volume and Strength of Training Data in Marine Bioacoustics.", Mar. 2022, [Online]. Available: https://dcase.community/documents/workshop2022/proceedings/DCASE2022Workshop_Napoli_48.pdf.

[32] B. McEwen, K. Soltero, S. Gutschmidt, A. Bainbridge-Smith, J. Atlas, and R. Green, "Active few-shot learning for rare bioacoustic feature annotation", *Ecological Informatics*, vol. 82, p. 102 734, Sep. 2024, [Online]. Available: https://www.sciencedirect.com/science/article/pii/S1574954124002760.

[33] C. Pérez-Granados, "BirdNET: Applications, performance, pitfalls and future opportunities", *Ibis*, vol. 165, no. 3, pp. 1068–1075, 2023, [Online]. Available: https://onlinelibrary.wiley.com/doi/abs/10.1111/ibi.13193.

[34] S. S. Sethi, F. Fossøy, B. Cretois, and C. M. Rosten, *Management relevant applications of acoustic monitoring for Norwegian nature – The Sound of Norway*. Norsk institutt for naturforskning (NINA), 2021, [Online]. Available: https://brage.nina.no/nina-xmlui/handle/11250/2832294.

[35] B. Krause, *Wild Soundscapes: Discovering the Voice of the Natural World, Revised Edition*. Yale University Press, May 2016, [Online]. Available: https://books.google.co.uk/books?hl=en&lr=&id=ZbEODAAAQBAJ&oi=fnd&pg=PR9&dq=Wild+Soundscapes:+Discovering+the+Voice+of+the+Natural+World&ots=-77waVcn-a&sig=mpfyaPoKm63nFiSjC-T5QY-264c#v=onepage&q=Wild%20Soundscapes%3A%20Discovering%20the%20Voice%20of%20the%20Natural%20World&f=false.

[36] A. Omprakash, R. Balakrishnan, R. Ewers, and S. Sethi, *Interpretable and Robust Machine Learning for Exploring and Classifying Soundscape Data*, Nov. 2024, [Online]. Available: https://www.biorxiv.org/content/10.1101/2024.11.07.622465v1.

[37] I. Alcocer, H. Lima, L. S. M. Sugai, and D. Llusia, "Acoustic indices as proxies for biodiversity: A meta-analysis", *Biological Reviews*, vol. 97, no. 6, pp. 2209–2236, Dec. 2022, [Online]. Available: https://onlinelibrary.wiley.com/doi/10.1111/brv.12890.

[38] B. Krause, "The Niche Hypothesis: A virtual symphony of animal sounds, the origins of musical expression and the health of habitats", *The Soundscape Newsletter*, vol. 6, pp. 6–10, Jun. 1993, [Online]. Available: https://www.researchgate.net/profile/Bernie-Krause/publication/295609070_The_niche_hypothesis/links/56dc834a08aebe4638c031b8/The-niche-hypothesis.pdf.

[39] D. Llusia, "The limits of acoustic indices", *Nature Ecology & Evolution*, vol. 8, no. 4, pp. 606–607, Apr. 2024, [Online]. Available: https://www.nature.com/articles/s41559-024-02348-1.

[40] A. Farina, "The acoustic complexity index (ACI): Theoretical foundations, applied perspectives and semantics", *Oikos*, vol. n/a, no. n/a, e10760, Oct. 2024, [Online]. Available: https://onlinelibrary.wiley.com/doi/abs/10.1111/oik.10760.

[41] E. Znidersic, D. M. Watson, and M. W. Towsey, "A new method to estimate abundance of Australasian Bittern (Botaurus poiciloptilus) from acoustic recordings", *Avian Conservation and Ecology*, vol. 19, no. 1, May 2024, [Online]. Available: https://ace-eco.org/vol19/iss1/art16/.

[42] T. Bradfer-Lawrence, N. Bunnefeld, N. Gardner, S. G. Willis, and D. H. Dent, "Rapid assessment of avian species richness and abundance using acoustic indices", *Ecological Indicators*, vol. 115, p. 106 400, Aug. 2020, [Online]. Available: https://www.sciencedirect.com/science/article/pii/S1470160X2030337X.

[43] T. Bradfer-Lawrence, B. Duthie, C. Abrahams, *et al.*, "The Acoustic Index User's Guide: A practical manual for defining, generating and understanding current and future acoustic indices", *Methods in Ecology and Evolution*, vol. 16, no. 6, pp. 1040–1050, 2025, [Online]. Available: https://onlinelibrary.wiley.com/doi/abs/10.1111/2041-210X.14357.

[44] T. Bradfer-Lawrence, N. Gardner, L. Bunnefeld, N. Bunnefeld, S. G. Willis, and D. H. Dent, "Guidelines for the use of acoustic indices in environmental research", *Methods in Ecology and Evolution*, vol. 10, no. 10, V. Zamora-Gutierrez, Ed., pp. 1796–1807, Oct. 2019, [Online]. Available: https://onlinelibrary.wiley.com/doi/10.1111/2041-210X.13254.

[45] S. S. Sethi, A. Bick, R. M. Ewers, *et al.*, "Limits to the accurate and generalizable use of soundscapes to monitor biodiversity", *Nature Ecology & Evolution*, vol. 7, no. 9, pp. 1373–1378, Sep. 2023, [Online]. Available: https://www.nature.com/articles/s41559-023-02148-z.

[46] K. M. Fristrup and D. Mennitt, "Bioacoustical Monitoring in Terrestrial Environments", *Acoustics Today*, vol. 8, no. 3, p. 16, 2012, [Online]. Available: https://acousticstoday.org/issues/2012AT/Jul2012/#?page=17.

[47] R. Gibb, E. Browning, P. Glover-Kapfer, and K. E. Jones, "Emerging opportunities and challenges for passive acoustics in ecological assessment and monitoring", *Methods in Ecology and Evolution*, vol. 10, no. 2, pp. 169–185, 2019, [Online]. Available: https://onlinelibrary.wiley.com/doi/abs/10.1111/2041-210X.13101.

[48] A. Potenza, R. Benocci, A. Bisceglie, J. Fouani, V. Zaffaroni-Caorsi, and G. Zambon, "Audio Equalization of Different Soundscape Recorders is Necessary to Perform a Correct Analysis", in *Proceedings of the 10th Convention of the European Acoustics Association Forum Acusticum 2023*, Turin, Italy: European Acoustics Association, Jan. 2024, pp. 4833–4840, [Online]. Available: https://dael.euracoustics.org/confs/landing_pages/fa2023/000748.html.

[49] C. Erbe and J. A. Thomas, Eds., *Exploring Animal Behavior Through Sound: Volume 1: Methods*. Cham: Springer International Publishing, 2022, [Online]. Available: https://link.springer.com/10.1007/978-3-030-97540-1.

[50] J. Bruyninckx, "For Science, Broadcasting, and Conservation: Wildlife Recording, the BBC, and the Consolidation of a British Library of Wildlife Sounds", *Technology and Culture*, vol. 60, no. 2 Supplement, S188–S215, Apr. 2019, [Online]. Available: https://www.proquest.com/docview/2249732993/abstract/E1EE5477C7144CC1PQ/1.

[51] K. Darras, P. Batáry, B. J. Furnas, I. Grass, Y. A. Mulyani, and T. Tscharntke, "Autonomous sound recording outperforms human observation for sampling birds: A systematic map and user guide", *Ecological Applications*, vol. 29, no. 6, e01954, 2019, [Online]. Available: https://onlinelibrary.wiley.com/doi/abs/10.1002/eap.1954.

[52] M. Anderson and B. Anderson, *An Analysis of Data Compression Algorithms in the Context of Ultrasonic Bat Bioacoustics*. 2022, [Online]. Available: https://urn.kb.se/resolve?urn=urn:nbn:se:lnu:diva-113872.

[53] C. M. Wood, J. Champion, C. Brown, *et al.*, "Challenges and opportunities for bioacoustics in the study of rare species in remote environments", *Conservation Science and Practice*, vol. 5, no. 6, e12941, 2023, [Online]. Available: https://onlinelibrary.wiley.com/doi/abs/10.1111/csp2.12941.

[54] B. Krause and A. Farina, "Using ecoacoustic methods to survey the impacts of climate change on biodiversity", *Biological Conservation*, vol. 195, pp. 245–254, Mar. 2016, [Online]. Available: https://www.sciencedirect.com/science/article/pii/S0006320716300118.

[55] K. Darras, B. Kolbrek, A. Knorr, V. Meyer, M. Zippert, and A. Wenzel, "Assembling cheap, high-performance microphones for recording terrestrial wildlife: The Sonitor system", *F1000Research*, vol. 7, p. 1984, Feb. 2021, [Online]. Available: https://www.ncbi.nlm.nih.gov/pmc/articles/PMC6338251/.

[56] J. J. Greenwood, "Citizens, science and bird conservation", *Journal of Ornithology*, vol. 148, no. Suppl 1, pp. 77–124, 2007, [Online]. Available: https://link.springer.com/article/10.1007/s10336-007-0239-9.

[57] R. Simpson, K. R. Page, and D. De Roure, "Zooniverse: Observing the world's largest citizen science platform", in *Proceedings of the 23rd International Conference on World Wide Web*, Seoul Korea: ACM, Apr. 2014, pp. 1049–1054, [Online]. Available: https://dl.acm.org/doi/10.1145/2567948.2579215.

[58] D. Jäckel, K. G. Mortega, U. Sturm, U. Brockmeyer, O. Khorramshahi, and S. L. Voigt-Heucke, "Opportunities and limitations: A comparative analysis of citizen science and expert recordings for bioacoustic research", *PLOS ONE*, vol. 16, no. 6, e0253763, Jun. 2021, [Online]. Available: https://journals.plos.org/plosone/article?id=10.1371/journal.pone.0253763.

[59] H. Heffner and R. Heffner, "Hearing ranges of laboratory animals", *J. Am. Assoc. Lab. Anim. Sci*, pp. 21–23, Jan. 2007, [Online]. Available: https://pubmed.ncbi.nlm.nih.gov/17203911/.

[60] P. M. Narins, A. S. Stoeger, and C. O'Connell-Rodwell, "Infrasonic and Seismic Communication in the Vertebrates with Special Emphasis on the Afrotheria: An Update and Future Directions", in *Vertebrate Sound Production and Acoustic Communication*, R. A. Suthers, W. T. Fitch, R. R. Fay, and A. N. Popper, Eds., Cham: Springer International Publishing, 2016, pp. 191–227, [Online]. Available: https://doi.org/10.1007/978-3-319-27721-9_7.

[61] A. Staniewicz, G. McCabe, and M. Holderied, "The low-frequency vocal repertoire of adult African dwarf crocodiles", *African Journal of Herpetology*, vol. 72, no. 2, pp. 103–118, 2023, [Online]. Available: https://journals.co.za/doi/abs/10.1080/21564574.2023.2237035.

[62] A. L. Mack and J. Jones, "Low-Frequency Vocalizations by Cassowaries (Casuarius Spp.)", *The Auk*, vol. 120, no. 4, pp. 1062–1068, Oct. 2003, [Online]. Available: https://doi.org/10.1093/auk/120.4.1062.

[63] T. Rossing, *Springer Handbook of Acoustics*. Springer Science & Business Media, Jun. 2007, [Online]. Available: https://dl.acm.org/doi/abs/10.5555/1535484.

[64] F. Ladich and H. Winkler, "Acoustic communication in terrestrial and aquatic vertebrates", *Journal of Experimental Biology*, vol. 220, no. 13, pp. 2306–2317, Jul. 2017, [Online]. Available: https://doi.org/10.1242/jeb.132944.

[65] R. Nakano, N. Skals, T. Takanashi, *et al.*, "Moths produce extremely quiet ultrasonic courtship songs by rubbing specialized scales", *Proceedings of the National Academy of Sciences*, vol. 105, no. 33, pp. 11 812–11 817, Aug. 2008, [Online]. Available: https://www.pnas.org/doi/abs/10.1073/pnas.0804056105.

[66] B. Chivers, T. Jonsson, O. J. Cadena-Castaneda, and F. Montealegre-Z, "Ultrasonic reverse stridulation in the spider-like katydid Arachnoscelis (Orthoptera: Listrosceledinae)", *Bioacoustics*, vol. 23, no. 1, pp. 67–77, Jan. 2014, [Online]. Available: https://doi.org/10.1080/09524622.2013.816639.

[67] W. Metzner and R. Müller, "Ultrasound Production, Emission, and Reception", in *Bat Bioacoustics*, M. B. Fenton, A. D. Grinnell, A. N. Popper, and R. R. Fay, Eds., New York, NY: Springer, 2016, pp. 55–91, [Online]. Available: https://doi.org/10.1007/978-1-4939-3527-7_3.

[68] I. Branchi, D. Santucci, and E. Alleva, "Ultrasonic vocalisation emitted by infant rodents: A tool for assessment of neurobehavioural development", *Behavioural Brain Research*, vol. 125, no. 1, pp. 49–56, Nov. 2001, [Online]. Available: https://www.sciencedirect.com/science/article/pii/S0166432801002777.

[69] J. R. Barber, D. Plotkin, J. J. Rubin, *et al.*, "Anti-bat ultrasound production in moths is globally and phylogenetically widespread", *Proceedings of the National Academy of Sciences*, vol. 119, no. 25, e2117485119, Jun. 2022, [Online]. Available: https://www.pnas.org/doi/abs/10.1073/pnas.2117485119.

[70] G. Sales and D. Pye, "The Songs of Bush Crickets (Tettigoniidae)", in *Ultrasonic Communication by Animals*, G. Sales and D. Pye, Eds., Dordrecht: Springer Netherlands, 1974, pp. 98–130, [Online]. Available: https://doi.org/10.1007/978-94-011-6901-1_5.

[71] S. Brinkløv, M. B. Fenton, and J. M. Ratcliffe, "Echolocation in Oilbirds and swiftlets", *Frontiers in Physiology*, vol. 4, May 2013, [Online]. Available: https://www.frontiersin.org/journals/physiology/articles/10.3389/fphys.2013.00123/full.

[72] F. Goller, "The syrinx", *Current Biology*, vol. 32, no. 20, R1095–R1100, Oct. 2022, [Online]. Available: https://www.sciencedirect.com/science/article/pii/S0960982222013112.

[73] N. Fletcher, "The Variety of Information Transfer in Animal Sonic Communication: Review from a Physics Perspective", *Entropy*, vol. 11, pp. 888–906, Nov. 2009, DOI: 10.3390/e11040888.

[74] G. Ubiema, M. Siwiaszczyk, C. Parias, *et al.*, "The use and impact of auditory stimulation in animals", *Journal of Interdisciplinary Methodologies and Issues in Sciences*, vol. Unlabeled volume, Sep. 2022, DOI: 10.46298/jimis.9971.

[75] L. Pater, T. Grubb, and D. Delaney, "Recommendations for Improved Assessment of Noise Impacts on Wildlife", *Journal of Wildlife Management*, vol. 73, pp. 788–795, Dec. 2010, DOI: 10.2193/2006-235.

[76] J. N. Zeyl, O. den Ouden, C. Köppl, *et al.*, "Infrasonic hearing in birds: A review of audiometry and hypothesized structure–function relationships", *Biological Reviews*, vol. 95, no. 4, pp. 1036–1054, 2020, [Online]. Available: https://onlinelibrary.wiley.com/doi/abs/10.1111/brv.12596.

[77] G. S. Pollack, "Hearing for Defense", in *Insect Hearing*, G. S. Pollack, A. C. Mason, A. N. Popper, and R. R. Fay, Eds., vol. 55, Cham: Springer International Publishing, 2016, pp. 81–98, [Online]. Available: http://link.springer.com/10.1007/978-3-319-28890-1_4.

[78] A. J. Zuckerwar, *Handbook of the Speed of Sound in Real Gases*. Academic Press, Sep. 2002, [Online]. Available: https://books.google.co.uk/books?hl=en&lr=&id=FiZPT_FVdQEC&oi=fnd&pg=PP1&dq=Handbook+of+the+Speed+of+Sound+in+Real+Gases&ots=fkf6dGQxpt&sig=-viWynq1pd7cJU2AuvA9DyG7MKk#v=onepage&q=Handbook%20of%20the%20Speed%20of%20Sound%20in%20Real%20Gases&f=false.

[79] N. Bilaniuk and G. S. K. Wong, "Speed of sound in pure water as a function of temperature", *The Journal of the Acoustical Society of America*, vol. 93, no. 3, pp. 1609–1612, Mar. 1993, [Online]. Available: https://doi.org/10.1121/1.406819.

[80] M. L. Oelze, W. D. O'Brien, and R. G. Darmody, "Measurement of Attenuation and Speed of Sound in Soils", *Soil Science Society of America Journal*, vol. 66, no. 3, pp. 788–796, 2002, [Online]. Available: https://onlinelibrary.wiley.com/doi/abs/10.2136/sssaj2002.7880.

[81] O. N. Larsen and M. Wahlberg, "Sound and Sound Sources", in *Comparative Bioacoustics: An Overview*, Bentham Science Publishers, Jan. 2017, pp. 3–61, [Online]. Available: https://www.benthamdirect.com/content/books/9781681083179.chapter-1.

[82] R. Kapoor, S. Ramasamy, A. Gardi, R. Schyndel, and R. Sabatini, "Acoustic Sensors for Air and Surface Navigation Applications", *Sensors*, vol. 18, no. 2, p. 499, Feb. 2018, [Online]. Available: https://www.mdpi.com/1424-8220/18/2/499.

[83] C. Brown and T. Riede, *Comparative Bioacoustics: An Overview*. Bentham Science Publishers, Jan. 2017, [Online]. Available: https://www.tandfonline.com/doi/full/10.1080/09524622.2017.1348672.

[84] M. O. Lammers, R. E. Brainard, W. W. L. Au, T. A. Mooney, and K. B. Wong, "An ecological acoustic recorder (EAR) for long-term monitoring of biological and anthropogenic sounds on coral reefs and other marine habitats", *The Journal of the Acoustical Society of America*, vol. 123, no. 3, pp. 1720–1728, Mar. 2008, [Online]. Available: https://asa.scitation.org/doi/abs/10.1121/1.2836780.

[85] A. P. Hill, P. Prince, J. L. Snaddon, C. P. Doncaster, and A. Rogers, "AudioMoth: A low-cost acoustic device for monitoring biodiversity and the environment", *HardwareX*, vol. 6, e00073, Oct. 2019, [Online]. Available: https://www.sciencedirect.com/science/article/pii/S2468067219300306.

[86] Wildlife Acoustics, *Products: Wildlife Sound Analysis Tools*, Apr. 2023, [Online]. Available: https://www.wildlifeacoustics.com/products.

[87] S. S. Sethi, R. M. Ewers, N. S. Jones, C. D. L. Orme, and L. Picinali, "Robust, real-time and autonomous monitoring of ecosystems with an open, low-cost, networked device", *Methods in Ecology and Evolution*, vol. 9, no. 12, pp. 2383–2387, 2018, [Online]. Available: https://onlinelibrary.wiley.com/doi/abs/10.1111/2041-210X.13089.

[88] R. D. Beason, R. Riesch, and J. Koricheva, "AURITA: An affordable, autonomous recording device for acoustic monitoring of audible and ultrasonic frequencies", *Bioacoustics*, vol. 28, no. 4, pp. 381–396, Jul. 2019, [Online]. Available: https://www.tandfonline.com/doi/full/10.1080/09524622.2018.1463293.

[89] E. C. M. Karlsson, H. Tay, P. Imbun, and A. C. Hughes, "The Kinabalu Recorder, a new passive acoustic and environmental monitoring recorder", *Methods in Ecology and Evolution*, vol. 12, no. 11, pp. 2109–2116, 2021, [Online]. Available: https://onlinelibrary.wiley.com/doi/abs/10.1111/2041-210X.13671.

[90] S. Van Parijs, C. Clark, R. Sousa-Lima, *et al.*, "Management and research applications of real-time and archival passive acoustic sensors over varying temporal and spatial scales", *Marine Ecology Progress Series*, vol. 395, pp. 21–36, Dec. 2009, [Online]. Available: http://www.int-res.com/abstracts/meps/v395/p21-36/.

[91] K. Chan, D. N. Schillereff, A. C. Baas, *et al.*, "Low-cost electronic sensors for environmental research: Pitfalls and opportunities", *Progress in Physical Geography: Earth and Environment*, vol. 45, no. 3, pp. 305–338, Jun. 2021, [Online]. Available: https://doi.org/10.1177/0309133320956567.

[92] M. R. Idris, M. N. Irdayanti, and M. Ramlee, "A review of microcontroller design in future industrial revolution", *AIP Conference Proceedings*, vol. 2750, no. 1, p. 050 031, Jun. 2023, [Online]. Available: https://doi.org/10.1063/5.0149680.

[93] T. R. Lambert, "An introduction to microcontrollers and embedded systems", *Auburn University. July*, vol. 344, 2017, [Online]. Available: https://www.researchgate.net/profile/Tyler-Lambert/publication/340062601_Introduction_to_Microcontrollers_and_Embedded_Systems/links/5e7a4332299bf1f3873f8a24/Introduction-to-Microcontrollers-and-Embedded-Systems.pdf.

[94] J. Ganssle, *The art of designing embedded systems*. Newnes, 2008, [Online]. Available: https://books.google.co.uk/books?hl=en&lr=&id=MMfCP3KTNZoC&oi=fnd&pg=PP1&dq=The+art+of+designing+embedded+systems&ots=lv9a8vMrZg&sig=Qq0g8LTV2DrYcN741FjKUlAo3Cg#v=onepage&q=The%20art%20of%20designing%20embedded%20systems&f=false.

[95] J. W. Valvano, *Introduction to the Arm® Cortex(TM)-M3* (Embedded systems / Jonathan W. Valvano 1), 4. ed. s.l.: Eigenverl. d. Verf, 2013, [Online]. Available: https://digilib.politeknik-pratama.ac.id/assets/dokumen/ebook/feb_2bc5029aaea34ed45f9d04fa8d43827ace71db4d_1641460443.pdf.

[96] S. Heath, *Embedded Systems Design*. Elsevier, Oct. 2002, [Online]. Available: https://books.google.co.uk/books?hl=en&lr=&id=BjNZXwH7HlkC&oi=fnd&pg=PP1&dq=Embedded+Systems+Design&ots=xk4iF3wMfP&sig=5fNWAyhIPvH8aNrnltT0XcGNb98#v=onepage&q=Embedded%20Systems%20Design&f=false.

[97] K. Dewald and D. Jacoby, "Signal Processing In Embedded Systems", *Latin America Transactions, IEEE (Revista IEEE America Latina)*, vol. 11, pp. 664–667, Feb. 2013, DOI: 10.1109/TLA.2013.6502881.

[98] H.-S. Wong, D. Frank, P. Solomon, C. Wann, and J. Welser, "Nanoscale CMOS", *Proceedings of the IEEE*, vol. 87, no. 4, pp. 537–570, Apr. 1999, [Online]. Available: http://ieeexplore.ieee.org/document/752515/.

[99] N. S. Widmer, G. L. Moss, and R. J. Tocci, *Digital systems: principles and applications*, Twelfth edition. Boston: Pearson, 2017, [Online]. Available: https://books.google.co.uk/books?hl=en&lr=&id=zm2TR30y0-8C&oi=fnd&pg=PR13&dq=Digital+systems:+principles+and+applications&ots=2cMy673T3n&sig=dWmKGVwv7GGi_v7Fv2btPzesA2c#v=onepage&q=Digital%20systems%3A%20principles%20and%20applications&f=false.

[100] H. H. Radamson, H. Zhu, Z. Wu, *et al.*, "State of the Art and Future Perspectives in Advanced CMOS Technology", *Nanomaterials*, vol. 10, no. 8, p. 1555, Aug. 2020, [Online]. Available: https://www.mdpi.com/2079-4991/10/8/1555.

[101] R. W. Keyes, "The Impact of Moore's Law", *IEEE Solid-State Circuits Society Newsletter*, vol. 11, no. 3, pp. 25–27, Sep. 2006, [Online]. Available: https://ieeexplore.ieee.org/abstract/document/4785857.

[102] Texas Instruments, "CMOS Power Consumption and CPD Calculation", Jul. 1997, [Online]. Available: https://www.ti.com/lit/an/scaa035b/scaa035b.pdf?ts=1734312195947.

[103] A. Chandrakasan, A. Wang, and B. H. Calhoun, *Sub-threshold Design for Ultra Low-Power Systems*. Boston, MA: Springer US, 2006, [Online]. Available: https://link.springer.com/chapter/10.1007/978-0-387-34501-7_7.

[104] D. A. Patterson and J. L. Hennessy, *Computer Organization and Design ARM Edition: The Hardware Software Interface*. Morgan Kaufmann, May 2016, [Online]. Available: https://books.google.co.uk/books?hl=en&lr=&id=Pz-XCgAAQBAJ&oi=fnd&pg=PP1&dq=Computer+Organization+and+Design+ARM+Edition:+The+Hardware+Software+Interface&ots=GcPd-ksS7X&sig=tKBxPaXYGQVnsdBEKiO2j3amlRA#v=onepage&q=Computer%20Organization%20and%20Design%20ARM%20Edition%3A%20The%20Hardware%20Software%20Interface&f=false.

[105] S. F. Barrett and D. J. Pack, *Embedded Systems Design and Applications with the 68HC12 and HCS12*. Prentice Hall, 2005.

[106] A. Di Nisio, T. Di Noia, C. G. C. Carducci, and M. Spadavecchia, "High Dynamic Range Power Consumption Measurement in Microcontroller-Based Applications", *IEEE Transactions on Instrumentation and Measurement*, vol. 65, no. 9, pp. 1968–1976, Sep. 2016, [Online]. Available: https://ieeexplore.ieee.org/abstract/document/7452656?casa_token=-OIvKoTy9ocAAAAA:23FlJ5QIRnC2YyWq7qPHyEIM1EfbuzAo_eyqZqVrBBYJWkrDDB3jDOeCbQaKlaI5FaFhvT4.

[107] S. Labs, *EFM32 Gecko Family, EFM32WG Data Sheet*, Jan. 2024, [Online]. Available: https://www.silabs.com/documents/public/data-sheets/efm32wg-datasheet.pdf.

[108] J. W. Jolles, "Broad-scale applications of the Raspberry Pi: A review and guide for biologists", *Methods in Ecology and Evolution*, vol. 12, no. 9, pp. 1562–1579, 2021, [Online]. Available: https://onlinelibrary.wiley.com/doi/abs/10.1111/2041-210X.13652.

[109] R. C. Whytock and J. Christie, "Solo: An open source, customizable and inexpensive audio recorder for bioacoustic research", *Methods in Ecology and Evolution*, vol. 8, no. 3, pp. 308–312, 2017, [Online]. Available: https://onlinelibrary.wiley.com/doi/abs/10.1111/2041-210X.12678.

[110] M. Gor, J. Vora, S. Tanwar, *et al.*, "GATA: GPS-Arduino based Tracking and Alarm system for protection of wildlife animals", in *2017 International Conference on Computer, Information and Telecommunication Systems (CITS)*, Jul. 2017, pp. 166–170, DOI: 10.1109/CITS.2017.8035325.

[111] F. L. AU, *BAR-LT | Bioacoustic Recorder*, Feb. 2022, [Online]. Available: https://www.frontierlabs.com.au/product-page/bar-lt.

[112] A. P. Hill, P. Prince, E. Piña Covarrubias, C. P. Doncaster, J. L. Snaddon, and A. Rogers, "AudioMoth: Evaluation of a smart open acoustic device for monitoring biodiversity and the environment", *Methods in Ecology and Evolution*, vol. 9, no. 5, N. Isaac, Ed., pp. 1199–1211, May 2018, [Online]. Available: https://onlinelibrary.wiley.com/doi/10.1111/2041-210X.12955.

[113] O. A. Devices, *AudioMoth Dev 1.0.1 Datasheet*, Feb. 2021, [Online]. Available: https://github.com/OpenAcousticDevices/Datasheets/blob/main/AudioMoth_Dev_Datasheet/AudioMoth_Dev_Datasheet.pdf.

[114] GroupGets, *AudioMoth Dev (Group Order - Round 1)*, Feb. 2022, [Online]. Available: https://groupgets.com/products/audiomoth-dev.

[115] W. Acoustics, *SONG METER MINI 2*, Feb. 2022, [Online]. Available: https://www.wildlifeacoustics.com/products/song-meter-mini.

[116] Google Finance, *USD/GBP Currency Exchange Rate & News*, Feb. 2022, [Online]. Available: https://www.google.com/finance/quote/USD-GBP.

[117] Google Finance, *AUD/GBP Currency Exchange Rate & News*, Feb. 2022, [Online]. Available: https://www.google.com/finance/quote/AUD-GBP.

[118] K. Roedel, *Reno startup helps fund global production of acoustic recording device*, Sep. 2021, [Online]. Available: http://www.nnbw.com/news/2021/sep/21/reno-startup-helps-fund-global-production-acoustic/.

[119] S. M. Barber-Meyer, V. Palacios, B. Marti-Domken, and L. J. Schmidt, "Testing a New Passive Acoustic Recording Unit to Monitor Wolves", *Wildlife Society Bulletin*, vol. 44, no. 3, pp. 590–598, 2020, [Online]. Available: https://onlinelibrary.wiley.com/doi/abs/10.1002/wsb.1117.

[120] G. Bota, R. Manzano Rubio, L. Catalán, J. Gómez Catasús, and C. Pérez Granados, "Hearing to the Unseen: AudioMoth and BirdNET as a Cheap and Easy Method for Monitoring Cryptic Bird Species", *Sensors*, vol. 23, p. 7176, Aug. 2023, [Online]. Available: https://www.mdpi.com/1424-8220/23/16/7176.

[121] R. Manzano-Rubio, G. Bota, L. Brotons, E. Soto-Largo, and C. Pérez-Granados, "Low-cost open-source recorders and ready-to-use machine learning approaches provide effective monitoring of threatened species", *Ecological Informatics*, vol. 72, p. 101 910, Dec. 2022, [Online]. Available: https://www.sciencedirect.com/science/article/pii/S1574954122003600.

[122] Open Acoustic Devices, *An Injection Moulded Case for AudioMoth*, Jan. 2024, [Online]. Available: https://github.com/OpenAcousticDevices/Application-Notes/blob/master/An_Injection_Moulded_Case_for_AudioMoth/An_Injection_Moulded_Case_for_AudioMoth.pdf.

[123] P. E. Osborne, T. Alvares-Sanches, and P. R. White, "To Bag or Not to Bag? How AudioMoth-Based Passive Acoustic Monitoring Is Impacted by Protective Coverings", *Sensors*, vol. 23, no. 16, p. 7287, Jan. 2023, [Online]. Available: https://www.mdpi.com/1424-8220/23/16/7287.

[124] S. Lapp, N. Stahlman, and J. Kitzes, "A Quantitative Evaluation of the Performance of the Low-Cost AudioMoth Acoustic Recording Unit", *Sensors*, vol. 23, no. 11, p. 5254, Jan. 2023, [Online]. Available: https://www.mdpi.com/1424-8220/23/11/5254.

[125] S. Bennett, L. Williamson, M. Hernández-González, *et al.*, "Bioacoustics as a Measure of Population Size and Breeding Success of European Storm Petrels Hydrobates pelagicus", *Ecology and Evolution*, vol. 15, no. 8, e71893, 2025, [Online]. Available: https://onlinelibrary.wiley.com/doi/abs/10.1002/ece3.71893.

[126] R. Snyder, M. Clark, L. Salas, *et al.*, "The Soundscapes to Landscapes Project: Development of a Bioacoustics-Based Monitoring Workflow with Multiple Citizen Scientist Contributions | Citizen Science: Theory and Practice", Jan. 2022, [Online]. Available: https://theoryandpractice.citizenscienceassociation.org/articles/10.5334/cstp.391.

[127] Wildlife Acoustics, "Song Meter Mini 2 User Guide", Apr. 2024, [Online]. Available: https://www.wildlifeacoustics.com/uploads/user-guides/Song_Meter_Mini_2_User_Guide_mobile-friendly_2024-04-18-en.pdf.

[128] M. Fueldner, "Microphones", in *Handbook of Silicon Based MEMS Materials and Technologies*, Elsevier, 2020, pp. 937–948, [Online]. Available: https://linkinghub.elsevier.com/retrieve/pii/B9780128177860000487.

[129] Y. Torabi, S. Shirani, J. P. Reilly, and G. M. Gauvreau, "MEMS and ECM Sensor Technologies for Cardiorespiratory Sound Monitoring—A Comprehensive Review", *Sensors (Basel, Switzerland)*, vol. 24, no. 21, p. 7036, Oct. 2024, [Online]. Available: https://www.ncbi.nlm.nih.gov/pmc/articles/PMC11548498/.

[130] CUI Devices, *Comparing MEMS and Electret Condenser (ECM) Microphones*, Jan. 2019, [Online]. Available: https://www.cuidevices.com/blog/comparing-mems-and-electret-condenser-microphones.

[131] M. Fueldner, "Chapter 48 - Microphones", in *Handbook of Silicon Based MEMS Materials and Technologies (Third Edition)*, ser. Micro and Nano Technologies, M. Tilli, M. Paulasto-Krockel, M. Petzold, H. Theuss, T. Motooka, and V. Lindroos, Eds., Elsevier, Jan. 2020, pp. 937–948, [Online]. Available: https://www.sciencedirect.com/science/article/pii/B9780128177860000487.

[132] Knowles, *Product Datasheet, SPU0410LR5H-QB, Zero-Height SiSonic Microphone*, Mar. 2013, [Online]. Available: https://micbooster.com/ultrasonic-microphones/128-knowles-spu0410lr5h-qb.html.

[133] Open Acoustic Devices, "Using AudioMoth with External Electret Condenser Microphones", Jun. 2024, [Online]. Available: https://github.com/OpenAcousticDevices/Application-Notes/blob/master/Using_AudioMoth_with_External_Electret_Condenser_Microphones/Using_AudioMoth_with_External_Electret_Condenser_Microphones.pdf.

[134] D. Self, "Preamplifier architectures", in *Small Signal Audio Design*, 2nd ed., Routledge, 2014.

[135] M. K. Obrist, G. Pavan, J. Sueur, K. Riede, D. Llusia, and R. Márquez, "Chapter 5 Bioacoustics approaches in biodiversity inventories", Jan. 2010.

[136] W. W. Au and M. C. Hastings, "Signal Recording and Data Acquisition", in *Principles of Marine Bioacoustics*, W. W. L. Au and M. C. Hastings, Eds.,

New York, NY: Springer US, 2008, pp. 121–175, [Online]. Available: https://doi.org/10.1007/978-0-387-78365-9_5.

[137] L. Bengtsson, "ADCs and Sampling", in *Electrical Measurement Techniques: For the Physics Laboratory*, L. Bengtsson, Ed., Singapore: Springer Nature, 2024, pp. 229–265, [Online]. Available: https://doi.org/10.1007/978-981-99-8187-8_11.

[138] A. V. Oppenheim, *Discrete-time signal processing*. Pearson Education India, 1999.

[139] J. N. Oswald, A. M. Van Cise, A. Dassow, *et al.*, "A Collection of Best Practices for the Collection and Analysis of Bioacoustic Data", *Applied Sciences*, vol. 12, no. 23, p. 12 046, Jan. 2022, [Online]. Available: https://www.mdpi.com/2076-3417/12/23/12046.

[140] B. C. Pijanowski, L. J. Villanueva-Rivera, S. L. Dumyahn, *et al.*, "Soundscape Ecology: The Science of Sound in the Landscape", *BioScience*, vol. 61, no. 3, pp. 203–216, Mar. 2011, [Online]. Available: https://doi.org/10.1525/bio.2011.61.3.6.

[141] T. Napier, E. Ahn, S. Allen-Ankins, L. Schwarzkopf, and I. Lee, "Advancements in preprocessing, detection and classification techniques for ecoacoustic data: A comprehensive review for large-scale Passive Acoustic Monitoring", *Expert Systems with Applications*, vol. 252, p. 124 220, Oct. 2024, [Online]. Available: https://linkinghub.elsevier.com/retrieve/pii/S0957417424010868.

[142] K. Selvan, "SD card based Data Logging and Data Retrieval for Microcontrollers to using micro-c/os-II", *International Journal of Engineering Research & Technology*, vol. 2, p. 1.76, Nov. 2013.

[143] K. O'Brien, D. C. Salyers, A. D. Striegel, and C. Poellabauer, "Power and performance characteristics of USB flash drives", in *2008 International Symposium on a World of Wireless, Mobile and Multimedia Networks*, Jun. 2008,

pp. 1–4, [Online]. Available: https://ieeexplore.ieee.org/document/4594868.

[144] A. K. Schulz, C. Shriver, S. Stathatos, *et al.*, "Conservation tools: The next generation of engineering–biology collaborations", *Journal of The Royal Society Interface*, vol. 20, no. 205, p. 20 230 232, Aug. 2023, [Online]. Available: https://royalsocietypublishing.org/doi/full/10.1098/rsif.2023.0232.

[145] D. Ibrahim, *SD Card Projects Using the PIC Microcontroller*. Newnes, May 2010.

[146] M. Dabas, K. Tandel, and H. Diwanji, *Analyze the Power Consumption of NAND Flash Memory*, Mar. 2013, [Online]. Available: https://www.ijera.com/papers/Vol3_issue2/DV32754758.pdf.

[147] Silicon Power, *Industrial Micro-SD Card 3.0 SDT330 Series Datasheet*, Jan. 2018, [Online]. Available: https://csi.pl/wp-content/uploads/2019/10/SDT335.pdf.

[148] Primo, *EM258 Electret Condenser Microphone Electret Condenser Microphone Tehcnical Data*, Jan. 2015, [Online]. Available: https://primomic.com/pdf/EM258.pdf.

[149] Autodesk, *Compare Autodesk Fusion vs Autodesk Fusion for Personal Use | Autodesk*, Feb. 2022, [Online]. Available: https://www.autodesk.com/products/fusion-360/personal.

[150] Prusament, *PrusaSlicer | Original Prusa 3D printers directly from Josef Prusa*, Feb. 2022, [Online]. Available: https://www.prusa3d.com/page/prusaslicer_424/.

[151] Prusament, *Prusament PC Blend Urban Grey 970g | Original Prusa 3D printers directly from Josef Prusa*, Feb. 2022, [Online]. Available: https://www.prusa3d.com/product/prusament-pc-blend-urban-grey-970g/.

[152] Prusament, *Prusament ASA Jet Black 850g | Original Prusa 3D printers directly from Josef Prusa*, Feb. 2022, [Online]. Available: https://www.prusa3d.com/product/prusament-asa-jet-black-850g/.

[153] KiCad EDA, *KiCad - A Cross Platform and Open Source Electronics Design Automation Suite*, Feb. 2022, [Online]. Available: https://www.kicad.org/.

[154] M. McDonald and R. Owen, "Sheep Grazing Behaviour on Cwm Hesgyn. Hollistic Restoration LLP", Tech. Rep., Jan. 2023, [Online]. Available: https://www.uplandecosystemresearch.com/uploads/1/4/6/1/146150710/rhiwlasgrazingstudy.pdf.

[155] UK Habitat Classification Working Group, "UK Habitat Classification – Habitat Definitions V1.0", May 2018, [Online]. Available: https://ecountability.co.uk/wp-content/uploads/2018/05/UK-Habitat-Classification-Habitat-Definitions-V1.0-May-2018-1.pdf.

[156] Open Acoustic Devices, *Apps*, Feb. 2022, [Online]. Available: https://www.openacousticdevices.info/applications.

[157] Audacity Team, *Audacity(R): Free Audio Editor and Recorder*, Apr. 2014, [Online]. Available: http://audacity.sourceforge.net/.

[158] S. Kahl, C. M. Wood, M. Eibl, and H. Klinck, "BirdNET: A deep learning solution for avian diversity monitoring", *Ecological Informatics*, vol. 61, p. 101 236, Mar. 2021, [Online]. Available: https://linkinghub.elsevier.com/retrieve/pii/S1574954121000273.

[159] Xeno-Canto, *Xeno-canto - Sharing wildlife sounds from around the world*, Sep. 2022, [Online]. Available: https://xeno-canto.org/.

[160] Wildlife Acoustics, *Kaleidoscope Pro Analysis Software*, Feb. 2022, [Online]. Available: https://www.wildlifeacoustics.com/products/kaleidoscope-pro.

[161] R Core Team, "R: A language and environment for statistical computing", R Foundation for Statistical Computing, Vienna, Austria, manual, 2021, [Online]. Available: https://www.R-project.org/.

[162] H. Wickham, R. François, L. Henry, K. Müller, and D. Vaughan, "Dplyr: A grammar of data manipulation", manual, 2023, [Online]. Available: https://CRAN.R-project.org/package=dplyr.

[163] H. Wickham, "Stringr: Simple, consistent wrappers for common string operations", manual, 2023, [Online]. Available: https://CRAN.R-project.org/package=stringr.

[164] J. Sueur, T. Aubin, and C. Simonis, "Seewave: A free modular tool for sound analysis and synthesis", *Bioacoustics-the International Journal of Animal Sound and Its Recording*, vol. 18, pp. 213–226, 2008, [Online]. Available: https://www.tandfonline.com/doi/abs/10.1080/09524622.2008.9753600.

[165] L. J. Villanueva-Rivera and B. C. Pijanowski, "Soundecology: Soundscape ecology", manual, 2018, [Online]. Available: https://CRAN.R-project.org/package=soundecology.

[166] Texas Instruments, *INA1x8 High-Side Measurement Current Shunt Monitor*, Jan. 2017, [Online]. Available: https://www.ti.com/lit/ds/symlink/ina138.pdf?ts=1733987708177&ref_url=https%253A%252F%252Fwww.google.com%252F.

[167] Texas Instruments, *OPAx340 Single-Supply, Rail-to-Rail Operational Amplifiers MicroAmplifier™ Series*, Jan. 2016, [Online]. Available: https://www.ti.com/lit/ds/symlink/opa340.pdf?ts=1734266125612&ref_url=https%253A%252F%252Fwww.ti.com%252Fproduct%252FOPA340%252Fpart-details%252FOPA340PA.

[168] Multisim, *Multisim*, Sep. 2024, [Online]. Available: https://www.ni.com/en-gb/shop/product/multisim.html.

[169] Tektronix, *Mixed Signal Oscilloscopes MSO2000 Series, DPO2000 Series Data Sheet*, May 2009, [Online]. Available: https://www.testequipmenthq.com/datasheets/TEKTRONIX-DPO2014-Datasheet.pdf.

[170] Tektronix, *Arbitrary/Function Generator, AFG1000 Series Datasheet*, Jun. 2023, [Online]. Available: https://www.tek.com/en/datasheet/arbitrary-function-generator.

[171] Keithley, *Multi-Channel USB and USB/GPIB Programmable DC Power Supplies*, Nov. 2013, [Online]. Available: https://octopart.com/datasheet/2230-30-1-keithley-24728821.

[172] Graphtec, *GL900 Midi Logger User Manual, Manual No. GL900-UM-151*, Jan. 2008, [Online]. Available: https://static1.squarespace.com/static/5900b1a3c534a5aa8149a65c/t/595eae5a5016e1f4ba32f167/1499377255833/INS+GL900+User+Manual+UM-151.pdf.

[173] D. Gil and D. Llusia, "The Bird Dawn Chorus Revisited", in *Coding Strategies in Vertebrate Acoustic Communication*, T. Aubin and N. Mathevon, Eds., Cham: Springer International Publishing, 2020, pp. 45–90, [Online]. Available: https://doi.org/10.1007/978-3-030-39200-0_3.

[174] RSPB, BTO, Game and Wildlife Conservation Trust, *et al.*, "Birds of Conservation Concern 5. The status of all regularly occurring birds in the UK, Channel Islands and Isle of Man.", Tech. Rep., Jan. 2021, [Online]. Available: https://www.bto.org/sites/default/files/publications/bocc-5-a5-4pp-single-pages.pdf.

[175] N. Sato and K. Yagi, "Thermal behavior analysis of nickel metal hydride batteries for electric vehicles", *JSAE Review*, vol. 21, no. 2, pp. 205–211, Apr. 2000, [Online]. Available: https://www.sciencedirect.com/science/article/pii/S038943049900096X.

[176] L. Fuller, M. Shewring, and F. M. Caryl, "A novel method for targeting survey effort to identify new bat roosts using habitat suitability modelling", *European Journal of Wildlife Research*, vol. 64, no. 3, p. 31, May 2018, [Online]. Available: https://doi.org/10.1007/s10344-018-1191-0.

[177] S. E. Newson, Y. Bas, A. Murray, and S. Gillings, "Potential for coupling the monitoring of bush-crickets with established large-scale acoustic monitoring of bats", *Methods in Ecology and Evolution*, vol. 8, no. 9, pp. 1051–1062, 2017, [Online]. Available: https://onlinelibrary.wiley.com/doi/abs/10.1111/2041-210X.12720.

[178] P. Devos, "The Bird Dawn Chorus Strength of an Urban Soundscape and Its Potential to Assess Urban Green Spaces", *Sustainability*, vol. 15, no. 8, p. 7002, Jan. 2023, [Online]. Available: https://www.mdpi.com/2071-1050/15/8/7002.

[179] J. M. Bryant, "9 - Analog Breadboarding", in *The Art and Science of Analog Circuit Design*, ser. EDN Series for Design Engineers, J. Williams, Ed., Woburn: Newnes, Jan. 1998, pp. 103–119, [Online]. Available: https://www.sciencedirect.com/science/article/pii/B9780750670623500121.

[180] A. Rogers, *Power consumption features on oscilloscope*, Jul. 2024, [Online]. Available: https://www.openacousticdevices.info/support/device-support/power-consumption-features-on-oscilloscope.

[181] Open Acoustic Devices, *SD Cards*, Feb. 2024, [Online]. Available: https://www.openacousticdevices.info/sd-card-guide.

[182] Linear Technology, *LT1761 Series 1, 100mA, Low Noise, LDO Micropower, Regulators in TSOT-23*, Jan. 2005, [Online]. Available: https://www.analog.com/media/en/technical-documentation/data-sheets/1761sff.pdf.

[183] A. Rogers, *1600 files of noise*, May 2021, [Online]. Available: https://www.openacousticdevices.info/support/device-support/1600-files-of-noise.

[184] A. Rogers, *Noise at 53 kHz*, Jul. 2022, [Online]. Available: https://www.openacousticdevices.info/support/configuration-support/noise-at-53-khz.

[185] A. Pires and R. R. Hoy, "Temperature coupling in cricket acoustic communication", *Journal of Comparative Physiology A*, vol. 171, no. 1, pp. 79–92, Aug. 1992, [Online]. Available: https://doi.org/10.1007/BF00195963.